The Concept of Weak Values
Jan Dziewior

Munich, 18th of May, 2016

The Concept of Weak Values
Jan Dziewior

Master Thesis
Faculty of Physics
Ludwig-Maximilians-Universität
München

Author:
Jan Dziewior

Munich, 18th of May, 2016

Supervisor: Prof. Dr. Harald Weinfurter

Das Konzept von Weak Values
Jan Dziewior

Masterarbeit
Fakultät für Physik
Ludwig-Maximilians-Universität
München

vorgelegt von
Jan Dziewior

München, 18. Mai 2016

Betreuer: Prof. Dr. Harald Weinfurter

Mais Sisyphe enseigne la fidélité supérieure qui nie les dieux et soulève les rochers. Lui aussi juge que tout est bien. Cet univers désormais sans maître ne lui paraît ni stérile ni futile. Chacun des grains de cette pierre, chaque éclat minéral de cette montagne pleine de nuit, à lui seul, forme un monde. La lutte elle-même vers les sommets suffit à remplir un coeur d'homme. Il faut imaginer Sisyphe heureux.

Le Mythe de Sisyphe - Albert Camus

Contents

Contents

List of Figures

List of Figures

Abstract

Weak values, which have been introduced in 1988 by Aharonov, Albert and Vaidman, to this day constitute an interesting and controversial element in the debate about the foundations of quantum mechanics. This thesis analyzes this concept together with its most important applications and interpretations. Weak values are introduced based on a discussion of standard quantum measurement, which is applied to pre- and postselected systems with a weak interaction. Thereby, a quantitative definition of weakness is proposed, which is based on the amount of correlation between measured and measuring system. Furthermore, the properties of a quantum tomography technique which employs the formalism of weak values are discussed in the context of a tomography experiment that was reproduced in the course of the thesis. Eventually in dependence on an operational definition of physical reality, also a proof for the reality of weak values as a property of pre- and postselected system is presented.

Abstract

1. Introduction

While quantum mechanics succeeded in the description of phenomena inexplicable by classical physics, as the famous Stern-Gerlach experiment [1], it did so at the cost of the introduction of the postulated "collapse" of the wavefunction. In the standard formalism of quantum mechanics, the duality between the particle and wave properties of quantum particles is bridged by the random transition of a superposition of alternative possibilities expressed in the form of a wave into the definite properties of a particle. The necessity of the measurement postulate, which describes the properties of physical systems as fundamentally dependent on their observation, is denoted as the "measurement problem" and presents a controversial subject also for the contemporary debate about the fundamental interpretation of quantum mechanics [2, 3].

The introduction of the concept of a "weak value of a quantum variable" in the momentous article of Aharanov, Albert and Vaidman in 1988 [4], which implied the possibility of conducting measurements on quantum systems without the consequence of a collapse, brought a new perspective into the standard debate. Because of the inception of weak values from the "time-symmetric formulation" of quantum mechanics as developed by Aharonov, Bergmann and Lebowitz in 1964 [5] and the controversial interpretation of weak values as highly unusual measurement outcomes of quantum measurements, this concept has fueled an intense debate, which began immediately after the initial introduction [6–9] and continues until today [10–20].

Independently of the interpretational controversies surrounding weak values and measurements, however, the concept has proven useful in at least some experimental applications. Since the first implementation of a weak measurement by Ritchie et al. [21] shortly after the initial introduction of weak measurements, a number of experiments has been performed, which employed the formalism of weak values in diverse ways. The two main applications for which weak values have proven useful is the amplification of small effects in quantum metrology as the famous weak measurement of the spin Hall effect of light [22] and the novel procedure for the determination of unknown quantum states, denoted as "direct state tomography" as most prominently presented in [23–25].

The goal of this thesis is the presentation of the concept of weak values alongside its most relevant interpretations and applications. A particular emphasis is given to the relation between weak values and the standard theory of quantum mechanics. In the course of the practical part of the thesis an experiment relating

to direct state tomography was performed, which is also presented in the context of the discussion of the basic principles of the procedure. Two review articles should be mentioned as important resources, one of which is the review of Kofman et al. [26], where the formalism of weak values is developed and analyzed in great detail. The other important source is a review article by Aharonov and Vaidman [27], which derives the concept of weak values from a systematic discussion of the time-symmetric approach to quantum mechanics.

This work is divided into four chapters and begins with an overview over the elements and structures of standard quantum theory. The mathematical formalism of Hilbert spaces is introduced and subsequently its application for the representation of physical systems is delineated. While the presentation of these basic principles is relatively extensive, this approach is justified by the aim to provide a clear and well-defined foundation for the following discussions.

The next chapter focuses on the subject of quantum measurement and introduces the notion of measurement strength after a more detailed discussion of the quantum mechanical measurement process. On this foundation it is possible to define the concepts of weak measurements and weak values and to provide an analysis of their properties in the second part of the chapter. The chapter is concluded by a graphical illustration of the effects of the weak measurement procedure on the pointer system.

In the third main chapter the principles of direct state tomography are explained in comparison to standard quantum tomography procedures. Subsequently, based on a detailed analysis of the Gaussian laser beam as a pointer system for weak measurements, an account of the conducted experiment and its results is given. As it was not possible to resolve two non-negligible discrepancies between theoretical predictions and experimental data, some possible explanations for this problem are discussed as well.

As a conclusion of the main content the last chapter delineates the interpretational controversies regarding weak values based on a discussion of the prominent "Three Box Paradox". It is pointed out that weak values should be rather regarded as relative probability amplitudes and not as measurement outcomes with the same meaning as expectation values. However, a strictly operational interpretation of weak values is presented as well, which allows to understand them as definite properties of pre- and postselected systems, in the same way as eigenvalues represent definite properties of standard quantum systems. A proof for this relation in the context of a strictly operational definition physical reality was developed in the course of this thesis and is described at the end of the last chapter, alongside the concept of an experiment which could confirm the connection between weak values and eigenvalues.

Concluding this introduction two technical remarks should be given about standard conventions employed in the text. The first pertains to quotation marks, which are used in two ways, either to signify verbatim quotations with a following

reference or to highlight the non-referential use of notions. The other relates to the writing of notions in italics, which points to a mention of these notions in a defining context for the first time.

1. Introduction

2. Fundemantals of Quantum Mechanics

The goal of this chapter is to summarize and present the fundamental framework of quantum mechanics as a basis for the discussion of weak values. Even though its aim is not to give a complete and mathematically exact account of quantum theory, which would of course extend far beyond the scope of this thesis, the intent is still to delineate a coherent and clear mathematical description of the relevant formalism as well as its connection to the physical world. Therefore, most of the chapter is based mainly on three introductory textbooks [28–30] that present, each in its own way, a far more detailed picture of quantum mechanics than this thesis. With respect to certain key issues, these three accounts are then complemented with additional material. The subject of measurement is purposefully left out and is discussed in more detail in the chapter 3.

2.1. Structure and Mathematical Formalism

This section provides a general overview of the relevant mathematical formalism of quantum mechanics. It is kept rather basic, in order to give a short but concise account of quantum mechanics with a special emphasis on the formulation of those elements that will be relevant for the discussions in the following chapters.

2.1.1. Structure of Quantum Theory

The presentation of quantum mechanics begins with a short overview of its structure and the principal difficulties that arise with the interpretation of physical theories in general.

Formalism, Postulates and Models

At first glance the elements of quantum mechanics can be roughly divided into two groups, the mathematical "Hilbert space" formalism and the quantum mechanical "postulates". While the former is a strictly mathematical structure, which can be labeled as the "internal principles", the postulates are additional "bridge principles", which form a set of rules that determine how the empirical systems of physics are to be encompassed by the formalism [29, 31, 32]. Even though

the explicit formulation of the postulates may vary between different accounts of quantum theory, all address three fundamental principles, the mathematical representation of physical states, the representation of their evolution and the representation of the physical measurement process, thus forming "schemata for getting into and out of the mathematical language of the theory" [31].

Apart from these two groups of principles, however, there arguably exists another important class of elements that constitutes quantum mechanics. As Cartwright eloquently states,

> "...one may know all this and not know any quantum mechanics. In a good undergraduate text these two sets of principles are covered in one short chapter. It is true that the Schroedinger equation tells us how a quantum system evolves subject to the Hamiltonian; but to do quantum mechanics, one has to know how to pick the Hamiltonian. The principles that tell us how to do so are the real bridge principles of quantum mechanics. These give content to the theory ..." [31]

The quantum mechanical description is thus based on "models", in which a set of physical systems along with their interactions is at least approximately expressed as "mathematical structures containing sets of elements on which certain operations and relations are defined" [32]. This expression, which is constructed along the rules of the quantum mechanical postulates but not determined by them, then makes the physical system accessible to the mathematical formalism of Hilbert spaces. The descriptive power of quantum mechanics arguably stems from the fact that many different physical systems can be described sufficiently well by a small number of relatively simple models, which are well known and understood, as for example a harmonic oscillator [31].

Status of Quantum Mechanical Models

An important and controversial issue is the representational status of quantum mechanical models and should be briefly illuminated at this point. The "relation between mathematical model and physical theory" is in general a "complicated question" [32] and while it is not the goal of this thesis to discuss this problem in a complete manner, two opposing positions will be presented for clarification of the problem and its possible implications.

One account as presented in [31] describes physical models as "constructions" with respect to specific physical systems, which allow to approximate the relevant processes and phenomena with the apparatus of the mathematical theory. It is not essential and even impossible for these models to describe every aspect of the system accurately and thus to represent it completely. In fact initially simple models are augmented ad hoc with various corrections and additions to account for the observed phenomena. According to this perspective the merit of

quantum mechanics can be seen as the ability to provide an excellent framework for the creation and optimization of models, which allow for a sufficiently accurate mathematical treatment of physical systems. This, however, does not necessarily imply that the basic mathematical structures of quantum mechanics represent the physical reality.

An objection to this view is provided by the argument [32] that the mathematical theory of quantum mechanics is able to provide representational models for at least some quantum systems. Namely for example the "essentially probabilistic interdependence" of spin observables and the fact that they are "mutually transformable" is precisely captured by the Hilbert space formalism. It can be argued that at least in these specific cases the mathematical structure of quantum mechanics has physical significance and for the description of those systems the "full representational capacity of Hilbert spaces" is employed.

While there seem to exist good arguments for both positions, their discussion is not in the scope of this thesis. However, the presented notions, definitions and distinctions have been introduced to form a framework, in which the discussed elements of quantum mechanics can be fitted.

2.1.2. Hilbert Spaces

The following subsection discusses the first element of quantum mechanics, namely the mathematical structure of Hilbert spaces, which incorporates the internal principles of the quantum mechanical description.

Vector Space

A *Hilbert space* is defined as a *complex vector space* with an *inner product*, which is *complete* [29, 32]. Vector spaces are basic objects of linear algebra and consist of a set of elements called *vectors*, for which the basic operations *addition* and *multiplication by a complex scalar* are defined. Following the notation introduced by Dirac [29, 30] an element of the Hilbert space $\mathcal{H}$ is denoted by a *ket* as

$$|v\rangle \in \mathcal{H}. \tag{2.1}$$

The minimal number of elements needed to *span* a vector space, which is to construct all of its elements through linear combinations, is defined as its *dimension*. In general finite and infinite dimensional vector spaces share the same properties, except of certain restrictions to be observed in the infinite dimensional case [28–30, 32]. For example Hilbert spaces have to be restricted to complete vector spaces because of the existence of properly defined infinite dimensional vector spaces that are not complete in the mathematical sense. The most important distinctions between the two cases emerge in the definition of possible state spaces as well as in the description of quantum measurements and will be mentioned explicitly in the respective sections.

2. Fundemantals of Quantum Mechanics

In a Hilbert space $\mathcal{H}$ all linear combinations of its elements $\{|v_i\rangle\} \subset \mathcal{H}$ are again elements of the same vector space, so that

$$\sum_j c_j |v_j\rangle \in \mathcal{H} \tag{2.2}$$

with $c_i \in \mathbb{C}$ [29]. This property, which translates into the quantum mechanical superposition principle, has important consequences for the structure of physical systems described by quantum mechanics as will be presented below.

Inner Product

As mentioned above to form a Hilbert space from the vector space $\mathcal{V}$, it is necessary to define an inner product between the elements of the vector space. The inner product (v, w) between two vectors $|v\rangle$ and $|w\rangle$ is written as [28–30]

$$(v, w) := \langle v | \cdot | w \rangle := \langle v | w \rangle, \tag{2.3}$$

where the *bra* $\langle v|$ represents the element of the *dual space* corresponding to the ket $|v\rangle$.

The inner product is defined as a function $\mathcal{V} \otimes \mathcal{V} \to \mathbb{C}$ that satisfies three relations. It has to be *linear* in the second argument, a commutation of the elements has to be equivalent to a conjugation of the value, which together with (1) implies *antilinearity* in the first argument and finally it has to be positive semi-definite

$$\langle v | v \rangle \geq 0, \tag{2.4}$$

with $\langle v | v \rangle = 0$ if only if $v = 0$ [29].

Using the inner product it is possible to define two important properties of vectors. Two elements of a Hilbert space are *orthogonal* if and only if their inner product is 0 and the *norm* $\| |v\rangle \|$ of a vector can be consistently expressed as

$$\| |v\rangle \| = \sqrt{\langle v | v \rangle}. \tag{2.5}$$

This allows to *normalize* any non-zero vector $|v\rangle$ by dividing it by its norm with [28, 29]

$$|v_N\rangle := \frac{|v\rangle}{\| |v\rangle \|}. \tag{2.6}$$

Representation of Hilbert Spaces

Each element of a vector space can be expressed as a linear combination of *basis vectors*, which are defined as a *linearly independent spanning set* of that particular space [29]. An especially convenient type of bases are *orthonormal* bases, the

elements of which are all normalized and pairwise orthogonal. An arbitrary vector $|v\rangle$ can therefore be expanded in the orthonormal basis $\{|a_j\rangle\}$ as [28, 29]

$$|v\rangle = \sum_j c_j |a_j\rangle \tag{2.7}$$

Any element of a finite dimensional vector space is therefore uniquely specified by a set of coefficients $c_j \in \mathbb{C}$ with respect to some basis. In the infinite dimensional case the elements are represented by a function $f : \mathbb{R} \to \mathbb{C}$ of some continuous parameter α with respect to an orthonormal basis $\{|\alpha\rangle\}$ consisting of infinitely many elements labeled by the same parameter as [28, 32]

$$|w\rangle = \int f(\alpha)|\alpha\rangle \, \mathrm{d}\alpha \tag{2.8}$$

The complex numbers defining a vector can be expressed using the inner product as $c_j = \langle a_i|v\rangle$ and $f(\alpha) = \langle \alpha|v\rangle$ respectively. It should be noted that in the infinite dimensional case the basis is "orthonormalized in the Dirac sense" [28] which is defined as: $\langle \alpha|\alpha'\rangle = \delta(\alpha - \alpha')$.

Using the representation of vectors with orthonormal bases it is possible to write the inner product in terms of the coefficients $\{c_j\}$ and the function f [28]. For the two elements of a finite dimensional vector space $|v\rangle = \sum_j c_j|a_j\rangle$ and $|\tilde{v}\rangle = \sum_j \tilde{c}_j|a_j\rangle$ the inner product becomes

$$\langle v|\tilde{v}\rangle = \sum_{j,k} c_j^* \tilde{c}_k \langle a_j|a_k\rangle = \sum_{j,k} c_j^* \tilde{c}_k \delta_{jk} = \sum_j c_j^* \tilde{c}_j. \tag{2.9}$$

Analogously for two elements of a infinite dimensional vector space $|w\rangle = \int f(\alpha)|\alpha\rangle \, \mathrm{d}\alpha$ and $|\tilde{w}\rangle = \int \tilde{f}(\alpha)|\alpha\rangle \, \mathrm{d}\alpha$ the inner product can be written as [28, 30]

$$\langle w|\tilde{w}\rangle = \iint f^*(\alpha)\tilde{f}(\alpha')\langle \alpha|\alpha'\rangle \, \mathrm{d}\alpha \, \mathrm{d}\alpha' = \int f^*(\alpha)\tilde{f}(\alpha) \, \mathrm{d}\alpha. \tag{2.10}$$

2.1.3. Operators

Another crucial element of the quantum mechanical formalism are linear operators, which represent functional relations between the elements of Hilbert spaces as presented in the following subsection.

Linear Operators

Apart from the vectors itself another important class of objects are *linear operators* defined on a Hilbert space $\mathcal{H}$. They represent functions $\hat{A} : \mathcal{H} \to \mathcal{H}$ that are linear in their inputs as [29, 30]

$$\hat{A}\left(\sum_j c_j|a_j\rangle\right) = \sum_j c_j \hat{A}|a_j\rangle. \tag{2.11}$$

In the equation above the action of the operator was expressed as a multiplication on a ket from the left as $\hat{A}\left(|v\rangle\right) := \hat{A}|v\rangle$, which makes sense because the action of linear operators is associative and therefore $\hat{A}(\hat{B}\left(|v\rangle\right)) = \hat{A}\hat{B}|v\rangle$ [28–30]. It should be noted, however, that linear operators do not commute in general and therefore the *commutator* $[\hat{A}, \hat{B}] := \hat{A}\hat{B} - \hat{B}\hat{A}$ is in general non-zero. To consistently define the action of an operator on a bra from the right it is necessary to introduce the *adjoint* $\hat{A}^\dagger$ of an operator $\hat{A}$, which is uniquely defined via the dual space with [28–30]

$$|v'\rangle = \hat{A}|v\rangle \Leftrightarrow \langle v'| = \langle v|\hat{A}^\dagger. \tag{2.12}$$

Another important notation is the representation of a linear operator by an *outer product* written as $|v\rangle\langle w|$ [29, 30]. This expression constitutes a natural extension of the multiplicative notation and is a well defined linear operator on $\mathcal{H}$ created out of the vectors $|v\rangle, |w\rangle \in \mathcal{H}$. Its action on an arbitrary ket $|u\rangle$ from the left maps the latter on a multiple of the ket $|v\rangle$ and vice versa for an action on a bra from the right as [30]

$$|v\rangle\langle w| \cdot |u\rangle := |v\rangle \cdot \langle w|u\rangle = \langle w|u\rangle \cdot |v\rangle. \tag{2.13}$$

In the equation above, the dots are inserted just for clarity and are usually not written explicitly. Any linear combination of outer products is again a linear operator and for its adjoint it follows that [29, 30]

$$\left(\sum_j c_j |v_j\rangle\langle w_j|\right)^\dagger = \sum_j c_j^* |w_j\rangle\langle v_j|. \tag{2.14}$$

Using the outer product notation it is possible to formulate the *closure* [28] or *completeness relation* [29] for orthonormal bases, $\sum_j |a_j\rangle\langle a_j| = \mathbb{1}$ in the finite dimensional basis $\{a_i\}$ and respectively $\int |\alpha\rangle\langle\alpha|\, d\alpha = \mathbb{1}$ for basis $\{\alpha\}$ of an infinite dimensional vector space. The *unity operator* $\mathbb{1}$ is defined with $\mathbb{1}|v\rangle = |v\rangle$ for all $|v\rangle \in \mathcal{H}$. The closure relation corresponds to an expansion of the unity operator in terms of the respective basis, and just as it is possible to expand any vector with respect to a basis, representing it with a set of complex numbers or a complex valued function, any operator can be expressed as a *matrix* with complex entries relative to a certain basis. Operator $\hat{A}$ acting on a finite dimensional Hilbert space can be written as [28, 29]

$$\hat{A} = \sum_{jk} \langle a_j|\hat{A}|a_k\rangle |a_j\rangle\langle a_k| := \sum_{jk} A_{jk} |a_j\rangle\langle a_k| \tag{2.15}$$

and operator $\hat{B}$ defined for an infinite dimensional space as [28]

$$\hat{B} = \iint \langle\alpha|\hat{B}|\alpha'\rangle |\alpha\rangle\langle\alpha'|\, d\alpha\, d\alpha' := \iint B_{\alpha\alpha'} |\alpha\rangle\langle\alpha'|\, d\alpha\, d\alpha'. \tag{2.16}$$

The complex numbers $A_{jk} = \langle a_j|\hat{A}|a_k\rangle$ and $B_{\alpha\alpha'} = \langle\alpha|\hat{B}|\alpha'\rangle$ are called the *matrix elements* of the operators in the respective bases.

Eigenvectors and functions of operators

A concept that is especially relevant for quantum measurement are *eigenvectors* of an operator defined on the Hilbert space $\mathcal{H}$ and the corresponding *eigenspaces*. The action of an operator $\hat{A}$ on one of this operators eigenstates $|a\rangle$, preserves the state up to a multiplication with the factor $a \in \mathbb{C}$ called *eigenvalue*: [28–30]

$$\hat{A}|a\rangle = a|a\rangle \tag{2.17}$$

The ket representing the eigenvector is usually labeled with the same symbol as the corresponding eigenvalue. While the eigenvalue can have the value 0, the zero element of the Hilbert space is not considered an eigenvector. An eigenspace of operator $\hat{A}$ corresponding to a certain eigenvalue a is defined as the subspace of $\mathcal{H}$ spanned by all eigenvectors of $\hat{A}$ with that particular eigenvalue. If the dimensionality of an eigenspace is greater than one, the corresponding eigenvalue is called *degenerate* [29, 30]. In general, however, not every linear operator needs to have eigenvectors.

If there exists an orthonormal basis $\{|a_j\rangle\}$ of the relevant Hilbert space $\mathcal{H}$, consisting entirely of eigenvectors of some operator $\hat{A}$, this basis is denoted as this operators *eigenbasis*. In this basis the operator has a *diagonal* representation which means that it can be written in the form [29]

$$\hat{A} = \sum_j a_j |a_j\rangle\langle a_j| \tag{2.18}$$

and analogously in the infinite dimensional case.

Suitable functions with complex arguments, which can be expanded into series, can be generalized for linear operators. In agreement with the definitions presented so far it is natural to define $\hat{A}^n$ as a n-fold application of operator $\hat{A}$ and $\hat{A}^{-1}$ as its inverse application [28]. A function that can be expanded to the series $f(z) = \sum_n c_n z^n$ can then be defined for operators as [28, 30]

$$f(\hat{A}) = \sum_n c_n \hat{A}^n. \tag{2.19}$$

For an operator with a diagonal representation this expression can be further simplified employing the orthonormality of the basis elements $|a_j\rangle$ [28, 29]

$$f(\hat{A}) = \sum_n c_n \hat{A}^n = \sum_n c_n \left(\sum_j a_j^n |a_j\rangle\langle a_j| \right) = \sum_j f(a_j)|a_j\rangle\langle a_j|. \tag{2.20}$$

It should be noted that in the latter case the diagonal form is conserved by the function because the last expression in the equation above still represents a diagonal operator with the same eigenstates.

2. Fundemantals of Quantum Mechanics

Hermitian and Unitary Operators

Two types of linear operators should be mentioned explicitly because of their great importance in quantum mechanics, the *Hermitian* and *unitary* operators. Hermitian or *selfadjoint* operators $\hat{X}$ are defined by the relation $\hat{X} = \hat{X}^\dagger$ [29, 30]. This property has many consequences, the most important of which will be briefly mentioned. All eigenvalues of Hermitian operators are real and the corresponding eigenspaces are all orthogonal. For each potentially degenerate eigenspace, a decomposition into an orthonormal basis can always be found. Such a decomposition consequently consists of eigenvectors with the eigenvalue corresponding to that eigenspace. Therefore, each Hermitian operator has an eigenbasis in which it can be represented in diagonal form. The set of eigenvalues of a Hermitian operator is called its *spectrum*, the decomposition in the eigenbasis a *spectral decomposition* [28–30].

An important subtype of Hermitian operators are *projection operators* or *projectors*. The projector $\hat{\Pi}_W$ onto the subspace W of the Hilbert space $\mathcal{H}$ is defined as [29]

$$\hat{\Pi}_W := \sum_{j=1}^{k} |a_j\rangle\langle a_j|, \tag{2.21}$$

where $\{|a_1\rangle....|a_k\rangle\}$ is the subset of an orthonormal basis $\{|a_j\rangle\}$ of $\mathcal{H}$ spanning W. An important property of projection operators is idempotency $\hat{\Pi}^n = \hat{\Pi}$ with $n \in \mathbb{N}$.

The other fundamental type of operators, the unitary operators $\hat{U}$ are defined by the property $\hat{U}^\dagger \hat{U} = \mathbb{1}$ or equivalently by $\hat{U}^{-1} = \hat{U}^\dagger$ [29]. Just as Hermitian operators, unitary operators always have a spectral decomposition but their eigenvalues can in general be complex. All eigenvalues, however, have a modulus of 1 which means they can be written as $e^{i\theta}$ with a $\theta \in \mathbb{R}$ [29].

Unitary operators can be constructed from Hermitian operators with [28, 30]

$$\hat{U} = \exp\left(-i\alpha\hat{F}\right), \tag{2.22}$$

where $\hat{F}$ is a Hermitian operator and α a real parameter. For sufficiently small α the operator can be approximately expressed as an *infinitesimal* unitary operator with $\hat{U} \approx \mathbb{1} - i\alpha\hat{F}$ [28, 30].

Operators and Product Space

To complete the presentation of the basic mathematical structures of quantum mechanics a final aspect should be briefly mentioned, namely the composition of Hilbert spaces. The *product space* $\mathcal{H} = \mathcal{V} \otimes \mathcal{W}$ constructed out of the Hilbert spaces $\mathcal{V}$ and $\mathcal{W}$ with dimension m and n respectively is itself a Hilbert space with dimension $m \cdot n$ [28, 29]. Its elements are linear combinations of *tensor products*

of elements of the constituent spaces, $|v\rangle \otimes |w\rangle \in \mathcal{H}$ with $|v\rangle \in \mathcal{V}$ and $|w\rangle \in \mathcal{W}$. If $\{|a_j\rangle\}$ and $\{|b_k\rangle\}$ are orthonormal bases of $\mathcal{V}$ and $\mathcal{W}$ then $\{|a_j\rangle \otimes |b_k\rangle\}$ is an orthonormal basis of $\mathcal{H}$ containing $m \cdot n$ elements [28, 29].

It is possible to define linear operators acting on $\mathcal{H}$ using operators $\hat{A} : \mathcal{V} \rightarrow \mathcal{V}$ and $\hat{B} : \mathcal{W} \rightarrow \mathcal{W}$. The operator $\hat{A} \otimes \hat{B}$ acts on an arbitrary element $\sum_j a_j |v_j\rangle \otimes |w_j\rangle$ of $\mathcal{H}$ as [29]

$$\left(\hat{A} \otimes \hat{B}\right)\left(\sum_j a_j |v_j\rangle \otimes |w_j\rangle\right) := \sum a_j \hat{A}|v_j\rangle \otimes \hat{B}|w_j\rangle. \tag{2.23}$$

Any linear operator $\hat{C}$ acting on $\mathcal{H}$ can be expressed as a linear combination of such operator products $\hat{C} = \sum_j c_j \hat{A}_j \otimes \hat{B}_j$ the action of which is defined as [29]

$$\left(\sum_j c_j \hat{A}_j \otimes \hat{B}_j\right) |v\rangle \otimes |w\rangle := \sum_j c_j \hat{A}_j |v\rangle \otimes \hat{B}_j |w\rangle. \tag{2.24}$$

The definition of the inner product on $\mathcal{H}$, which is necessary for a Hilbert space is based on the inner products of the constituent spaces with

$$\left(\sum_j a_j |v_j\rangle \otimes |w_j\rangle, \sum_k b_k |v_k'\rangle \otimes |w_k'\rangle\right) = \sum_{j,k} a_j^* b_k \langle v_j | v_k'\rangle \langle w_j | w_k'\rangle. \tag{2.25}$$

From the inner product defined in this way the product space "inherits" the other structural elements presented above, as unitarity and Hermiticity [29].

2.2. Representation of physical systems

After the structure of Hilbert spaces has been summarized, the next sections describe how this mathematical formalism is applied to physical systems in quantum mechanics. As mentioned in section 2.1.1 the translation of physical systems into the mathematical formalism is governed by postulates that can be roughly separated into three groups, first, postulates about the representation of physical states, second, postulates about the representation of their evolution, and eventually, postulates about the nature of measurement. While the latter subject is discussed separately in more detail in chapter 3, the following subsections present the first two topics. Because there is no unique formulation of the postulates of quantum mechanics, which can be seen by comparing [28–30, 33], this thesis presents the propositions of the three groups of postulates in a summarized way as three single "postulates".

2.2.1. Physical States

The first step in the quantum mechanical representation of physical systems is the formulation of a suitable abstract space corresponding to the physical states. This subsection presents the principles which govern this representation.

Quantum State

The first type of postulates ascertains that a Hilbert space can be "associated" with "any isolated physical system" [29]. The system at a given time is then "completely described" by a *state vector* which is a normalized vector in the corresponding Hilbert space, which is then called a *state space* [28–30, 32]. Picking up the distinction presented in section 2.1.1 the Hilbert space, which describes a particular empirical system sufficiently well, would be considered to be the physical model for that system. While the postulates determine that the state of a physical system has to be represented as a state in a suitable state space they do not specify any rules for the creation of such models, which means that each system has to be modeled depending on its particular behavior [29, 31].

Because only normalized vectors are considered to represent physical states, it can be argued that the state really corresponds to the 1-dimensional subspace or *ray* of the Hilbert space spanned by that vector [30]. Therefore, the vectors $|v\rangle$ and $c|v\rangle$ with $c \neq 0$ correspond to the same physical state and whenever an operation on a system would result in a not normalized state, as for example in the case of a projective measurement, which is presented in chapter 3, the resulting state has to be renormalized to represent the system in a consistent way.

It follows from the structure of Hilbert spaces that any linear combination of states is itself an element of the state space, which constitutes the *superposition principle* of quantum mechanics. In particular this implies that it is possible

to expand any state into an orthonormal basis of the state space [28, 29]. For the states $|v\rangle = \sum_j c_j |a_j\rangle$ and $|w\rangle = \int f(\alpha)|\alpha\rangle \, d\alpha$, which are expanded with respect to the orthonormal bases $\{|a_j\rangle\}$ and $\{|\alpha\rangle\}$, respectively, the set of complex numbers $\{c_j\}$ are called the *amplitudes* of the basis elements and the complex valued function f is called the *wavefunction* of that state for the particular basis [29, 30]. In general, however, both notions are interchangeable to a certain extent.

An additional restriction of potential state spaces has to be made in the case of infinite dimensional systems. While any vector in a finite dimensional space can be normalized, in the infinite dimensional case there exist well defined states that cannot. Therefore, infinite dimensional physical systems can only be represented by states with wavefunctions that are *square integrable functions* denoted as L^2 in mathematics [28, 32]. Furthermore, it is postulated that physical systems always correspond to "sufficiently regular" wavefunctions that are among other things "everywhere defined, continuous and everywhere differentiable"[28]. The set of these functions, which is a subset of L^2, constitutes the space of vectors $\mathcal{F}$ that can represent physical states. $\mathcal{F}$ itself is a well defined Hilbert space and any infinite dimensional physical system has to be represented as a subspace of $\mathcal{F}$.

It should be noted however, that while the states mentioned above have to be elements of $\mathcal{F}$, it is still possible to expand them in a basis that does not fulfill that requirement. In particular there exist Hermitian operators $\hat{\alpha}$ defined on a Hilbert space $\tilde{\mathcal{F}} \subseteq \mathcal{F}$, as the position operator $\hat{x}$, which will be discussed later, with eigenbases $\{|\alpha\rangle\}$ that do not consist of elements of $\tilde{\mathcal{F}}$ or even of $\mathcal{F}$ [28, 32]. While such bases are well defined and satisfy the orthonormalization as well as the closure relation, the system can only be represented by certain linear combinations of the basis states that lie in $\tilde{\mathcal{F}}$ and for example never by a single element of the basis. Regardless of their intermediary status, however, such operators and the corresponding bases are very useful and constitute important elements of quantum mechanics.

Mixed States

Apart from the standard representation of physical states as vectors, the same states can be expressed by *density operators* in an equivalent way. The density operator $\hat{\rho}$ corresponding to a state $|\psi\rangle$ is defined as [28, 29]

$$\hat{\rho} := |\psi\rangle\langle\psi|. \tag{2.26}$$

Density operators are Hermitian by construction, possess only non-negative eigenvalues and have a normalized trace with $\text{tr}(\hat{\rho}) = 1$ [29, 30]. The latter requirement can be regarded as an equivalent to the normalization condition for state vectors.

The formalism of quantum mechanics presented so far can be fully reproduced using density operators but at the same time they allow the extension of the formalism towards a representation of states that usually cannot be expressed as

vectors. In the state vector formalism the only possible way to combine different quantum states of one system is a normalized linear combination and according to the superposition principle of quantum mechanics any such combination is again a physical state that describes the system completely. A scenario where the system is in a state of statistical uncertainty and the state of the system is consequently not completely known, can therefore not be expressed in the usual formalism [28–30, 32]. However, with the formulation of a suitable density operator $\hat{\rho}$ it is possible to consistently represent a system in such a state with [29, 30, 32]

$$\hat{\rho} := \sum_j P_j |\psi_j\rangle\langle\psi_j|. \tag{2.27}$$

In the above definition the states $\{\psi_j\} \in \mathcal{H}$ define a set of projectors $\{|\psi_j\rangle\langle\psi_j|\}$ with corresponding coefficients P_j that are normalized with $\sum_j P_j = 1$ and can be interpreted as probabilities as will be discussed in section 3.1.

In general an arbitrary density operator cannot be expressed as an outer product of a state vector as in eq. (2.26). States for which this is possible can effectively be represented as state vectors and describe the system completely [28]. Such states are denoted as *pure* states. If the state of a system can only be expressed as a density operator, this implies that the system is in a state of statistical uncertainty or *statistical mixture* and the corresponding state is called a *mixed state* [28, 29]. Just as the density operators of pure states, the ones of mixed states are Hermitian and have a trace of 1.

It should be noted that the description of the density operator as a representation of a statistical uncertainty is not unique [29, 32]. For a mixed state there exist infinite many representations as weighted sums of projectors as defined in eq. (2.27). The states $\{|\psi_j\rangle\}$ with probabilities P_j will generate the same density operator as the states $\{|\varphi_j\rangle\}$ with probabilities Q_j as long as they fulfill the relation [29]

$$\sqrt{P_j}|\psi_j\rangle = \sum_k u_{jk}\sqrt{Q_k}|\varphi_k\rangle, \tag{2.28}$$

where the numbers u_{jk} form a unitary matrix. For this relation to be well defined in the case where one of the sets has less elements than the other, it might be necessary to augment the former with suitable states that have probabilities of 0. This general undetermination of mixed density operators is called *unitary freedom* [29].

The proposition that the density operator corresponding to a mixed state is related to the probabilities of finding the system in different states is therefore always only true with respect to a certain decomposition into projectors. Only in the case of pure states it is possible to express the density operator uniquely by a state vector according to eq. (2.26). Consequently an "ignorance interpretation" which asserts that a mixed state simply describes a system that can be in one of certain pure states with respective probabilities is highly problematic and a mixed

state has to be considered as something fundamentally different from a pure state [29, 32]. This will be also made clear in the later discussion of coherence and interference.

Purity and Entropy

The density matrix of a pure state $\hat{\rho}_p$ is a projector and therefore idempotent, which implies that $\text{tr}\left(\hat{\rho}_p^2\right) = 1$ [28, 29]. In general, however, for a potentially mixed state $\hat{\rho}$ the relation changes to $\text{tr}\left(\hat{\rho}^2\right) \leq 1$. The expression is equal to 1 if and only if $\hat{\rho}$ is a pure state. For a mixed state $\hat{\rho}_m$ it holds that $\text{tr}\left(\hat{\rho}_m^2\right) < 1$ [28, 29]. The value $\text{tr}\left(\hat{\rho}^2\right)$, called *purity*, can therefore be used to quantify how mixed a state is. For the *maximally mixed state* in D dimensions, which is represented by the density matrix $\hat{\rho} = \mathbb{1}/D$, the minimal value of purity $1/D$ is achieved [2, 29, 33, 34].

Another measure for the statistical uncertainty of a state represented by a density operator $\hat{\rho}$ is the *von Neumann entropy* or simply *entropy* S which is defined as [29, 33–35]

$$S(\hat{\rho}) := -\text{tr}\left(\hat{\rho}\log\hat{\rho}\right). \tag{2.29}$$

This formulation of entropy is a generalization of the classical *Shannon Entropy* which is used in information theory to quantify the uncertainty of the probability distribution of random variables. While a pure state that is known with certainty has an entropy of 0, a maximally mixed state in a D-dimensional Hilbert space corresponds to an entropy of $\log D$.

Coherence and Interference

A crucial feature that distinguishes a superposition of states from a mixture is the emergence of *interference* effects [28]. The simplest example for that is the calculation of a norm of a potentially not normalized pure state $|\psi\rangle = c_1|\psi_1\rangle + c_2|\psi_2\rangle$ constructed from the normalized states $|\psi_1\rangle$ and $|\psi_2\rangle$ with

$$\|\psi\| = \sqrt{\langle\psi|\psi\rangle} = \sqrt{|c_1|^2 + |c_2|^2 + 2\text{Re}\left[c_1 c_2^* \langle\psi_1|\psi_2\rangle\right]}. \tag{2.30}$$

The value of the norm does not only depend on the moduli of the coefficients $\{c_j\}$ but also on their phase relation which is captured by the factor $c_1 c_2^*$ and on the inner product $\langle\psi_1|\psi_2\rangle$ of the two states. This dependence represents the interference of the two states [28, 36]. For example in the case $|\psi_1\rangle = |\psi_2\rangle$ with the coefficients $c_1 = -c_2$, state $|\psi\rangle$ would be the zero vector, which would correspond to fully destructive interference. It should be noted that the expression above could also be obtained by calculation of the trace of the density operator corresponding to this pure state with $\|\psi\| = \sqrt{\text{tr}\left(|\psi\rangle\langle\psi|\right)}$. The property of state superpositions, which entails the emergence of interference effects, is denoted as *coherence* [28].

Considering the same two states as a mixture $\hat{\rho} = P_1|\psi_1\rangle\langle\psi_1| + P_2|\psi_2\rangle\langle\psi_2|$ with probability coefficients $\{P_j\}$ and calculating the trace of the density operator yields the result

$$\sqrt{\text{tr}(\hat{\rho})} = \sqrt{P_1 + P_2}. \tag{2.31}$$

The lack of dependence on any parameters other than the two positive numbers P_1 and P_2 represents the fact that the two states $|\psi_1\rangle$ and $|\psi_2\rangle$ do not interfere in this case [28]. There is for example no possibility to adjust the parameters in a way to achieve any destructive interference even if $|\psi_1\rangle = |\psi_2\rangle$. Compositions of states that exhibit such behavior are therefore not coherent. Consequently the purity of a density operator can be used to quantify the coherence of a state or in other words its ability to produce interference effects.

Similarity of states

To conclude the presentation of the first group of postulates regarding the representation of physical states in quantum mechanics, this segment contains a brief remark about possible quantifications of state similarity. The two "most used, known and important" distance measures of states are *trace distance* and *fidelity* [29].

The trace distance D of two states expressed as the density operators $\hat{\rho}$ and $\hat{\sigma}$ is defined as [29, 35]

$$D(\hat{\rho}, \hat{\sigma}) := \frac{1}{2}\text{tr}\left(|\hat{\rho} - \hat{\sigma}|\right), \tag{2.32}$$

with $|\hat{A}| := \sqrt{\hat{A}^2}$ for Hermitian operators. The trace distance can take values in the interval $[0, 1]$ where a distance of 0 between two states indicates identity.

The most general definition of fidelity F also refers to states described by density matrices and can be written as [29, 35]

$$F(\hat{\rho}, \hat{\sigma}) := \text{tr}\left(\sqrt{\hat{\rho}^{1/2}\hat{\sigma}\hat{\rho}^{1/2}}\right). \tag{2.33}$$

Just as the trace distance the fidelity is symmetric in the arguments and has values in the interval $[0, 1]$. The fidelity of identical states is 1. If one of the two states is pure the fidelity simplifies to [29, 35]

$$F(|\psi\rangle, \hat{\rho}) = \sqrt{\langle\psi|\hat{\rho}|\psi\rangle} \tag{2.34}$$

and for two pure states to

$$F(|\psi\rangle, |\varphi\rangle) = |\langle\psi|\varphi\rangle|. \tag{2.35}$$

In general the two distances measures can be compared via the relation

$$1 - F(\hat{\rho}, \hat{\sigma}) \leq D(\hat{\rho}, \hat{\sigma}) \leq \sqrt{1 - F(\hat{\rho}, \hat{\sigma})^2}. \tag{2.36}$$

Only in the case when both states are pure, there exists an exact functional relationship between trace distance and fidelity with [37]

$$D = \sqrt{1 - F^2}. \tag{2.37}$$

This indicates that while the choice of an appropriate measure in general is not uniquely determined, trace distance and fidelity are at least "qualitatively equivalent measures for closeness of quantum states" [29].

2.2.2. Evolution of States

The first group of postulates as presented above, determine the proper manner to model the state of a physical system as a Hilbert space. The second group presented in the following subsection addresses the question of the systems evolution.

Unitary Transformation

Any evolution of a closed quantum system into a new state $|\psi'\rangle$ is represented by a unitary operator $\hat{U}$ acting on the initial quantum state $|\psi\rangle$ of the system with [28, 29]

$$|\psi'\rangle = \hat{U}|\psi\rangle. \tag{2.38}$$

The same evolution can be generalized to potentially mixed states expressed by density operators $\hat{\rho}$ and $\hat{\rho}'$ as [29]

$$\hat{\rho}' = \hat{U}\hat{\rho}\hat{U}^\dagger. \tag{2.39}$$

Thereby the unitarity of the evolution ensures the conservation of the normalization of the system state. It should be noted that the form of the evolution is determined solely by the unitary operator $\hat{U}$ and is therefore independent of the state of the system.

The evolution of a state in time is explicitly described by the *Schrödinger Equation* which can be written as [28–30]

$$i\hbar\frac{\mathrm{d}|\psi\rangle}{\mathrm{d}t} = \hat{H}|\psi\rangle, \tag{2.40}$$

where $\hbar$ is an empirical constant and $\hat{H}$ a Hermitian operator that uniquely determines the dynamical behaviour of the system. Because of its relation to the Hamiltonian of classical mechanics, $\hat{H}$ is denoted as the *Hamilton operator* or *Hamiltonian* [28, 29]. As already mentioned in section 2.1.1 the explicit form of the Hamiltonian is not determined by the postulates and alongside the definition of a suitable Hilbert space, the formulation of the correct Hamiltonian is a crucial and non-trivial element of the quantum mechanical description of a physical system [29, 30].

2. Fundemantals of Quantum Mechanics

Depending on the complexity of the Hamilton Operator general solutions of the Schrödinger equation can be given, which formulate a unitary operator $\hat{U}(t, t_0)$ that describes the evolution from a state $|\psi(t_0)\rangle$ at time t_0 into the state $|\psi(t)\rangle$ at time t with $|\psi(t)\rangle = \hat{U}(t, t_0)|\psi(t_0)\rangle$. In the most general case of an arbitrary time dependent Hamiltonian without any additional restrictions the unitary operator can be expressed as a *Dyson Series* with [30]

$$\hat{U}(t, t_0) = 1 + \sum_{n=1}^{\infty} \left(-\frac{i}{\hbar}\right)^n \int_{t_0}^{t} \mathrm{d}t_1 \int_{t_0}^{t_1} \mathrm{d}t_2 \cdots \int_{t_0}^{t_{n-1}} \mathrm{d}t_n \, \hat{H}(t_1)\hat{H}(t_2) \cdots \hat{H}(t_n). \tag{2.41}$$

If the Hamiltonians at different times commute this expression can be simplified to [30]

$$\hat{U}(t, t_0) = \exp\left(-\frac{i}{\hbar} \int_{t_0}^{t} \hat{H}(t') \, \mathrm{d}t'\right). \tag{2.42}$$

For a time independent Hamiltonian the solution of the Schrödinger equation can be written in the most simple form as [29, 30]

$$\hat{U}(t, t_0) = \exp\left(\frac{-i\hat{H}}{\hbar}(t - t_0)\right). \tag{2.43}$$

In reality, a physical system can be never completely separated from other systems but often it is possible to describe physical system as closed systems in good approximation. Furthermore, any not-closed system can be at least in principle expressed as part of larger system that evolves unitarily. Also often it is possible to capture the interaction with an outside system by a Hamiltonian that varies in time. In general, however, Hamiltonians of closed systems are time independent [29].

Translation

An example of evolution is the *translation* of a wavefunction $\psi(x) = \langle x|\psi\rangle$ of state $|\psi\rangle$ in a 1-dimensional continuous space expressed in the basis $\{|x\rangle\}$, which represents the position of the system and is the eigenbasis of the *position operator* $\hat{x}$. To constitute an infinitesimal translation of the wavefunction $\psi(x) \to \psi(x+\mathrm{d}x)$ by the amount $\mathrm{d}x$ the corresponding *translation operator* $\mathcal{T}(\mathrm{d}x)$ has to act on an arbitrary basis ket as $\mathcal{T}(\mathrm{d}x)|x\rangle = |x + \mathrm{d}x\rangle$ [30]. Furthermore, it has to fulfill typical requirements such as $\mathcal{T}(\mathrm{d}x)\mathcal{T}(\mathrm{d}x') = \mathcal{T}(\mathrm{d}x + \mathrm{d}x')$ and $\mathcal{T}(\mathrm{d}x)\mathcal{T}(-\mathrm{d}x) = \mathbb{1}$. Consequently an infinitesimal unitary translation operator can be represented as [28, 30]

$$\mathcal{T}(\mathrm{d}x) = \mathbb{1} - i\hat{k}\mathrm{d}x, \tag{2.44}$$

where $\hat{k}$ is a Hermitian operator that fulfills the commutation relation [28, 30]

$$\left[\hat{x}, \hat{k}\right] = i. \tag{2.45}$$

The operator $\hat{k}$ is called the *generator* of the translation and in analogy to classical mechanics the *momentum operator* $\hat{p}_x$ is defined with $\hat{p}_x := \hat{k}\hbar$ [30]. The commutator relation between $\hat{x}$ and $\hat{p}_x$ then becomes

$$[\hat{x}, \hat{p}_x] = i\hbar \tag{2.46}$$

which is called the *canoncial commutation relation* of quantum mechanics [30]. Relations of these type are typical for operators that are respective generators of translation. Another type of evolutions are rotations which correspond to another set of commutation relations and will be presented below.

A finite translation α can be expressed as a repetition of infinitesimal translations $\mathrm{d}x = \frac{\alpha}{N}$ for $N \to \infty$ with [30]

$$\mathcal{T}(\alpha) = \lim_{N\to\infty} \left(1 - \frac{i\hat{p}_x\alpha}{N\hbar}\right)^N = \exp\left(-\frac{i}{\hbar}\hat{p}_x\alpha\right). \tag{2.47}$$

The resulting unitary operator $\mathcal{T}$ can be understood as the solution of a Schrödinger equation with the Hamiltonian $\hat{H} := \hat{p}_x\frac{\alpha}{\Delta t}$ that is active for time Δt, which implies

$$\mathcal{T}(\alpha) = \exp\left(-\frac{i}{\hbar}\hat{H}\Delta t\right) = \exp\left(-\frac{i}{\hbar}\hat{p}_x\alpha\right). \tag{2.48}$$

If an interaction happens over a fixed time and the respective Hamiltonian is time independent, it is usually possible to incorporate the time parameter and all other constants into the Hamiltonian in this manner and therefore only write the final form of the evolution without explicit reference to the form of the Hamiltonian [29, 38].

Position and Momentum Operators

Because of the importance of the operators $\hat{x}$ and $\hat{p}$, some of their additional properties and relations should be presented in more detail. Both operators are Hermitian, have a non-degenerate eigenspectrum and therefore unique eigenbases $\{|x\rangle\}$ and $\{|p\rangle\}$. Employing the formulation of the minimal translation it is possible to express the actions of the two operators on a general quantum state $|\psi\rangle$ in each others eigenbases as [28, 30]

$$\langle x|\hat{p}|\psi\rangle = -i\hbar\frac{\partial}{\partial x}\langle x|\psi\rangle, \tag{2.49}$$

$$\langle p|\hat{x}|\psi\rangle = i\hbar\frac{\partial}{\partial p}\langle p|\psi\rangle. \tag{2.50}$$

Consequently the respective eigenstates can be represented in the other eigenbasis as [28, 30]

$$\langle x|p\rangle = \langle p|x\rangle^* = \frac{1}{\sqrt{2\pi\hbar}}\exp\left(\frac{i}{\hbar}px\right), \tag{2.51}$$

where the normalization factor $1/\sqrt{2\pi\hbar}$ can be obtained for example from the orthonormality condition $\langle x|x'\rangle = \delta(x - x')$. However, the wavefunction of state $|x\rangle$ in the eigenbasis of $\hat{p}$ can not be normalized and vice versa. The eigenstates of the position and momentum operators are therefore not possible physical states of a system that lie in $\tilde{\mathcal{F}}$ as presented in subsection 2.2.1.

The expression of $\langle x|p\rangle$ allows to formulate transformations between the wavefunctions $\psi(x) = \langle x|\psi\rangle$ and $\tilde{\psi}(p) = \langle p|\psi\rangle$ in the two bases with

$$\tilde{\psi}(p) = \frac{1}{\sqrt{2\pi\hbar}} \int_{-\infty}^{\infty} \exp\left(-\frac{ipx}{\hbar}\right) \psi(x)\,\mathrm{d}x, \tag{2.52}$$

$$\psi(x) = \frac{1}{\sqrt{2\pi\hbar}} \int_{-\infty}^{\infty} \exp\left(\frac{ipx}{\hbar}\right) \tilde{\psi}(p)\,\mathrm{d}p. \tag{2.53}$$

These transformations resemble Fourier Transforms and express, together with the other relations above, the symmetrical properties of the position and momentum operators [28, 30]. Just as the momentum operator is the generator of a shift in position, the position operator generates a momentum shift.

Rotation

Another basic and very important example of quantum evolution are *rotations* represented in a 2-dimensional quantum system. In analogy to the case of translation the quantum mechanical *angular momentum operator* is defined as the generator of rotations in real 3-dimensional space with $\vec{J} := (\hat{J}_x, \hat{J}_y, \hat{J}_z)^T$ [30]. An arbitrary infinitesimal rotation $\mathcal{D}(\mathrm{d}\phi)$ about angle $\mathrm{d}\phi$ around an axis $\vec{n}$ can then be expressed as [30]

$$\mathcal{D}(\mathrm{d}\phi) = \mathbb{1} - \frac{i}{\hbar}\left(\vec{J}\cdot\vec{n}\right)\mathrm{d}\phi. \tag{2.54}$$

A comparison of this formulation of rotation with the classical requirements and conditions for properly defined rotations yields the *fundamental commutation relations* of angular momentum [30]

$$\left[\hat{J}_j, \hat{J}_k\right] = i\hbar\epsilon_{jkm}\hat{J}_m, \tag{2.55}$$

where the indices $\{j, k, m\}$ represent the three dimensions denoted as x,y and z. Any group of operators, which represent rotations, has to fulfill these commutation relations.

While in real space the rotation operators $\mathcal{D}$ can be represented by the 3-dimensional $SO(3)$ group this structure is *locally isomorphic* to the 2-dimensional $SU(2)$ group in complex space. Therefore, it is possible to represent the corresponding generators of rotations in a two dimensional state space. Choosing the

states $|+\rangle_z := (1,0)^T$ and $|-\rangle_z := (0,1)^T$ as an orthonormal basis, which represents the positive and negative z-directions, the three corresponding rotation operators $\{\hat{S}_x, \hat{S}_y, \hat{S}_z\}$ can be expressed as [30]

$$\hat{S}_x = \frac{\hbar}{2}\sigma_x, \ \hat{S}_y = \frac{\hbar}{2}\sigma_y, \ \hat{S}_z = \frac{\hbar}{2}\sigma_z. \tag{2.56}$$

The matrices $\{\sigma_x, \sigma_y, \sigma_z\}$ are the Hermitian and unitary *Pauli matrices* that are defined as [29, 30]

$$\sigma_x := \begin{pmatrix} 0 & 1 \\ 1 & 0 \end{pmatrix}, \ \sigma_y := \begin{pmatrix} 0 & -i \\ i & 0 \end{pmatrix}, \ \sigma_z := \begin{pmatrix} 1 & 0 \\ 0 & -1 \end{pmatrix}. \tag{2.57}$$

With the additional bases $|\pm\rangle_x := \frac{1}{\sqrt{2}}\left(|+\rangle_z \pm |-\rangle_z\right)$ and $|\pm\rangle_y := \frac{1}{\sqrt{2}}\left(|+\rangle_z \pm i|-\rangle_z\right)$ corresponding to the x- and y-directions, it is possible to consistently represent the rotation group and all directions in 3-dimensional space as superpositions of states from one of these 2-dimensional bases [30]. An example of such a representation will be given in chapter 4 in the context of the qubit model for polarization.

2.2.3. Composite Systems

Another important aspect of the representation of physical states in quantum mechanics is the manner in which a composition of quantum systems can be expressed formally. In this context the important notion of entanglement is introduced as well.

Product States

The rule for the formal expression of composite systems is part of the postulates about the correct representation of physical systems. It can be stated as follows: "The state space of composite physical system" is equivalent to the "tensor product of the state spaces of the component physical systems" [29]. For a composite system made out of the subsystems 1 to n, with respective pure states $|\psi_1\rangle, |\psi_2\rangle, \ldots |\psi_n\rangle$, the overall state can be written as $|\psi_1\rangle \otimes |\psi_2\rangle \otimes \cdots \otimes |\psi_n\rangle$ [29].

As presented in subsection 2.1.2 all linear operators acting on the composite system, including unitary evolutions, can then be formulated as linear combinations of products of component operators acting only on the component systems. This "multiplicity of states" corresponds to different degrees of freedom of the composite system [28]. For example a photon can have a continuous degree of freedom $\mathcal{H}_1$, which can be expressed in the position or the momentum bases and a 2-dimensional polarization degree of freedom $\mathcal{H}_2$, which constitute the composite system "photon" $\mathcal{H}_1 \otimes \mathcal{H}_2$. Alternatively, the different degrees of freedom, which form the composite quantum system, can also belong to completely different particles.

Entanglement

In general not all possible states of composite systems can be expressed as tensor products of component states. States where the latter is possible are called *separable states* and states that are not product states are denoted as *entangled* states [29, 35, 39]. While a separable state corresponds to a simple "juxtaposition" of two systems, which can be in principle described and measured independently, the entanglement of two systems implies *correlations* between them [28, 35]. These correlations are generally introduced by the interaction of the systems and are crucial for quantum measurement which will be discussed in section section 3.1.

The state of a subsystem A, which is part of a larger composite system C represented by a product space $\mathcal{H}_C = \mathcal{H}_A \otimes \mathcal{H}_B$, can be expressed by performing a *partial trace* on the density operator $\hat{\rho}_C$ representing the state of the total system [29]. The state $\hat{\rho}_A$ of system A can be written as

$$\hat{\rho}_A := \operatorname{tr}_B\left(\hat{\rho}_C\right). \tag{2.58}$$

The partial trace tr_B over subsystem B is defined by its action on an operator expressed by the arbitrary states $\{|a_j\rangle, |a_j'\rangle\} \subset \mathcal{H}_A$ and $\{|b_j\rangle, |b_j'\rangle\} \subset \mathcal{H}_B$ with [29]

$$\operatorname{tr}_B\left(\sum_j \alpha_j |a_j\rangle\langle a_j'| \otimes |b_j\rangle\langle b_j'|\right) := \sum_j \alpha_j |a_j\rangle\langle a_j'| \operatorname{tr}\left(|b_j\rangle\langle b_j'|\right). \tag{2.59}$$

All information that is available when considering only the isolated subsystem is correctly represented by this reduced density operator [29, 36].

If the composite system is in an entangled state, the result of a partial trace is always a mixed state in the subsystems. This implies that while a composite system can be in a pure state that describes the system completely from the perspective of quantum mechanics, the composite systems can be in states of statistical mixture and thus not completely known. In these cases the description of the composite system contains "more information" in form of correlations than the separate descriptions of the subsystems [29, 32, 33].

Bipartite Entanglement Measures

To complete the discussion of entanglement the general approach of entanglement quantification is presented. However, this description is restricted to entanglement of just two systems which is denoted as *bipartite* entanglement in contrast to *multipartite* entanglement, which represents correlations between an arbitrary number of systems [33, 34, 39, 40]. Another simplification stems from the restriction to pure composite states. While in general also mixed product states can exhibit some entanglement and are in principle also interesting in the context of weak values, they do not fall in the scope of this thesis with the small exception of

weak tomography. In the case of mixed bipartite states, and even more so in the case of multipartite states, the relations and definitions of entanglement measures are problematic. For pure bipartite states, however, it is possible to formulate relatively simple and straightforward quantifications of entanglement [33, 39, 40].

The most basic approach to evaluate entanglement is the *Schmidt decomposition*. For any pure bipartite state $|\psi\rangle \in \mathcal{H} = \mathcal{H}_A \otimes \mathcal{H}_B$ there exist orthonormal bases $\{|a_j\rangle\} \subset \mathcal{H}_A$ and $\{|b_j\rangle\} \subset \mathcal{H}_B$ of the respective constituent spaces, which constitute a decomposition of $|\psi\rangle$ in with [29, 34, 35, 39, 40]

$$|\psi\rangle = \sum_j \lambda_j |a_j\rangle |b_j\rangle, \tag{2.60}$$

where the coefficients $\{\lambda_j\}$ are real and non-negative numbers that are called *Schmidt Coefficients*. The amount of non-zero Schmidt Coefficients is defined as the *Schmidt number*. The Schmidt decomposition corresponds to a simultaneous diagonalization of the reduced denstity operators $\hat{\rho}_A$ and $\hat{\rho}_B$ of the component systems which can be consequently written as [29, 34, 39, 40]

$$\hat{\rho}_A = \mathrm{tr}_B \left(|\psi\rangle\langle\psi| \right) = \sum_j \lambda_j^2 |a_j\rangle\langle a_j| \tag{2.61}$$

for system A and symmetrically for system B. Therefore, the component states are pure and the composite state separable if and only if the Schmidt Number is 1 [39].

Based on the relation of the degree of entanglement in the composite system and the amount of mixture in the composite systems, it is possible to gradually quantify the entanglement by relying on the quantifications of statistical uncertainty in the subsystems. The *concurrence* of an entangled state $|\psi\rangle_{AB}$ with $\hat{\rho}_{AB} = |\psi\rangle\langle\psi|$ is directly related to the purity $P = \mathrm{tr}\left(\mathrm{tr}_B\left(\hat{\rho}_{AB}\right)^2\right)$ of the reduced states as [39, 40]

$$C(|\psi\rangle) = \sqrt{\frac{D}{D-1}(1-P)}. \tag{2.62}$$

The above expression for the concurrence is normalized so that it ranges from 0 for a separable state to 1 for a maximally entangled state, where $D \geq 2$ is the dimension of the respective subsystem.

Another convenient measure is the *entropy of entanglement*, which is simply equal to the von Neumann entropy of the reduced states and ranges from 0 to $\log D$ for maximally entangled states [33, 34, 39]. Both the concurrence and the entropy of entanglement are monotonic functions of the degree of entanglement and can therefore be used consistently for its quantification. The entanglement of potentially mixed composite systems can be measured employing different measures as the *entanglement of formation*, *distillable entanglement* or *negativity*, which all simplify to the entropy of entanglement for pure bipartite states [34, 39].

3. Quantum Measurement

In this chapter the concept of weak measurement is introduced after a discussion of the standard description of the measurement process in quantum mechanics. Thereby, the representation of general quantum measurements as interactions between physical system constitutes the foundation for an account of weak values. The latter are introduced in section 3.2, which can be regarded to some extent as the central part of the thesis, as it contains the most of important definitions relevant in the field of weak values. As an illustration of the presented concepts, the diverse types of measurements are graphically compared in the final section of the chapter.

3.1. Standard Quantum Measurement

The following section presents the standard quantum theory of measurement. Apart from an overview of the fundamental description of measurement, another important aspect is the definition of measurement strength, which can be used to quantify measurements in general and which therefore represents a reference for the definition of weak measurements.

3.1.1. Measurement Postulate

As a basis for a more detailed discussion of the quantum mechanical measurement process in this subsection the third group of postulates is introduced.

Observables and Projective Measurements

According to the measurement postulates of quantum mechanics, all physical properties are based on *observables*, which are represented by Hermitian operators acting on the state space of a quantum system [28–30, 33]. The eigenvalues of these measurement operators represent the possible outcomes of quantum measurements. The expression of physical quantities by appropriate operators is the third fundamental task for the quantum mechanical description of physical systems, alongside a definition of a suitable Hilbert space and the formulation of the correct Hamiltonian. It should be noted that in this work the measurement operator itself is denoted as the "observable" in accordance with the definition of the notion as given in [29, 30].

3. Quantum Measurement

Because of the restriction of possible measurement outcomes to eigenvalues of linear operators, measurements in finite dimensional Hilbert spaces are necessarily quantized and can yield only a discrete set of results [28, 32]. The Hermiticity of the operators representing observables ensures that all outcomes are real and can therefore be interpreted meaningfully as values of the corresponding physical quantity. Furthermore, instead of stating the observable explicitly it is just possible to state that a measurement is conducted in an orthonormal basis, where a certain real value a_j is attributed to each basis state $|a_j\rangle$, which consequently implies the diagonal form of a Hermitian operator $\hat{A}$ with [29, 33]

$$\hat{A} = \sum_j a_j |a_j\rangle\langle a_j|. \tag{3.1}$$

This operator constructed out of the projectors $\{|a_j\rangle\langle a_j|\}$ represents the relevant observable of that measurement. The ideal form of quantum measurement expressed by such a set of orthogonal projectors is denoted as a *projective measurement* [29].

Probabilistic Interpretation

The crucial feature that is introduced by the standard measurement postulates of quantum mechanics is a fundamental indeterminacy of the quantum mechanical description of physical reality in the process of measurement. In general an arbitrary state of the system $|\psi\rangle$ is not an eigenstate of an observable $\hat{A}$, but rather a linear superposition of such orthonormal basis states $\{|a_j\rangle\}$ with $|\psi\rangle = \sum_j c_j |a_j\rangle$. In such a case it is not possible to predict the outcome of a measurement of $\hat{A}$ but only to specify probabilities P_j for each result a_j associated with state $|a_j\rangle$ as [29, 30, 41]

$$P_j := |\langle a_j|\psi\rangle|^2 = |c_j|^2. \tag{3.2}$$

In the continuous case with basis $\{|\alpha\rangle\}$ the amplitudes c_j are replaced by the wavefunction ψ with $\psi(\alpha) = \langle\alpha|\psi\rangle$. The squared modulus of this wavefunction then corresponds to a probability density in continuous state space for state $|\alpha\rangle$ or in other words the probability $P(\alpha, \alpha + d\alpha)$ of finding the system in the infinitesimal state interval between $|\alpha\rangle$ and $|\alpha + d\alpha\rangle$ is given by $|\psi(\alpha)|^2 d\alpha$ [28, 30, 41]. These measurement probabilities can be generalized to potentially mixed states represented by density operators $\hat{\rho}$ as [26, 28]

$$P_j = \langle a_j|\hat{\rho}|a_j\rangle = \operatorname{tr}(\hat{\rho}|a_j\rangle\langle a_j|). \tag{3.3}$$

Therefore, the usual interpretation of the amplitudes c_j and the wavefunction $\psi(\alpha)$ in quantum mechanics is a *probabilistic interpretation*. From this perspective, the meaning of these quantities is understood as a foundation for the calculation

of probabilities of certain measurement outcomes. In this context the normalization condition for quantum states ensures the consistent normalization of these distributions. While for a system in an eigenstate of the measured observable the result of the measuremet can be predicted with certainty, it is an implication of the superposition principle of quantum mechanics that there exist states for which the measurement is inherently indeterministic [32]. This uncertainty is distinct from the statistical uncertainty expressed by the density operator of a mixed state, which has its origin in an incomplete description of the system. The indeterminism of quantum measurement persists even if the system is completely described by a pure state vector [28, 32, 42].

The meaning of the quantum wavefunction beyond a probabilistic interpretation is still unclear and actively discussed in the scientific community [3, 42]. For the remainder of this thesis, however, it suffices to acknowledge the probabilistic character of the quantum mechanical description of measurement and treat the wavefunction simply as a mathematical tool for the description of physical systems without deciding on its ontological status.

Reduction of States

Closely associated to the projective theory of measurement is the postulate of the *reduction of the wavefunction* [41]. It states that after a certain eigenvalue of a measurement observable has been measured the system "jumps" into the corresponding eigenstate. This "collapse" of the wavefunction does not refer to some contingent backaction of a physical measuring device, which destroys or at least disturbs the system in the measurement process, as for example a photon detector that annihilates a photon. Instead it describes the fundamental effect that any potential interaction of the system with a measuring device necessarily must have to extract the relevant information about the quantum state [26, 28, 29, 41].

For a potentially degenerate eigenvalue a_j of observable $\hat{A}$ with the corresponding eigenspace $\mathcal{H}_j$, which is spanned by the orthonormal basis $\{|a_j^k\rangle\}$ labeled by the additional index k, the state $|\psi'\rangle$ of the system after an ideal projective measurement that yielded the value a_j, can be expressed as [29, 30, 33]

$$|\psi'\rangle = \frac{\hat{\Pi}_j|\psi\rangle}{\sqrt{\langle\psi|\hat{\Pi}_j|\psi\rangle}}, \tag{3.4}$$

where $|\psi\rangle$ denotes the initial state of the system and $\hat{\Pi}_j = \sum_k |a_j^k\rangle\langle a_j^k|$ the projector into the eigenspace corresponding to the eigenvalue. Because in general the initial state contains elements that are orthogonal to this eigenspace and which are consequently removed, the state after the projection $\hat{\Pi}_j|\psi\rangle$ is not normalized and the denominator is necessary because it is unequal to 1. This loss of normalization entails that the transformation $|\psi\rangle \to |\psi'\rangle$ caused by the measurement is in general non-unitary [29].

The definition of the post measurement state can be generalized to initially mixed states described by the density operator $\hat{\rho}$ with [26, 29, 35]

$$\hat{\rho}' = \frac{\hat{\Pi}_j \hat{\rho} \hat{\Pi}_j}{\mathrm{tr}\left(\hat{\Pi}_j \hat{\rho}\right)}. \tag{3.5}$$

It should be noted that for continuous observables with eigenbases which do not consist of normalizable states as the position operator $\hat{x}$ presented in subsection 2.2.2, measurements with projections onto a eigenstate are impossible because they would entail a collapse into a state which cannot be normalized. Therefore, in the case of such continuous observables the measurements must always consist in a projection on an interval of eigenstates [28, 30, 32].

In the standard interpretation this third postulate introduces a distinct kind of quantum evolution by measurement. Other than the essentially reversible and deterministic unitary evolution of quantum systems governed by the Schrödinger equation, the evolution implied by the collapse of the wavefunction is fundamentally irreversible and indeterministic [28, 32, 41, 43]. It is experimentally demonstrated [44] that the evolution of a physical system can be driven and influenced by repeated measurements, which is denoted as the *quantum Zeno effect* [45]. However, the relation between measurement and unitary evolution is still a highly debated topic in quantum physics. The introduction of the postulate of reduction into quantum mechanics is denoted as the "measurement problem" [2], which is highlighted again in subsection 3.1.2 after the concept of indirect measurement is presented.

Expectation Value

Because of the indeterministic quality of quantum measurements it is in general impossible to infer the wavefunction of the quantum state by a single measurement. In fact the only information that can be gained by measuring an outcome a_j for the measurement of state $|\psi\rangle$ is that the wavefunction $\psi_j = \langle a_j|\psi\rangle$ at the corresponding eigenstate $|a_j\rangle$ is non-zero [41]. To measure the complete wavefunction of a quantum state it is necessary to conduct a number of measurements on an *ensemble* of quantum systems prepared in the same initial state ψ [28, 30, 41]. However, such a repeated measurement of one observable yields only the probability distribution, which is the squared modulus of the wavefunction. The relative frequencies of measuring the outcome a_j corresponding to the state $|a_j\rangle$ approximate the probabilites $P_j = |\langle a_j|\psi\rangle|^2$ of finding the system in state $|a_j\rangle$ for a sufficiently high number of measurements. To gain information about the relative phases of the measured eigenstates, other observables have to be measured as well. The procedure of complete state determination is called "quantum state tomography" and is discussed in chapter 4.

If the wavefunction or at least the probability distribution of a state with respect to the eigenstates of some observable is known, it is possible to calculate the *expectation value E* of an observable $\hat{A} = \sum_j a_j \hat{\Pi}_j$ which is defined as [28, 29]

$$E_\psi(\hat{A}) := \sum_j a_j P_j^\psi = \langle \psi | \hat{A} | \psi \rangle \tag{3.6}$$

for pure states $|\psi\rangle = \sum_j c_j |a_j\rangle$ and the probabilities $P_j^\psi = |\langle a_j | \psi \rangle|^2 = |c_j|^2$. The expectation value corresponds to the statistical mean value of the measurement and is not necessarily equal to a possible outcome of the measurement [28, 30]. In quantum mechanics the expectation $E_\psi(\hat{A})$ is written as $\langle \hat{A} \rangle_\Psi$ or simply as $\langle \hat{A} \rangle$ if it is clear with respect to which state $|\psi\rangle$ the observable $\hat{A}$ is being evaluated.

The expectation value can be generalized to potentially mixed states represented by the density operator $\hat{\rho}$ with [28, 29, 33]

$$\langle \hat{A} \rangle_{\hat{\rho}} := \mathrm{tr}\left(\hat{\rho} \hat{A} \right) \tag{3.7}$$

where the ordering of the operators is insignificant because of the cyclicity of the trace operation.

Along with a mean value it is also possible to define the statistical *variance* $\mathrm{Var}(\hat{A})$ of some state $|\psi\rangle$ with respect to an observable $\hat{A}$ as [28, 29, 33]

$$\mathrm{Var}(\hat{A}) := \langle (\hat{A} - \langle \hat{A} \rangle)^2 \rangle = \langle \hat{A}^2 \rangle - \langle \hat{A} \rangle^2, \tag{3.8}$$

where the expectation values are calculated in relation to $|\psi\rangle$. Based on the variance, the *standard deviation* ΔA is defined as $\Delta A := \mathrm{Var}(\hat{A})^{\frac{1}{2}}$ [28, 29, 33]. A standard deviation of 0 corresponds to the case where the state of the system is an eigenstate of the observable and therefore the outcome of the measurement can be predicted with certainty.

Compatibility and Complementarity

The presentation of the standard measurement postulate of quantum mechanics is completed by the discussion of successive measurements of different observables. Because an ideal measurement consists of projections into the respective eigenspaces of observables, the properties of such successive measurements are determined by the relation between the eigenspaces of the relevant observables. It can be shown that two observables $\hat{A}$ and $\hat{B}$ can have a common eigenbasis if and only if they commute, thus if $[\hat{A}, \hat{B}] = 0$. Commuting obervables that can be simultaneously diagonalized are denoted as *compatible* [28–30].

If observables do not commute, there exists at least one eigenstate $|a_j^k\rangle$ of $\hat{A}$ that is not an eigenstate of $\hat{B}$ and which consequently has to be written as super-position of basis states of $\hat{B}$ [30]. If a measurement of observable $\hat{A}$, which yields

the result a_j and leaves the system in state $|\psi_j\rangle$ with $\langle a_j^k|\psi_j\rangle \neq 0$, is succeeded by a measurement of observable $\hat{B}$, the resulting state after that second measurement may contain components that are not in the subspace corresponding to the eigenvalue a_j. Therefore, measurements of non-commuting observables may disturb each other, which means that the information about the state gained by one measurement may become incomplete after the second measurement because the system evolves into a different state that has again an undetermined value with respect to the first observable [30].

While for non-compatible observables successive measurements might disturb the system with respect to previous measurements, this relation is extreme for *complementary* observables [36]. If $\hat{A}$ and $\hat{B}$ are complementary, then each eigenstate of $\hat{A}$ is an superposition of all possible eigenstates of $\hat{B}$ with equal probability amplitudes and vice versa. After an ideal measurement of one of the observables the outcome of a measurement of the second is thus maximally indetermined. All sets of "dynamical variables", which are generators of translations or rotations in each others eigenspaces, have this complementary relation [36]. The principle of complementarity implies that, in quantum mechanics contrary to classical physics, it is impossible to acquire simultaneous knowledge about the outcomes of all possible measurements [36, 41].

The fundamental uncertainty of states with respect to non-compatible observables $\hat{A}$ and $\hat{B}$ is expressed formally in the *Heisenberg uncertainty relation* [29]

$$\Delta A \Delta B \geq \frac{\left|\langle [\hat{A}, \hat{B}] \rangle\right|}{2}, \tag{3.9}$$

where the standard deviations on the left hand side as well as the expectation value on the right hand side are both evaluated with respect to the same state of the system. A special case of the uncertainty relation can be formulated for the complementary observables $\hat{x}$ and $\hat{p}_x$ already mentioned is section 2.1, the commutator of which is a constant. In this case the uncertainty relation has the form [28, 30, 41]

$$\Delta x \Delta p \geq \frac{\hbar}{2}. \tag{3.10}$$

This reflects the fact that a more precise knowledge of the position $\hat{x}$, which is reflected by a small deviation Δx, entails a greater uncertainty Δp in momentum.

3.1.2. Indirect Measurement

The fundamental description of the measurement process via the respective postulates can be refined by a more detailed account of the interaction between the measurement apparatus and the measured system as presented below.

Interaction

In practice the process of projective measurement is usually accompanied not only by a collapse of the system into an eigenspace of the measurement operator but also by a much greater and more complicated transformation of the system [41]. For example the detection of a photon with an initially extensive wavefunction in some small region interval, usually annihilates the photon, transforming the relatively simple quantum system of the particle into the complex system of the detection environment. This direct interaction of the system of interest or *object system* with some complicated detection device, which might induce other evolutions than the intended reduction of the system into the eigenspace of the measurement outcome, is denoted as a *direct measurement* [41].

To realize a measurement, which better reproduces the theoretical description of projective measurement, the concept of *indirect measurement* is introduced, where prior to the measurement inducing the collapse, the object system interacts with an ancillary system called *pointer system* [29, 33, 41]. Because of resulting entanglement between the two systems a projective measurement on the pointer system, which potentially destroys the latter, causes the object system to be reduced into a certain post measurement state as well. Any unintended backaction on the object system by the measurement device, however, can be avoided using this approach because a direct measurement is only performed on the pointer system [41].

In principle any unitary evolution $\hat{U}_{XY}$ acting on the systems X and Y, which cannot be expressed as a product evolution $\hat{U}_P$ of the form $\hat{U}_P = \hat{U}_A \otimes \hat{U}_B$, with operators $\hat{U}_A$ and $\hat{U}_B$ acting only on the respective subsystems, introduces some change in the correlation of the two systems [36, 39]. Such a non-product evolution is therefore denoted as an *interaction* of the two systems. An indirect measurement is realized by a simple and fundamental form of interaction $\hat{U}_\alpha$ already introduced by von Neumann in 1932 [43], which can be written as [29, 41, 46, 47]

$$\hat{U}_\alpha := \exp\left(-\frac{i}{\hbar}\alpha\hat{A} \otimes \hat{p}\right) \tag{3.11}$$

where $\hat{A}$ is the measured observable acting on the object system, α a constant parameter of the measurement and $\hat{p}$ a generator of evolution acting on the pointer system. The evolution operator $\hat{U}_\alpha$ can be seen as corresponding to the time independent interaction Hamiltonian $\hat{H} := \frac{\alpha}{\Delta t}\hat{A} \otimes \hat{p}_q$, which is active for a time of Δt [38, 48]. The other parts of the overall Hamiltonian containing the separate evolutions of the two subsystems are not relevant for the measurement and can be neglected without the loss of generality [26]. It should be noted than in this work the interaction observable $\hat{A}$ is taken to be dimensionless and its dimension is incorporated into the interaction parameter α as proposed in [49].

Correlation

The usual scenario for an ideal indirect measurement begins with a finite dimensional object system that is initially in the state $|\psi_0\rangle = \sum_j c_j |a_j\rangle$, where the basis $\{|a_j\rangle\}$ is the non-degenerate eigenbasis of the observable $\hat{A}$. Before the interaction the overall state $|I\rangle$ is a separable state that can be written as

$$|I\rangle = |\psi_0\rangle \otimes |\Phi_0\rangle, \tag{3.12}$$

with $|\Phi_0\rangle$ as the initial state of the pointer system, which is initially completely uncorrelated to the object system [28]. This composite state is subsequently transformed by the interaction operator $\hat{U}_\alpha$ into the correlated state $|C\rangle$ with [2, 28, 50]

$$
\begin{aligned}
|C\rangle = \hat{U}_\alpha |I\rangle &= \exp\left(-\frac{i}{\hbar}\alpha\hat{A}\otimes\hat{p}\right)\left(\sum_j c_j |a_j\rangle\right)\otimes|\Phi_0\rangle \\
&= \sum_j c_j |a_j\rangle \otimes \left(\exp\left(-\frac{i}{\hbar}\alpha a_j \hat{p}\right)|\Phi_0\rangle\right) = \sum_j c_j |a_j\rangle \otimes |\Phi_{\alpha a_j}\rangle,
\end{aligned}
\tag{3.13}
$$

where $|\Phi_\lambda\rangle := e^{-\frac{i}{\hbar}\lambda\hat{p}}|\Phi_0\rangle$ denotes the pointer state that is shifted or rotated by the amount λ. If the states $|\Phi_{\alpha a_j}\rangle$ are pairwise orthogonal this interaction results in a perfect correlation between pointer and object system states, which represents the ideal form of an indirect measurement interaction [35, 41].

In the case of such a correlation the probability $P_{\alpha a_j}^\Phi$ to measure the outcome corresponding to projective measurement on the pointer system represented by the projector $\Pi_{\alpha a_j}^\Phi = \mathbb{1}\otimes|\Phi_{\alpha a_j}\rangle\langle\Phi_{\alpha a_j}|$ is given by

$$P_{\alpha a_j}^\Phi = \langle C|\Pi_{\alpha a_j}^\Phi|C\rangle = |c_j|^2, \tag{3.14}$$

which is exactly the same as the probability of measuring the value a_j with a projective measurement directly on the object system in the initial state [26]. Furthermore, the state of the composite system $|C'\rangle$ after the measurement on the pointer system is

$$|C'\rangle = \frac{\Pi_{\alpha a_j}^\Phi|C\rangle}{\langle C|\Pi_{\alpha a_j}^\Phi|C\rangle} = e^{i\varphi}|a_j\rangle\otimes|\Phi_{\alpha a_j}\rangle \tag{3.15}$$

with some global phase φ that is of no relevance. This is again a separable state and the object system after measurement is reduced into the state $|a_j\rangle$, which is exactly the final state to be expected after a direct measurement of the value a_j on the object system.

For an observable $\hat{A}$ with potentially degenerate eigenvalues the situation is more or less the same with the difference that the relevant projectors project

onto potentially multidimensional subspaces and not necessarily onto single states. In any case for an indirect measurement to reproduce a direct measurement of observable $\hat{A}$, the pointer system needs to have a dimension that is equal to or higher than the number of distinct eigenvalues of $\hat{A}$. Only then it is possible for the respective eigenspaces to be correlated with pairwise orthogonal pointer states.

Distinguishability and Coherence

The procedure of indirect measurement can in principle be divided into two parts, the interaction that creates the correlations between object and pointer system and the subsequent direct measurement of the pointer system [7, 43, 50, 51]. The interaction by itself does not constitute a quantum measurement in the standard sense because it represents a deterministic and reversible unitary evolution. Instead of being measured, the eigenstates of the measurement operator only become *distinguishable* because of the correlation with orthogonal pointer states. This distinguishability, however, causes a loss of coherence in the object system [33, 36]. As a subsystem of a maximally entangled bipartite system the object system by itself is in a maximally mixed state and thus incoherent.

Because the interaction without a projective measurement, which would cause a reduction of the wavefunction, is reversible, it is possible to fully remove the introduced distinguishability and recover the coherence of the object system [36]. This can be either done by simply removing the correlation with a suitable unitary transformation, or by carrying out a suitable projective measurement on the pointer system that is symmetrical with respect to the orthogonal pointer states correlated with the object system states of interest. The entanglement of the two system is consequently removed and the composite system reduced to a separable state with the object system in its initial state.

Continuing the notation introduced in the previous subsections the correlated state $|C\rangle$ can be expressed as

$$|C\rangle = \sum_j c_j |a_j\rangle \otimes |\Phi_{\alpha a_j}\rangle. \tag{3.16}$$

A symmetric projective measurement on the pointer system expressed by the operator $\mathbb{1} \otimes |\Phi_s\rangle\langle\Phi_s|$ with $|\Phi_s\rangle = \frac{1}{\sqrt{N}} \sum_j |\Phi_{\alpha a_j}\rangle$, where N is the number of non-zero coefficients c_j, leaves the bipartite system in the state

$$(\mathbb{1} \otimes |\Phi_s\rangle\langle\Phi_s|) |C\rangle = \frac{1}{\sqrt{N}} \left(\sum_j c_j |a_j\rangle \right) \otimes |\Phi_s\rangle, \tag{3.17}$$

which is a separable state with the object system in the initial coherent pure state.

A *quantum erasure*, where the distinguishability is annuled by a unitary evolution, has been experimentally realized [51] employing single photon pairs in a

superposition state of two possible paths as a two dimensional which-path object system. The pointer systems used to *mark* a certain path of the photon pair making the paths dinstinguishable, were polarization and time delay between the photons of one pair. Amongst other things, it was demonstrated that even marking only one of the photons of a pair in one path resulted in a loss of interference between the two path states for both photons. Successive gradual removal of this dinstinguishability recovered the interference gradually, confirming the assertion of complementarity between dinstinguishabity and the ability to interfere.

Alternative to Measurement Postulate

The formulation of the measurement process via the entanglement of object and pointer system allows a new perspective on the measurement postulates of quantum mechanics. The question arises whether it is not possible to describe the irreversible and indeterminstic reduction of the wavefunction in terms of a reversible and deterministic unitary evolution described by the second group of postulates [2, 29]. In this context the physical universe as a whole, could be seen as a closed system that evolves only unitarily and all other effects as statistical uncertainty and collapsing wavefunctions would be effects of the description of reduced subsystems without the complete information about the global composite pure state.

In general any quantum measurement can be described via entanglement of the object system with some pointer system, on which the actual measurement is carried out. However, the latter measurement could in principle itself again be described as an interaction of the pointer with another pointer that carries the correlation forward. Therefore, the whole process of the measurement of some object system by an observer could be in principle expressed as such a chain of entangling interactions [43]. Nevertheless at some point some sort of collapse has to be introduced to account for the fact that in the end a definitive outcome of the measurement is observed. Thus, to conform with the observation of defined measurements results it seems necessary to "divide the world in two parts", namely a set of quantum systems, which evolve according to the Schrödinger equation and an observer system, which causes an indeterministic collapse of the overall superposition state into a definitive measurement value [2, 43]. While the existence of such a "borderline" is strongly implied by the postulates, it appears that the chain of entangled systems can in principle be extended arbitrarily close to the observer and thus there exists no definite distinction between the unitarily evolving quantum systems and the irreversible measurement process [41, 43].

The meaning of the collapse and its relation to the entanglement between various physical system is still very much debated. It is unclear if it is possible to replace the measurement postulates and the notion of collapse by a fully unitary description [2, 28, 29]. While some accounts tend to dismiss the fundamentality

of indeterministic and irreversible evolution [50, 52], others point to the problem of definitive outcomes as a yet insurmountable obstacle [2].

3.1.3. Measurement Strength

Based on the preceding discussion of quantum mechanical measurements, it is possible to introduce a quantification of measurements, according to their ability to provide precise information about the state of the object system.

Non-Ideal Measurements

In principle there are two distinct ways in which an indirect measurement can diverge from the ideal case. In one case the interaction does not create full one to one correlations between orthogonal object and pointer system states and in the other case the measurement of the pointer system is not an ideal projective measurement. The latter is a contingent property of the direct measurement of the pointer and usually depends on the technical realisation of the measurement process. The imperfection of correlations, however, is a fundamental feature of the measurement interaction, which crucially influences the coherence of the state of the object system. This discussion, therefore focusses on the modification of measurements resulting from properties of the interaction.

Continuing with state $|C\rangle$ after the interaction from eq. (3.13), which can be written as

$$|C\rangle = \sum_j c_j |a_j\rangle \otimes |\Phi_{\alpha a_j}\rangle, \tag{3.18}$$

it is now assumed that the states $\{|\Phi_{\alpha a_j}\rangle\}$ are potentially non-orthogonal states. A projective measurement on the pointer with the projector $\Pi^\Phi_{\alpha a_m} = \mathbb{1} \otimes |\Phi_{\alpha a_m}\rangle\langle\Phi_{\alpha a_m}|$ leaves the composite system in the final state

$$\Pi^\Phi_{\alpha a_m} |C\rangle = \sum_j c_j \langle\Phi_{\alpha a_m}|\Phi_{\alpha a_j}\rangle |a_j\rangle \otimes |\Phi_{\alpha a_m}\rangle. \tag{3.19}$$

This result corresponds to the action of the operator $\sum_j \langle\Phi_{\alpha a_m}|\Phi_{\alpha a_j}\rangle |a_j\rangle\langle a_j|$ on the object system in its initial state.

The action of such an operator is an instance of a *positive operator-valued measure* or *POVM* measurement, which represent a generalization of the measurement postulates to cases where the measurements cannot be described by projective measurements [29, 35, 41, 53, 54]. Contrary to a standard projective measurement, a POVM measurement is not necessarily defined by a set of orthogonal projectors, but instead by a set of operators $\{\hat{E}_j\}$, which fulfill the normalization condition $\sum_j \hat{E}_j = \mathbb{1}$ and have the form $\hat{E}_j = \hat{M}_j^\dagger \hat{M}_j$ with arbitrary operators $\hat{M}_j$. For the initial state $|\psi\rangle$ the probability P_j of measuring the value associated with

operator $\hat{E}_j$ can be written as $P_j = \langle\psi|\hat{M}_j^\dagger\hat{M}_j|\psi\rangle = \langle E_j\rangle$ and the reduced state $|\psi'\rangle$ after the measurement becomes [29, 33]

$$|\psi'\rangle = \frac{\hat{M}_j|\psi\rangle}{\langle\hat{E}_j\rangle}. \tag{3.20}$$

The overlap expressions $\langle\Phi_{\alpha a_j}|\Phi_{\alpha a_m}\rangle$ from eq. (3.19) quantify how strongly the eigenstates of the measurement observable are correlated with the outcomes of pointer measurements and thus the amount of information gained by a POVM measurement of the type presented above. The information is maximized when the states $\{|\Phi_{\alpha a_j}\rangle\}$ are pairwise orthogonal, which, however, also entails a maximal distortion of the initial state with a full collapse into an eigenstate of the observable [41, 47, 55]. In the other extreme case, all states $\{|\Phi_{\alpha a_j}\rangle\}$ are the same and the composite system is effectively in a separable state without any correlations. While in the latter case no information about the initial state is gained by the measurement, there is also no distortion and the reduced post measurement state resembles exactly the initial one [29, 41, 56, 57].

Quantification of Interaction Strength

The concept of non-ideal measurements, which depends on the amount of correlations between the object system and pointer, allows the definition of measurement *strength* corresponding to the strength of the measurement interaction [26, 46]. A *strong* interaction is defined as an interaction that creates perfect one to one correlations between the eigenstates of a measurement operator $\hat{A}$ and orthogonal states $\{|\Phi_{\alpha a_j}\rangle\}$ of the pointer system. For *weaker* interaction this condition is not fully realized with no correlation for an interaction of zero strength. To gradually assess the strength or respectively the *weakness* of an interaction subsequently a definition of interaction strength is proposed, which depends on the interaction parameter α, the relation of the initial object state $|\psi\rangle$ to the observable $\hat{A}$ and the relation of the initial pointer state $|\Phi_0\rangle$ to the generator $\hat{p}$ for an interaction defined as in eq. (3.11).

For a D-dimensional object system with the totally symmetric initial state $|\psi_S\rangle = \frac{1}{\sqrt{D}}\sum_j|a_j\rangle$ the interaction leaves the composite system in the state

$$|C\rangle = \frac{1}{\sqrt{D}}\sum_j|a_j\rangle\otimes|\Phi_{\alpha a_j}\rangle. \tag{3.21}$$

Tracing out the pointer system yields the potentially mixed state $\hat{\rho}_C$ of the object system after the interaction

$$
\begin{aligned}
\hat{\rho}_C &= \frac{1}{D}\mathrm{tr}_\Phi\left(\sum_{j,m}|a_j\rangle\langle a_m|\otimes|\Phi_{\alpha a_j}\rangle\langle\Phi_{\alpha a_m}|\right)\\
&= \frac{1}{D}\sum_{j,m}|a_j\rangle\langle a_m|\mathrm{tr}\left(|\Phi_{\alpha a_j}\rangle\langle\Phi_{\alpha a_m}|\right)\\
&= \frac{1}{D}\sum_{j,m}|a_j\rangle\langle a_m|\langle\Phi_{\alpha a_m}|\Phi_{\alpha a_j}\rangle.
\end{aligned}
\tag{3.22}
$$

As presented in subsection 2.2.3, there is a gradual relation between the statistical uncertainty of state $\hat{\rho}_C$ and the degree of correlation in state $|C\rangle$. Therefore, to evaluate the latter it is instructive to calculate the former.

The purity P of $\hat{\rho}_C$ can be written as

$$
P = \mathrm{tr}\left(\hat{\rho}_C^2\right) = \frac{1}{D^2}\sum_{j,m}\left|\langle\Phi_{\alpha a_m}|\Phi_{\alpha a_j}\rangle\right|^2,
\tag{3.23}
$$

which implies a measure for the interaction strength S, which is equal to the normalized concurrence with

$$
S = \sqrt{\frac{D}{D-1}\left(1-\frac{1}{D^2}\sum_{j,m}\left|\langle e^{-\frac{i}{\hbar}\alpha(a_j-a_m)\hat{p}}\rangle\right|^2\right)},
\tag{3.24}
$$

where the expectation value is taken with respect to the initial pointer state $|\Phi_0\rangle$ and the overlap has been written explicitly as

$$
\langle\Phi_{\alpha a_m}|\Phi_{\alpha a_j}\rangle = \langle\Phi_0|e^{\frac{i}{\hbar}\alpha a_m\hat{p}}e^{-\frac{i}{\hbar}\alpha a_j\hat{p}}|\Phi_0\rangle = \langle e^{-\frac{i}{\hbar}\alpha(a_j-a_m)\hat{p}}\rangle.
\tag{3.25}
$$

The minimal value of $S=0$ is achieved for no interaction when $\langle\Phi_{\alpha a_m}|\Phi_{\alpha a_j}\rangle = 1$ and the maximal value $S=1$ corresponds to a strong interaction with $\langle\Phi_{\alpha a_m}|\Phi_{\alpha a_j}\rangle = \delta_{jm}$.

Condition for Weakness

For a weak interaction, no significant decoherence is introduced into a initially pure object system, which requires that the purity after the interaction is still close to 1 [26, 27, 55, 58]. This will always be realized when the interaction parameter α is sufficiently small and can thus be replaced by the small parameter

ϵ. The purity P from eq. (3.23) can in this case be expanded in orders of ϵ around 0 which yields

$$P \approx \frac{1}{D^2} \sum_{j,m} \left| 1 - i\frac{\epsilon}{\hbar}(a_m - a_j)\langle \hat{p} \rangle - \frac{\epsilon^2}{2\hbar^2}(a_m - a_j)^2 \langle \hat{p}^2 \rangle \right|^2$$

$$\approx \frac{1}{D^2} \sum_{j,m} \left(1 - (a_j^2 + a_m^2 - 2a_j a_m)(\langle \hat{p}^2 \rangle - \langle \hat{p} \rangle^2)\frac{\epsilon^2}{\hbar^2} \right) \qquad (3.26)$$

$$= 1 - 2(\Delta A_S)^2 (\Delta p)^2 \frac{\epsilon^2}{\hbar^2},$$

where the expectation values $\langle \hat{A}^n \rangle_S = \frac{1}{D} \sum_j a_j^n$ are calculated with respect to the initial symmetric state $|\psi_S\rangle$, which also implies the standard deviation ΔA_S.

This result can easily be generalized for any state $|\psi\rangle$ and the corresponding $\Delta \hat{A}$. The choice of the symmetrical initial state $|\psi_S\rangle$ for the definition of the interaction strength is simply motivated by the aim to give a general definition of interaction strength, which is not dependent on the specific initial state of the object system. The state $|\psi_S\rangle$ can form a maximally entangled state with the pointer system as defined in [39] and is therefore maximally sensitive to a distortion by the interaction. Consequently it is most suitable to evaluate the maximal amount of correlations introduced by the interaction.

For the preservation of purity, and therefore, for minimal disturbance of the object state, the expression above implies

$$\epsilon \, \Delta p \ll \frac{\hbar}{\sqrt{2} \, \Delta A} \qquad (3.27)$$

as the defining condition for a weak interaction, which represents an upper bound for the product of ϵ and Δp, also defined in [49]. It should be noted that for this approximate condition it is assumed that factors for the terms of higher order of ϵ are not too large and can therefore be safely neglected. As various experiments show, this is a valid assumption for the relevant pointers and interactions.

In practice there exist two distinct manners, in which a weak interaction can be achieved. In accordance with eq. (3.27) either the interaction parameter ϵ or the generator uncertainty Δp of the initial pointer state is reduced. The former can be regarded as a "weakening at the separation stage" of the procedure and the latter as "weakening at the recording stage" [59]. The condition is of course meaningless if at least one of the standard deviations ΔA and Δp vanishes, which corresponds to the case where either the object system is in an eigenstate of $\hat{A}$ or the pointer is in an eigenstate of $\hat{p}$. In both cases the interaction does not create any correlations independent of the magnitude of the interaction parameter ϵ. While in the case of $\Delta A = 0$, where the object system is in an eigenstate of $\hat{A}$, the pointer might get shifted significantly, this interaction, however, does not disturb the object state in any way and is not suitable to extract any information from it.

Measurement with Weak Interaction

After establishing a criterion for a weak interaction, it remains to assess how much information can be gained by a measurement involving an interaction of this type. Because of the principle of complementarity there is an upper bound for information, which can be gained given a certain disturbance of the system [60]. In the following the resulting pointer state after a weak interaction $\hat{\rho}_F$ is analyzed together with the possible information, which can be gained by a strong measurement of this pointer with respect to the observable $\hat{q}$.

The reduced pointer state $\hat{\rho}_F$ after the interaction can be written as [61]

$$\hat{\rho}_F = \mathrm{tr}_A\left(|C\rangle\langle C|\right) = \sum_j |c_j|^2|\Phi_{\epsilon a_j}\rangle\langle\Phi_{\epsilon a_j}|, \tag{3.28}$$

where $|C\rangle$ is the composite state after the interaction defined in eq. (3.13). For this state the expectation value of observable $\hat{q}$ becomes

$$\begin{aligned}
\mathrm{tr}\left(\hat{\rho}_F\hat{q}\right) &= \sum_j |c_j|^2\langle\Phi_{\epsilon a_j}|\hat{q}|\Phi_{\epsilon a_j}\rangle = \sum_j |c_j|^2\langle e^{\frac{i}{\hbar}\epsilon a_j\hat{p}}\hat{q}e^{-\frac{i}{\hbar}\epsilon a_j\hat{p}}\rangle \\
&\approx \sum_j |c_j|^2\left(\langle\hat{q}\rangle + \frac{\epsilon}{\hbar}a_j\mathrm{Im}\left[\langle[\hat{q},\hat{p}]\rangle\right]\right) \\
&= \langle\hat{q}\rangle + \frac{\epsilon}{\hbar}\langle\hat{A}\rangle\mathrm{Im}\left[\langle[\hat{q},\hat{p}]\rangle\right]
\end{aligned} \tag{3.29}$$

in the limit of small ϵ as described in [26]. All expectation values are taken with respect to the initial state of object and pointer system with $q_0 := \langle\hat{q}\rangle$. Therefore, for a sufficiently weak interaction there exists a linear relation between the pointer shift $\delta q := \mathrm{tr}\left(\hat{\rho}_F\hat{q}\right) - q_0$ and the expectation value $\langle\hat{A}\rangle$ of the object system.

In the case of a pointer measurement in position space with $\hat{q} = \hat{x}$ and the generator $\hat{p}$ is the corresponding momentum operator $\hat{p}_x$, the shift in eq. (3.29) can be calculated without approximation. As described in subsection 2.2.2 the position expectation value of the shifted pointer state $|\Phi_{\epsilon a_j}\rangle$ can then be written explicitly as $\langle\hat{x}\rangle = \epsilon a_j + x_0$. The approximate solution above is therefore shown to be exact for position and momentum operators with the commutator $[\hat{x},\hat{p}_x] = i\hbar$ [27]. In the latter case, the exact shift in the mean value of the pointer becomes

$$\delta x = \epsilon\langle\hat{A}\rangle. \tag{3.30}$$

While this result is valid for all interaction strengths, for a sufficiently weak interaction, any non-commuting pair of interaction and measurement operators $\hat{q}$ and $\hat{p}$ produces approximately the same linear shift as calculated above [26].

The possibility to accurately measure a pointer shift δx of the magnitude $\epsilon|\langle\hat{A}\rangle|$ depends on the uncertainty Δx of the pointer state. To resolve a shift δx of the wavefunction with a single measurement it is required that [26]

$$\delta x = \epsilon|\langle\hat{A}\rangle| \gg \Delta x. \tag{3.31}$$

However, the weak interaction condition eq. (3.27), requires exactly the opposite as can be seen when it is evaluated for a pointer state that approximately saturates the uncertainty relation with $\Delta x \, \Delta p_x \approx \frac{\hbar}{2}$. In this case it can be written as

$$\epsilon \Delta A \ll \frac{\hbar}{\sqrt{2}\Delta p_x} \approx \sqrt{2}\Delta x. \tag{3.32}$$

As long as the magnitude of the expectation value $|\langle \hat{A} \rangle|$ does not significantly exceed the standard deviation ΔA, a single measurement of the pointer system, which satisfies the condition of weakness, will not yield the expectation value with good precision. In fact it is the non-vanishing position uncertainty and the corresponding finite momentum uncertainty that allow a weak interaction in the first place.

To measure the expectation value with precision even in the case of a weak interaction, it is therefore necessary to repeat the pointer measurement on an ensemble of many identical systems [9, 58, 62]. With a signal to noise ratio ("SNR") that scales with $\frac{1}{\sqrt{N}}$, where N is the number of pointer measurements, it is possible to express the minimal number of events N_0, which are necessary to resolve a pointer shift of δx given a standard deviation of Δx as [26, 27, 37, 46]

$$N_0 \approx \left(\frac{\Delta x}{\delta x} \right)^2 = \left(\frac{\Delta x}{\epsilon \langle \hat{A} \rangle} \right)^2. \tag{3.33}$$

This requirement limits the suitability of measurements with weak interaction for cases in which only a small ensemble of object systems is available.

Weakly Disturbed Pointer

Apart from the expectation value, it is also possible to make general claims about the probability distribution $P(x)$ of the pointer. The probability density can be written as

$$P(x) = \langle x | \hat{\rho}_F | x \rangle = \sum_j |c_j|^2 \left| \langle x | \Phi_{\epsilon a_j} \rangle \right|^2. \tag{3.34}$$

This can be expanded in orders of ϵ to obtain an approximate expression for the probability distribution of the pointer after the interaction as

$$\begin{aligned} P_x &\approx \sum_j |c_j|^2 \left| \langle x | \left(1 - i\frac{\epsilon}{\hbar} a_j \hat{p}_x \right) | \Phi_0 \rangle \right|^2 \\ &\approx \sum_j |c_j|^2 \left(|\langle x | \Phi_0 \rangle|^2 + 2\frac{\epsilon}{\hbar} a_j \mathrm{Im} \left[\langle x | \hat{p}_x | \Phi_0 \rangle \langle \Phi_0 | x \rangle \right] \right) \\ &= |\langle x | \Phi_0 \rangle|^2 + 2\frac{\epsilon}{\hbar} \langle \hat{A} \rangle \mathrm{Im} \left[\langle x | \hat{p}_x | \Phi_0 \rangle \langle \Phi_0 | x \rangle \right] \\ &\approx \left| \langle x | \left(1 - i\frac{\epsilon}{\hbar} \langle \hat{A} \rangle \hat{p}_x \right) | \Phi_0 \rangle \right|^2 \approx |\langle x | \Phi_{\epsilon \hat{A}} \rangle|^2, \end{aligned} \tag{3.35}$$

as long as $\mathrm{Im}\left[\langle x|\hat{p}_x|\Phi_0\rangle\langle\Phi_0|x\rangle\right] = -\hbar\left(\frac{\partial}{\partial x}\langle x|\Phi_0\rangle\right)\langle\Phi_0|x\rangle$ is non-vanishing. Therefore, at least for a class of pointer distributions, the probability distribution after the interaction resembles approximately the original distribution shifted by the expectation value $\langle\hat{A}\rangle$ [27]. For example this is realized in the case of a Gaussian pointer as introduced in subsection 3.3.

In conclusion, there exists a range of ϵ, where the object system is minimally disturbed by the interaction, where the pointer system is just shifted without a significant change in the shape of the probability distribution and it is still possible to measure the expectation value, which is proportional to the amount the pointer shift. For a strong measurement with orthogonal pointer states corresponding to different eigenvalues of the measured observable, it is possible to estimate the probability of each eigenvalue separately by measuring the relative frequencies of each outcome. The eigenstates are *resolved* and the expectation value is calculated as a sum of the eigenvalues, weighted with the corresponding probabilities. In the case of a weak interaction, the particular pointer states overlap almost completely and it is therefore impossible to measure the explicit form of the probability distribution of the object state [4, 9, 21, 26, 63]. However, as shown above, it is still possible to obtain the expectation values in a direct way. In a certain sense this resembles the case where the object system is initially in an eigenstate of observable $\hat{A}$ and the pointer system is consequently only shifted proportionally to the eigenvalue without changing its shape [27]. This property of weak interactions emerges again in the context of weak measurements, which are discussed in the next section.

3.2. Weak Measurements

Based on the standard description of quantum measurement, this central section deals with the theoretical formulation of the complex field of weak measurements. After the concept of weak values is introduced, its relation to the measurement process is discussed in more detail.

3.2.1. Weak Value

In the following paragraphs the concept of weak values is defined in relation to an account of the procedure of pre- and postselected measurements. Eventually the distinctions between the various types of measurements are presented in the final part of this subsection.

Postselection

Contrary to a standard quantum measurement where the probability distribution of an initial state is determined with respect to a certain observable, in *postselected* measurements the additional condition of successful projection of the measured state into a specific final state is introduced. This final state is denoted as the postselection state and the initial state as the *preselection* state. The measurement is conducted as an initially standard indirect measurement with an object system that interacts with a pointer system. After the interaction, a direct projective measurement of the object system is carried out and the corresponding pointer state is only considered as a relevant outcome if the direct measurement on the object system yields the outcome associated with the specified postselection state. When this procedure is carried out on an ensemble of identical preselected sates, the postselection effectively represents a filtering process, where only a certain subensemble of the initial systems is considered [11, 26, 46].

The procedure of a pre- and postselected ("PPS") measurement as illustrated in Fig. 3.1 can be formally expressed in the following way. For a preselection on the initial state $|\psi_I\rangle = \sum_j c_j |a_j\rangle$, the initial pointer state $|\Phi_0\rangle$ and an indirect measurement of observable $\hat{A}$ with eigenbasis $\{|a_j\rangle\}$, the composite state $|C\rangle$ after the interaction becomes

$$|C\rangle = \sum_j c_j \left(|a_j\rangle \otimes |\Phi_{\alpha a_j}\rangle \right) \tag{3.36}$$

as already presented in section 3.1. Applying a pure projective postselection $\hat{\Pi}_F = |\psi_F\rangle\langle\psi_F|$ with the final state $|\psi_F\rangle = \sum_j d_j |a_j\rangle$, yields the final composite state $|F\rangle$ with

$$|F\rangle = \mathcal{N}\,\hat{\Pi}_F |C\rangle = \mathcal{N}|\psi_F\rangle \otimes \left(\sum_j c_j d_j^* |\Phi_{\alpha a_j}\rangle \right), \tag{3.37}$$
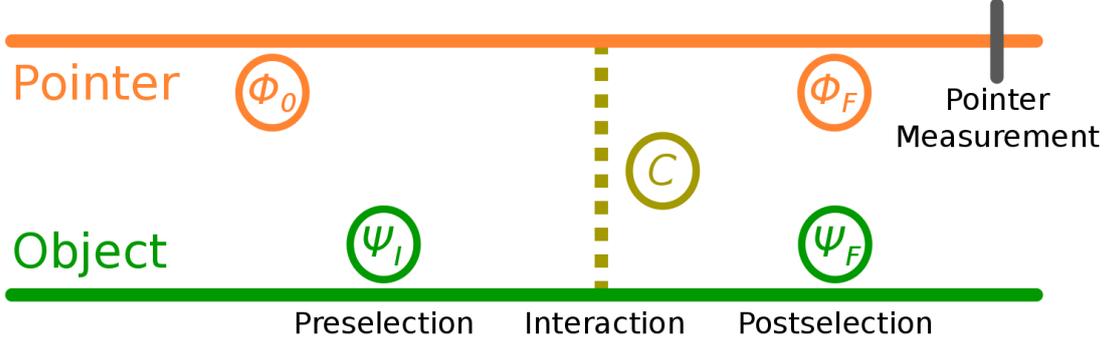
Figure 3.1.: Scheme for a PPS measurement. The pointer system is initially in state $|\Phi_0\rangle$ and the object system is prepared in state $|\psi_I\rangle$, which constitutes the preselection. Subsequently the systems interact and become correlated forming the entangled state $|C\rangle$. After the interaction the object system is projected into its final postselection state $|\psi_F\rangle$, which separates the two systems again. Eventually a direct measurement of the final pointer state $|\Phi_F\rangle$ is performed.

which is a separable state. The factor $\mathcal{N}$ represents a suitable normalization coefficient, which is necessary because of the filtering effect of the postselection. A direct measurement of the final pointer state $|\Phi_F\rangle = \sum_j c_j d_j^* |\Phi_{\alpha a_j}\rangle$ yields what is considered to be the outcome of the PPS measurement.

Conditioned Probability

While the notion of a conditioned probability for measurement outcomes is not defined in standard quantum measurement theory, there exist several approaches to interpret a PPS measurement as conditioned measurement and to formulate a probability of a quantum measurement under the condition of a certain postselection in analogy to Bayes theorem [26, 35, 53, 56, 58, 61, 64]. According to the latter the conditioned probability $P(A|B)$ of event A under condition B can be expressed as $P(A|B) = \frac{P(A \cap B)}{P(B)}$, where $P(A \cap B)$ is the joint probability of A and B and $P(B)$ the unconditioned probability of B.

In the account of ABL the joint probability of measuring outcome a_j with a projective measurement on the object system and of successful postselection onto $|\Phi_F\rangle$ is given by $|\langle\psi_F|\hat{\Pi}_j|\psi_I\rangle|^2$, where $\hat{\Pi}_j$ is the projector on the corresponding eigenspace and $|\psi_I\rangle$ the initial state of the system. The unconditioned probability of successful postselection is the sum of all joined probabilities with respect to a decomposition of unity into the set of projectors $\{\hat{\Pi}_m\} \ni \hat{\Pi}_j$ as $\sum_m |\langle\psi_F|\hat{\Pi}_m|\psi_I\rangle|^2$. Therefore, the probability P_j^{IF} of measuring outcome a_j conditioned on the pre- and postselection given above becomes

$$P_j^{IF} = \frac{|\langle\psi_F|\hat{\Pi}_j|\psi_I\rangle|^2}{\sum_m |\langle\psi_F|\hat{\Pi}_m|\psi_I\rangle|^2}, \qquad (3.38)$$

which is known as the *ABL formula* or *ABL rule* for conditioned probabilities [26, 27, 65–68].

The probability calculated via the ABL formula is well defined in the sense that it takes real values from the interval $[0, 1]$ and is furthermore normalized to unity if the conditioned probabilities over all measurements $\{\hat{\Pi}_j\}$ are summed, with [26]

$$\sum_j P_j^{IF} = 1. \tag{3.39}$$

However, as will be elaborated in section 5.1, the ABL probability is context dependent. For different projector decompositions of unity, which all contain $\hat{\Pi}_j$, the numerator stays the same while the value of the denominator may vary. Therefore, the conditional probability of outcome a_j calculated by the ABL rule depends in general on the other eigenspaces of the observable that is measured. In the case of non-projective measurements, this formula can be extended to incorporate POVM operators instead of projectors as discussed in [57].

Another approach to conditioned probabilities as presented in [64] defines the concept of a "conditioned expectation value". Unlike in the ABL rule, the joint probability is calculated as the expectation value of the the product of the projectors $\hat{\Pi}_j$ and $\hat{\Pi}_F$ with respect to the initial state. The resulting expression $\langle\psi_I|\hat{\Pi}_j\hat{\Pi}_F|\psi_I\rangle$ may be negative or even complex because the product of two projectors is not necessarily Hermitian. This approach therefore represents an extension of the usual notion of probability to complex probabilities. If the unconditioned probability for successful postselection is taken simply as the squared modulus of the overlap between pre- and postselection $|\langle\psi_F|\psi_I\rangle|^2 = \langle\psi_I|\hat{\Pi}_F|\psi_I\rangle$, the modified conditional probability $\tilde{P}(a_j|F)$ of measuring value a_j under the condition of successful postselection of the system becomes

$$\tilde{P}(a_j|F) = \frac{\langle\psi_I|\hat{\Pi}_F\hat{\Pi}_j|\psi_I\rangle}{\langle\psi_I|\hat{\Pi}_F|\psi_I\rangle} = \frac{\langle\psi_F|\hat{\Pi}_j|\psi_I\rangle}{\langle\psi_F|\psi_I\rangle}. \tag{3.40}$$

Expanding the standard definition of the expectation value $E(\hat{A}) = \sum_j a_j P_j$, the conditioned expectation value $\tilde{E}^F$ can be defined as [26, 64]

$$\tilde{E}^F(\hat{A}) = \sum_j a_j \tilde{P}(a_j|F) = \sum_j \frac{\langle\psi_F|a_j\Pi_j|\psi_I\rangle}{\langle\psi_F|\psi_I\rangle} = \frac{\langle\psi_F|\hat{A}|\psi_I\rangle}{\langle\psi_F|\psi_I\rangle}. \tag{3.41}$$

While this value is in general a complex number, which makes it difficult to interpret it as an expectation value, the formulation, which employs a conditioned probability distribution, is consistent in the sense that the particular probabilities $\tilde{P}(a_j|F)$ are normalized as well, with $\sum_j \tilde{P}(a_j|F) = 1$ [26].

Furthermore, it is possible to calculate the standard expectation value of an observable with respect to the initial state $|\psi_I\rangle$ from the complex conditioned

expectation values as defined above. A sum of the conditioned expressions $\tilde{E}_j^F(\hat{A})$ for a complete basis of postselection states $\{|\psi_F^{(j)}\rangle\}$, weighted by the probabilities of successful postselection $|\langle\psi_F^{(j)}|\psi_I\rangle|^2$ for each postselection state, yields [26, 54]

$$\sum_j \left|\langle\psi_F^{(j)}|\psi_I\rangle\right|^2 \tilde{E}_j^F(\hat{A}) = \sum_j \langle\psi_I|\psi_F^{(j)}\rangle\langle\psi_F^{(j)}|\hat{A}|\psi_I\rangle = \langle\psi_I|\hat{A}|\psi_I\rangle. \tag{3.42}$$

Definition of Weak Values

The final pointer state after the postselected indirect measurement, which is written in eq. (3.37) as an expansion into pointer states corresponding to the eigenstates of observable $\hat{A}$, can also be expressed in a different manner, by expanding the interaction operator $\hat{U}_\alpha = \exp\left(-\frac{i}{\hbar}\alpha\hat{A}\otimes\hat{p}\right)$ from eq. (3.11) in a power series. The final pointer state $|\Phi_F\rangle$ can then be expressed as

$$\begin{aligned}
|\Phi_F\rangle &= \mathcal{N}\,\mathrm{tr}_{OS}\left[(|\psi_F\rangle\langle\psi_F|\otimes\mathbb{1})\exp\left(-\frac{i}{\hbar}\alpha\hat{A}\otimes\hat{p}\right)(|\psi_I\rangle\otimes|\Phi_0\rangle)\right] \\
&= \mathcal{N}\sum_n \frac{(-i)^n}{\hbar^n n!}\alpha^n\langle\psi_F|\hat{A}^n|\psi_I\rangle\hat{p}^n|\Phi_0\rangle \\
&= \mathcal{N}\langle\psi_F|\psi_I\rangle\sum_n \frac{(-i)^n}{\hbar^n n!}\alpha^n\frac{\langle\psi_F|\hat{A}^n|\psi_I\rangle}{\langle\psi_F|\psi_I\rangle}\hat{p}^n|\Phi_0\rangle,
\end{aligned} \tag{3.43}$$

where tr_{OS} denotes the trace over the object system and $\mathcal{N}$ a suitable normalization.

In the last line of eq. (3.43) it is possible to identify the conditioned expectation values as defined in above. The expansion of the final pointer state after postselection motivates the definition of a quantity that is known as the *weak value*. The nth order weak value A_w^n of operator $\hat{A}$ is defined with respect to preselection $|\psi_I\rangle$ and postselection $|\psi_F\rangle$ as [26, 38, 49]

$$A_w^n = \frac{\langle\psi_F|\hat{A}^n|\psi_I\rangle}{\langle\psi_F|\psi_I\rangle}, \tag{3.44}$$

where the weak value of first order A_w^1 is denoted as the standard weak value A_w and the zero order weak value is simply 1. While this quantity was introduced by Aharanov, Albert and Vaidman ("AAV") in [4] in the context of a PPS measurement with a weak interaction, several authors [38, 48, 53] have pointed out that the concept is independent of the weakness of the measurement and should be regarded in a more general way as the property of a PPS system. First and foremost weak values represent well defined quantities, which can be assigned to observables in pre- and postselected systems.

A useful property of first order weak values is their linearity with respect to the corresponding operator. The weak value of the operator $\hat{A} = \sum_j \nu_j \hat{A}_j$ can be written as

$$A_w = \frac{\langle \psi_F | \hat{A} | \psi_I \rangle}{\langle \psi_F | \psi_I \rangle} = \sum_j \nu_j \frac{\langle \psi_F | \hat{A}_j | \psi_I \rangle}{\langle \psi_F | \psi_I \rangle} = \sum_j \nu_j (A_j)_w. \qquad (3.45)$$

In particular, as demonstrated in eq. (3.41), a weak value of observable $\hat{A}$ can be decomposed into corresponding projector weak values, which will be useful for the procedure of direct tomography presented in chapter 4.

Types of Measurements

As mentioned above weak values are sometimes defined as "outcomes of weak measurements" [27, 62], which motivates some clarification of the terminology. The standard quantum measurement as expressed in the fundamental postulates, is a direct or indirect strong measurement without any postselection. The notion of weakness was introduced in connection with a weak interaction between object system and pointer, which disturbs the object system in minimal way. Therefore, the first criterion (1) of classification of measurements is whether the interaction disturbs the object system strongly or weakly, which corresponds to the criterion of interaction strength. The second criterion (2) discriminates measurements with respect to the property of being postselected or not. However, as will be presented in the next subsection there is a third criterion (3) of weakness in PPS measurements. While the latter is connected to the weakness of the interaction (1), it still imposes different requirements on the interaction strength, which depend on the pre- and postselection [49].

In accordance to the definition presented by AAV, in this work a *weak measurement* is defined as a PPS measurement (2), that fulfills the weakness requirement for PPS measurements (3) [4, 26, 27, 49, 55, 69]. This terminology is not unique because in principle it would also make sense to refer to measurements fulfilling conditions (1) and (2), or even only condition (1) as "weak measurements". In this thesis, however, measurements without postselection, which are only characterized by condition (1), are referred to as *standard measurements with weak interaction*. Outcomes of weak measurement in the sense of AAV have a very specific relation to weak values as will be presented in the next subsection.

3.2.2. Linear Regime

The specific manner, in which weak values emerge in the case of weak measurements, is presented in the following subsection.

Pointer Expectation Value

Just as in the case of standard measurements with weak interaction, the outcomes of weak measurements are obtained by calculation of expectation values of pointer observables. Continuing from eq. (3.43) the final pointer state $|\Phi_F\rangle$ after postselection and a weak interaction described by the small interaction parameter ϵ, which replaces α, can be written as

$$|\Phi_F\rangle = \mathcal{N}\langle\psi_F|\psi_I\rangle \sum_n \frac{(-i)^n}{\hbar^n n!}\epsilon^n A_w^n \hat{p}_q^n |\Phi_0\rangle. \tag{3.46}$$

The expectation value of an arbitrary operator $\langle\hat{q}\rangle_F = \langle\Phi_F|\hat{q}|\Phi_F\rangle$ acting on the pointer system consequently becomes [49]

$$\langle\hat{q}\rangle_F = \mathcal{N}^2 |\langle\psi_F|\psi_I\rangle|^2 \sum_{mn} \frac{(-1)^m i^{m+n}}{\hbar^{m+n} n! m!}\epsilon^{m+n} A_w^m (A_w^n)^* \langle\Phi_0|\hat{p}^n \hat{q}\hat{p}^m|\Phi_0\rangle, \tag{3.47}$$

where the normalization coefficient $\mathcal{N}$ can be expressed as

$$\frac{1}{\mathcal{N}^2} = |\langle\psi_F|\psi_I\rangle|^2 \sum_{mn} \frac{(-1)^m i^{m+n}}{\hbar^{m+n} n! m!}\epsilon^{m+n} A_w^m (A_w^n)^* \langle\Phi_0|\hat{p}^{m+n}|\Phi_0\rangle. \tag{3.48}$$

The weakness of interaction strength controlled by the parameter ϵ in weak measurements, motivates an approximation of the expectation value by an expansion to low orders of ϵ. While it is highly non-trivial to specify the general conditions for the validity of such an approximation, in any case there exist some finite ϵ, for which the higher order terms can be safely neglected. Up to second order of ϵ the expectation value becomes

$$\langle\hat{q}\rangle_F \approx \frac{\langle\hat{q}\rangle + \frac{2}{\hbar}\mathrm{Im}\left[A_w\langle\hat{q}\hat{p}\rangle\right]\epsilon - \frac{1}{\hbar^2}\left(\mathrm{Re}\left[A_w^2\langle\hat{q}\hat{p}^2\rangle\right] - |A_w|^2\langle\hat{p}\hat{q}\hat{p}\rangle\right)\epsilon^2}{1 + \frac{2}{\hbar}\mathrm{Im}\left[A_w\right]\langle\hat{p}\rangle\epsilon - \frac{1}{\hbar^2}\left(\mathrm{Re}\left[A_w^2\right] - |A_w|^2\right)\langle\hat{p}^2\rangle\epsilon^2}, \tag{3.49}$$

where all expectation values except $\langle\hat{q}\rangle_F$ are calculated with respect to the initial pointer states. Eq. (3.49) as described in [26] represents a general approximate expression for the shifts of the pointer in the course of a weak measurement, which is valid for arbitrary observables $\hat{q}$ and $\hat{p}$ and for arbitrary initial pointer states.

For the position observable $\hat{x}$ with the corresponding momentum $\hat{p}_x$ and a pointer state $\langle\hat{x}\rangle = \langle\hat{p}_x\rangle = 0$, the expectation value $\langle\hat{x}\hat{p}\rangle$ can be rewritten employing the commutator relation $[\hat{x}, \hat{p}_x] = i\hbar$ with

$$\langle\hat{x}\hat{p}_x\rangle = \frac{\langle\{\hat{x}, \hat{p}_x\}\rangle}{2} + \frac{\langle[\hat{x}, \hat{p}_x]\rangle}{2} = c_{xp} + \frac{i\hbar}{2}, \tag{3.50}$$

where $c_{xp} := \frac{\langle\{\hat{x},\hat{p}_x\}\rangle}{2}$ is introduced as the "quantum analog" of the statistical *covariance*, which is a measure for the correlation between position and momentum

in the initial pointer state [26]. The covariance, as the expectation value of anti-commutator $\{\hat{x}, \hat{p}_x\} := \hat{x}\hat{p}_x + \hat{p}_x\hat{x}$, is a real quantity because it can be written as a sum of complex conjugates. Approximating the expectation value of the pointer to first order in ϵ consequently yields [26, 49]

$$\delta x = \epsilon \text{Re}\left[A_w\right] + \epsilon \text{Im}\left[A_w\right]\frac{2}{\hbar}c_{xp} \tag{3.51}$$

for the position shift. While the relevance of eq. (3.51) will become apparent in the context of Gaussian beams used as pointers as discussed in section 4.2, the usual expressions for the outcomes of weak measurements assume an initial pointer state with no correlation between position and momentum. This allows the simplification of the shift expressions to the usual form, which was first introduced by AAV only for the shift in position [4]. The standard linear pointer shift in weak measurements can be represented as [26, 38, 47–49, 53, 62, 70]

$$\delta x = \epsilon \text{Re}\left[A_w\right], \tag{3.52}$$

$$\delta p = \epsilon\frac{2}{\hbar}(\Delta p)^2\text{Im}\left[A_w\right] \approx \epsilon\frac{\Delta p}{\Delta x}\text{Im}\left[A_w\right], \tag{3.53}$$

where the shift in pointer momentum was simply calculated from eq. (3.49) with $\hat{q} = \hat{p}$ and $\langle\hat{p}\rangle = 0$ up to first order in ϵ. The last approximation in eq. (3.53) is only valid for pointers that approximately saturate the uncertainty relation between position and momentum [26]. Scenarios where these relations are valid are denoted as the *linear regime* of weak measurements. While in principle "weak measurements" could be defined as PPS measurements that exhibit such a linear relationship between the pointer expectation values and the weak value, the condition for weak measurements, which is presented below, is related to the shape of the final wavefunction of the pointer system. In this work the emergence of the linear regime is considered a necessary but not a sufficient condition for weak measurements in the most strict sense.

Linear Weak Measurements

The linear relations between pointer expectation values and weak values for weak measurements, as expressed in equations (3.52) and (3.53) are a central reason for the usefulness of weak measurements. At the same time they invite a particular type of interpretations, which are responsible for most of the controversy surrounding weak values and weak measurements, as will be delineated in chapter 5.

One of the notable properties of weak measurements in the linear regime is their formal similarity to the expressions obtained for standard measurements of arbitrary strength. As discussed in section 3.1, there exists also a linear relationship between the shift of a pointer δx and the expectation value $\langle\hat{A}\rangle$ of the object system. For an interaction characterized by the parameter ϵ the change

in the position expectation value is related to the expectation of the system observable $\hat{A}$ with $\delta x = \epsilon \langle \hat{A} \rangle$. The similarity between the latter expression and the linear formulas in the weak measurement case, motivated interpretations similar to the one presented in subsection 3.2.1, where the weak value is considered as a "weak expectation value", corresponding to weakly interacting pre- and postselected systems in the same way as an expectation corresponds to a standard quantum system. In this context it should be noted that for identical pre- and postselection the weak value is equal to the expectation value with [24, 27]

$$A_w = \frac{\langle \psi | \hat{A} | \psi \rangle}{\langle \psi | \psi \rangle} = \langle \psi | \hat{A} | \psi \rangle = \langle \hat{A} \rangle. \tag{3.54}$$

In contrast to expectation values, however, that always lie in the range of the eigenvalue of the observable, weak values can be arbitrarily large or even complex [4, 27, 47]. In principle for a given preselection state, which is not an eigenstate of the measurement observable, it is possible to create an arbitrary complex weak value by choosing a suitable postselection state. While the interpretation of real weak values as physical quantities is less problematic, the meaning of complex weak values has been regarded as a greater problem. The measurements of both parts of the weak value are well defined as shifts of initial expectation values of the two pointer observables caused by the double action of the weak measurement procedure. In contrast to the standard quantum measurement, in this case both the position and the momentum of the pointer carry information about the object system [26, 53, 71].

Whatever information is gained by a weak measurement, in many accounts [23, 24, 26, 71–73] it is pointed out that the state of the object system which is projected onto the postselection state, is essentially the undisturbed initial preselection state. This motivates a range of theoretical and experimental scenarios which aim to get some amount of information about complementary observables from a single preselected system. Examples for such procedures are presented in chapter 4 in the context of direct tomography and are also discussed in chapter 5 as mentioned above.

Minimal Ensemble Size

Just as in the case of weak standard measurements the information gained from the pointer shifts proportional to ϵ is small because of the large uncertainty of the corresponding observable [4, 27, 62]. Assuming a weak measurement of observables $\hat{x}$ and $\hat{p}_x$ with uncertainties Δx and Δp, in the linear regime of a weak measurement of observable $\hat{A}$ both shifts exhibit the same SNR proportional to the corresponding part of the weak value with

$$\frac{\delta p}{\Delta p} = \frac{\epsilon}{\Delta x} \text{Im} \left[A_w \right] \tag{3.55}$$

$$\frac{\delta x}{\Delta x} = \frac{\epsilon}{\Delta x} \text{Re} \left[A_w \right], \tag{3.56}$$

where the formulation of momentum shift from eq. (3.53) for a pointer state saturating the uncertainty relation was used.

The approximate minimal ensemble size required to resolve both shifts can be calculated in analogy to the case of weak standard measurements by substituting the modulus of the weak value $|A_w|$ for the expectation value $\langle \hat{A} \rangle$ in eq. (3.33). The minimal number N_0 of measurements on the pointer system becomes [26, 62]

$$N_0 \approx \frac{1}{|\langle \psi_F | \psi_I \rangle|} \left(\frac{\Delta x}{\epsilon |A_w|} \right)^2 \tag{3.57}$$

where the factor $|\langle \psi_F | \psi_I \rangle|$ takes into account the filtering losses caused by the postselection. In principle it is thus possible to measure the weak value for an arbitrary small interaction by repeated measurements on many identical systems [27, 62]. It should be noted that for the above expression it is assumed that the uncertainty of the final pointer is approximately the same as the uncertainty of the initial state Δx [26].

In the next subsection the validity of this assumption for weak measurements in the strict sense will be presented. Just as in the case of standard measurements with weak interaction the measurement outcome is obtained in a direct manner by averaging over the pointer distributions. In the case of $A_w = 0$ the condition obviously fails because there are no shifts to be measured. However, the definition is consistent in the sense that in principle an infinite amount of measurements would need to be conducted to assure that actually no shift has taken place.

3.2.3. Effects on Pointer

By considering the pointer state after the weak PPS measurement the conditions for a weak measurement are eventually specified in this subsection. Furthermore, the emergence of the final pointer state from the procedure of weak measurements is discussed as well.

Final Pointer Shape

The analysis of the pointer wavefunction after interaction and postselection can be continued from eq. (3.46). Assuming a small enough interaction parameter ϵ,

all contribution of the order $\epsilon \geq 2$ can be neglected, which yields the approximate expression for the final pointer state $|\Phi_F\rangle$ with [9, 55, 69, 74]

$$
\begin{aligned}
|\Phi_F\rangle &= \mathcal{N}\langle\psi_F|\psi_I\rangle \sum_n \frac{(-i)^n}{\hbar^n n!}\epsilon^n A_w^n \hat{p}^n|\Phi_0\rangle \\
&\approx \mathcal{N}\langle\psi_F|\psi_I\rangle\left(|\Phi_0\rangle - \frac{i}{\hbar}\epsilon A_w\hat{p}|\Phi_0\rangle\right) \\
&\approx \mathcal{N}\langle\psi_F|\psi_I\rangle \sum_n \frac{(-i)^n}{\hbar^n n!}\epsilon^n (A_w)^n\hat{p}^n|\Phi_0\rangle \\
&= \mathcal{N}\langle\psi_F|\psi_I\rangle|\Phi_{\epsilon A_w}\rangle,
\end{aligned}
\tag{3.58}
$$

where $|\Phi_{\epsilon A_w}\rangle = e^{-\frac{i}{\hbar}\epsilon A_w\hat{p}}|\Phi_0\rangle$ as defined in eq. (3.11).

The property expressed in the relation above can be seen as the fundamental defining property of weak measurements. In the case of weak measurements the interaction simply shifts the pointer wavefunction in good approximation proportional to A_w [4, 27]. This behavior shows a striking similarity to the case of standard quantum measurements, where the initial object system is in an eigenstate of the observable $\hat{A}$ corresponding to eigenvalue a and the pointer successively evolves into the state $|\Phi_{\alpha a}\rangle$. While the latter property holds for any interaction interaction strengths α, the proportionality of the shift to the weak value remains always an approximation, which, however, becomes arbitrarily good with decreasing interaction strength ϵ.

Calculating the expectation values of the final pointer state for the observables $\hat{x}$ and $\hat{p}_x$ recovers the linear expression formulated above. With $\mathcal{N}^{-1} = |\langle\psi_F|\psi_I\rangle|$ the position expectation value to first order in ϵ becomes

$$
\begin{aligned}
\langle\hat{x}\rangle_F &= \langle\Phi_0|e^{\frac{i}{\hbar}\epsilon A_w^*\hat{p}_x}\hat{x}e^{-\frac{i}{\hbar}\epsilon A_w\hat{p}_x}|\Phi_0\rangle \\
&= \langle\Phi_0|e^{\frac{2}{\hbar}\epsilon\mathrm{Im}[A_w]\hat{p}_x}\hat{x}|\Phi_0\rangle + \epsilon A_w\langle\Phi_0|e^{\frac{2}{\hbar}\epsilon\mathrm{Im}[A_w]\hat{p}_x}|\Phi_0\rangle \\
&\approx \langle\hat{x}\rangle + \frac{2\epsilon}{\hbar}\mathrm{Im}\,[A_w]\,\langle\hat{p}_x\hat{x}\rangle + \epsilon A_w = \langle\hat{x}\rangle + \frac{2\epsilon}{\hbar}\mathrm{Im}\,[A_w]\left(c_{xp} - \frac{i\hbar}{2}\right) + \epsilon A_w \\
&= \epsilon\mathrm{Re}\,[A_w] + \epsilon\mathrm{Im}\,[A_w]\frac{2}{\hbar}c_{xp},
\end{aligned}
\tag{3.59}
$$

where it was assumed that $\langle\hat{x}\rangle = 0$ and the covariance from eq. (3.51) was used. In an analog fashion the momentum expectation value can be calculated for $\langle\hat{p}_x\rangle = 0$ as

$$
\begin{aligned}
\langle\hat{p}_x\rangle_F &= \langle\Phi_0|e^{\frac{i}{\hbar}\epsilon A_w^*\hat{p}_x}\hat{p}_x e^{-\frac{i}{\hbar}\epsilon A_w\hat{p}_x}|\Phi_0\rangle = \langle\Phi_0|e^{\frac{2}{\hbar}\epsilon\mathrm{Im}[A_w]\hat{p}_x}\hat{p}_x|\Phi_0\rangle \\
&\approx \langle\hat{p}_x\rangle + \frac{2\epsilon}{\hbar}\mathrm{Im}\,[A_w]\,\langle\hat{p}_x^2\rangle \\
&= \epsilon\frac{2}{\hbar}(\Delta p_x)^2\mathrm{Im}\,[A_w].
\end{aligned}
\tag{3.60}
$$

It has thus been shown that for any weak measurement satisfying eq. (3.58) the pointer shifts in position and momentum space exhibit a linear dependence on the weak value. While the opposite implication is also true for most types of pointers, in general the linear regime does not imply a weak measurement in the sense presented here [26]. It should be noted that while the shape of the pointer distribution is unaltered for weak measurements, the whole wavefunction is rescaled by the factor $|\langle\psi_F|\psi_I\rangle|$ as a consequence of the postselection.

Regime of Weak Measurement

Beside the definition of the weak regime of measurements the other point of interest are of course the conditions under which a PPS measurement exhibits the property of weakness. In the derivation of the approximate final pointer state in weak measurements in eq. (3.58) two approximations are made. For the first it is assumed that

$$\|\frac{i}{\hbar}\epsilon A_w\hat{p}_x|\Phi_0\rangle\| \gg \|\frac{(-i)^n}{\hbar^n n!}\epsilon^n A_w^n\hat{p}_x^n|\Phi_0\rangle\| \ \ \forall n \geq 2 \tag{3.61}$$

$$\text{and} \quad \frac{\epsilon}{\hbar}|A_w|\Delta p_x \gg \frac{\epsilon^n}{\hbar^n n!}|A_w^n|(\Delta p_x)^n \ \ \forall n \geq 2, \tag{3.62}$$

where $\|\hat{p}_x|\Phi_0\rangle\| = \sqrt{\langle\hat{p}_x^2\rangle} = \Delta p_x$ for $\langle\hat{p}_x\rangle = 0$. Thus, for pointer states that saturate the uncertainty relation the first condition can be expressed as [9, 26]

$$\frac{\epsilon}{\Delta x} \ll \min_{n\geq 2}\left[n!\left|\frac{A_w}{A_w^n}\right|^{\frac{1}{n-1}}\right]. \tag{3.63}$$

The second condition is much simpler, requiring that

$$\frac{\epsilon}{\hbar}|A_w|\Delta p_x \gg \frac{\epsilon^n}{\hbar^n n!}|A_w|^n(\Delta p_x)^n \ \ \forall n \geq 2, \tag{3.64}$$

which leads to [9, 26, 53]

$$\frac{\epsilon}{\Delta x}|A_w| \ll 1. \tag{3.65}$$

It should be noted that the ratio of ϵ and Δx is the relevant quantity to be considered for all bounds concerning weakness in indirect measurements with pointers, for which $\Delta x\Delta p_x \approx \frac{\hbar}{2}$. This reflects the already mentioned property that weakness can be achieved either by weakening the interaction, or by increasing the pointer uncertainty. Unlike in the case of standard measurements, however, where the condition of weakness corresponds to minimal disturbance of the object system, in the case of PPS measurements the relevant criterion for weakness is a minimal disturbance of the pointer because the object system is postselected. A comparison of eq. (3.32) and eq. (3.65) clearly shows that the condition of a weak interaction does not suffice to guarantee weak measurements in the case of large weak values with $|A_w| \gg \Delta A$ [49].

Emergence of Final Pointer State

The question arises, how the shape of the pointer distribution changes under the influence of the postselection. Employing eq. (3.13) the probability distribution $P(x)$ of the pointer state $\hat{\rho}_F$ after an interaction of arbitrary strength α can be written as

$$P(x) = \sum_j |c_j|^2 |\Phi_j(x)|^2, \tag{3.66}$$

where $\Phi_j(x) := \langle x | \Phi_{\alpha a_j} \rangle$ is the wavefunction of a pointer state shifted by αa_j. The probability distribution $P_F(x)$ of the final pointer state $|\Phi_F\rangle$ resulting from a postselection of the state above, can be interpreted as the joint probability $P(x \cap F)$ of measuring the pointer in state x and the object system in postselection state $|\psi_F\rangle$. It can be calculated as

$$
\begin{aligned}
P_F(x) &= \sum_{j,m} c_j d_j^* c_m^* d_m \Phi_j(x) \Phi_m^*(x) \\
&= \sum_j |c_j d_j^*|^2 |\Phi_j(x)|^2 + \sum_{j \neq m} c_j d_j^* c_m^* d_m \Phi_j(x) \Phi_m^*(x).
\end{aligned}
\tag{3.67}
$$

From the last expression it can be seen that the probability distribution of the pointer state after postselection does not only contain the contributions of the particular components $|\Phi_j(x)|^2$, but also several interference terms with arbitrary complex coefficients determined by the choice of the postselection state $\sum_j d_j |a_j\rangle$ [9]. Therefore, the action of the postselection can be seen as the action of a quantum eraser, which in some sense restores coherence between the components of the pointer state. This allows for various interference effects, such as the emergence of extraordinary large pointer expectation values, which are not caused by a putative increase of probability of measuring a high spatial value, but rather by a decrease in probability for lower values, caused by destructive interference of the particular components [9, 10, 21, 26, 46, 54]. In fact the action of postselection as a local filtering process ensures that $P(x) \geq P_F(x) \ \forall x$. For a strong interaction, designed to resolve the eigenvalues in the pointer distribution, it is, however, impossible for the postselection to restore coherence, which is the reason why in general weak measurements also need to satisfy the usual condition of weak interaction [26].

A slightly different form of explanation has to be employed in the case when the pointer system is measured prior to the postselection. While the procedure of weak measurements was formulated in subsection 3.2.1 with a pointer measurement after the postselection, in principle an opposite procedure is also in agreement with the theory of weak measurements [26, 62]. In this variant the pointer expectation values are measured for each system of the ensemble and the outcomes of measurements on systems, which did not pass postselection are discarded afterwards. The only requirement for this procedure is the possibility to separate the outcomes after postselection, which can be for example achieved by

an interaction of each system with a separate pointer system [4, 62]. This is for example achieved in [54] where the polarizations of two single photons represent the object and pointer systems. In the case of the measurement of a continuous observable as $\hat{x}$, an ideal projective measurement is of course impossible, but for the sake of clarity an idealized projective measurement of the observable with $\hat{x} = \int_{-\infty}^{\infty} x|x\rangle\langle x|\,\mathrm{d}x$ will be assumed, without loss of generality.

Starting from $|C\rangle$, the weakly entangled state by means of weak interaction, as described in eq. (3.13), the first step of the alternative measurement procedure is a direct projective measurement of the pointer represented by the projector $\hat{\Pi}_x = |x\rangle\langle x|$. With tr_Φ as the partial trace on the pointer system, the state of the object system after the pointer measurement $|\psi_M\rangle$ becomes

$$|\psi_M\rangle = \mathcal{N}_x \, \mathrm{tr}_\Phi\left(\hat{\Pi}_x|C\rangle\right) = \mathcal{N}_x \sum_j c_j \Phi_j(x)|a_j\rangle, \qquad (3.68)$$

where the normalization $\mathcal{N}_x = \sqrt{\sum_j |c_j|^2|\Phi_j(x)|^2}$ corresponds to the probability $P(x) = \mathcal{N}_x^2$ of measuring the outcome x. This measurement can be interpreted as a weak POVM measurement with measurement operators close to unity [54, 57, 75]. Thus, in the case of a weak interaction with almost identical wavefunctions $\{\Phi_j\}$, the expression above represents approximately the initial state of the object system, which is only slightly modified by the coefficients $\Phi_j(x)$ depending on the outcome of the pointer POVM measurements. However, this backaction of the pointer measurements is exactly what changes the probability of successfull postselection of the resulting state. A value of x, at which the pointers would interfere less destructively even for almost orthogonal postselection in the standard weak measurement procedure described above, is a value for which the x dependent coefficients modify the object state in such a way that it becomes less orthogonal to the postselection. This can be seen straightforward by projecting onto the postselection state, which yields

$$\langle\psi_F|\psi_M\rangle = \mathcal{N}_x \sum_j c_j d_j^* \Phi_j(x). \qquad (3.69)$$

Consequently the expression $|\langle\psi_F|\psi_M\rangle|^2 = P(F|x)$ denotes the probability of postselection conditioned of a prior pointer measurement of the value x. The probability of the pointer measurement of $\hat{x}$ after filtering of the results with respect to successful postselection, effectively corresponds to a correction of the pointer probability distribution $P(x)$ by multiplication with the conditioned probability $P(F|x)$. According to Bayes' theorem, however, this expression is equal to the joint probability of measuring x and successful postselection with $P(x \cap F) = P(x) \cdot P(F|x)$ and a simple calculation confirms that the expression calculated in the case of an antecedent pointer measurement is exactly the same as the probability distribution calculated in eq. (3.67). This proves that the backaction of the weak measurement

onto the object system exactly corresponds to the effect of the postselection on the pointer distribution. In fact, some accounts also denote the pointer measurement itself as a "postselection" [38].

Annihilation Operator Description

To conclude the presentation of weak measurements, an extraordinary formulation of this concept should be mentioned, where the process of postselection is described as the action of an annihilation operator on the pointer system [47]. The standard dimensionless *annihilation* or *lowering* operator $\hat{a}$ for a harmonic potential is defined as [47]

$$\hat{a} = \sqrt{\frac{m\omega}{2\hbar}}\hat{x} + i\sqrt{\frac{1}{2m\omega\hbar}}\hat{p}_x, \tag{3.70}$$

with the parameters m and ω. Applying a reparametrization with $\Delta x := \sqrt{\frac{\hbar}{2m\omega}}$ makes it possible to express the annihilation operator in the form

$$\hat{a} = \frac{1}{2\Delta x}\hat{x} + i\frac{\Delta x}{\hbar}\hat{p}_x. \tag{3.71}$$

With the linear dependencies of the real and imaginary parts of the weak value on position and momentum shifts, the weak value can be written as [47]

$$\begin{aligned} A_w = \text{Re}\,[A_w] + i\text{Im}\,[A_w] &= \frac{\langle\hat{x}\rangle_F}{\epsilon} + i\frac{\Delta x}{\epsilon\Delta p}\langle\hat{p}_x\rangle_F \\ &= \frac{2\Delta x}{\epsilon}\langle\hat{a}\rangle_F, \end{aligned} \tag{3.72}$$

with $\frac{2\Delta x}{\hbar} = \frac{1}{\Delta p}$. The weak value can therefore be understood as proportional to the expectation of the final pointer state with respect to the annihilation operator.

The authors of [47] also provide a possible interpretation for this representation. In this perspective, the interaction can be seen as small excitation of the pointer, which is initially in the ground state. Consequently the final pointer state has some non-vanishing amplitude for the excited state. The action of the annihilation operator then removes the ground state component, with a remaining amplitude proportional to $\frac{\epsilon}{\Delta x}A_w$. "In other words, the annihilation operator isolates only that part of the pointer state that is changed by the interaction." [47]

It should be noted that all these expressions were obtained for a specific type of pointer and are of course only valid in the linear regime of weak interaction. Nevertheless, they represent an interesting relation and it remains to be seen whether they contain any physical significance.

3.3. Examples with Gaussian Pointers

To illustrate the nature of weak measurements in comparison with quantum measurements without postselection, in the following section the final pointer distributions for both scenarios are compared graphically.

3.3.1. Definition of States and Observables

As a basis for the graphical examples, the corresponding observable and states are defined in the following paragraphs.

Object System

The object system in this example has five dimensions and the measured quantity is represented by the non-degenerate observable $\hat{A}$, which is defined as

$$\hat{A} := \sum_j a_j |a_j\rangle\langle a_j|, \tag{3.73}$$

with the orthonormal states $\{|a_j\rangle\}$ and the eigenvalues $\{a_j\} = \{0, 1, 2, 3, 4\}$.

The two initial states $|\psi_{I1}\rangle$ and $|\psi_{I2}\rangle$ are defined as

$$|\psi_{I1}\rangle = \frac{1}{5}\left(|0\rangle + 2|1\rangle + \sqrt{15}|2\rangle + 2|3\rangle + |4\rangle\right), \tag{3.74}$$

$$|\psi_{I2}\rangle = \frac{1}{6}\left(4|0\rangle + |1\rangle + \sqrt{2}|2\rangle + |3\rangle + 4|4\rangle\right), \tag{3.75}$$

which both have the expectation value $\langle \hat{A} \rangle = 2$. They differ, however, with respect to their standard deviations, which are $\Delta A^{(1)} \approx 0.64$ and $\Delta A^{(2)} \approx 3.61$.

Furthermore the two postselection state $|\psi_{F1}\rangle$ and $|\psi_{F2}\rangle$ are employed with

$$|\psi_{F1}\rangle = \frac{1}{\mathcal{N}_1}\left(-|0\rangle - |1\rangle + \frac{1}{\sqrt{3}}|2\rangle + |3\rangle + |4\rangle\right), \tag{3.76}$$

$$|\psi_{F2}\rangle = \frac{1}{\mathcal{N}_2}\left(\sqrt{4}|0\rangle + 5|1\rangle - 5|2\rangle - 3|3\rangle + |4\rangle\right). \tag{3.77}$$

Together with the corresponding preselections this implies the weak values $A_w^{(1)} \approx 5.58$ and $A_w^{(2)} \approx -0.31$. These weak values are ideal for a demonstration of the pointer behavior as both lie outside the range of eigenvalues while having moduli which differ about more than one order of magnitude. Furthermore while for the first PPS pair the weak value is larger than the standard deviation, for the second pair the weak value is about one order of magnitude smaller than the standard deviation.

Pointer

The pointer system is an infinitely dimensional spatial system, on which the observable $\hat{x}$ is measured. The initial pointer state $|\Phi_0\rangle$ is a Gaussian distribution which is defined as [28]

$$\langle x|\Phi_0\rangle = \left(\frac{1}{2\pi\sigma}\right)^{\frac{1}{4}} e^{-\frac{x^2}{4\sigma^2}}, \tag{3.78}$$

where the parameter σ is equal to the standard deviation in position space with $\Delta x = \sigma$. The standard deviation in momentum space is related to σ via $\Delta p = \frac{\hbar}{2\sigma}$. Thus, the Gaussian function as a quantum wavefunction saturates the uncertainty relation with $\Delta x \Delta p = \frac{\hbar}{2}$.

As discussed above, for this type of pointers the condition for weakness of interaction (3.32) and the condition for weak measurements (3.65) depend on the parameter $\frac{\epsilon}{\Delta x} = \frac{\epsilon}{\sigma}$. In the following examples ϵ is fixed at 1 and the interaction is weakened by increasing σ. Employing the two conditions for weakness, the boundary values for the object system states defined above are given in Tab. 3.1.

Case	Value		Condition
Preselection 1 only	ΔA	≈ 0.64	$\sigma \gg 0.45$
Preselection 2 only	ΔA	≈ 3.61	$\sigma \gg 2.55$
PPS-pair 1	$A_w^{(1)}$	≈ 5.58	$\sigma \gg 5.58$
PPS-pair 2	$A_w^{(2)}$	≈ -0.31	$\sigma \gg 0.31.$

Table 3.1.: Conditions for weakness calculated from ΔA and $A_w^{(j)}$ using eqs. (3.32) and (3.65).

3.3.2. Final Pointer States

In Fig. 3.2 the pointer states after both kinds of postselection are depicted for different interaction strengths parametrized by σ. For the first PPS pair, the two limiting values for weakness are 0.45 and 5.58, respectively. Therefore, in the case of $\sigma = 0.25$ as depicted in a) both measurements are relatively strong, as the eigenvalues are still resolved and it is possible to distinguish the five peaks. In graph b) the value of σ is twice as high as the limiting value in the non-postselected case and indeed it can be seen that the corresponding pointer shape is starting to resemble the initial Gaussian profile centered at the expectation value of 2. Only when σ becomes much larger, as depicted in graph c), also the weak measurement condition becomes satisfied and the postselected profile approaches a Gaussian centered at the weak value of 5.58 as well.

In the case of the second PPS pair, the situation is somehow reversed, because the weak value is much smaller than the standard deviation of the preselection
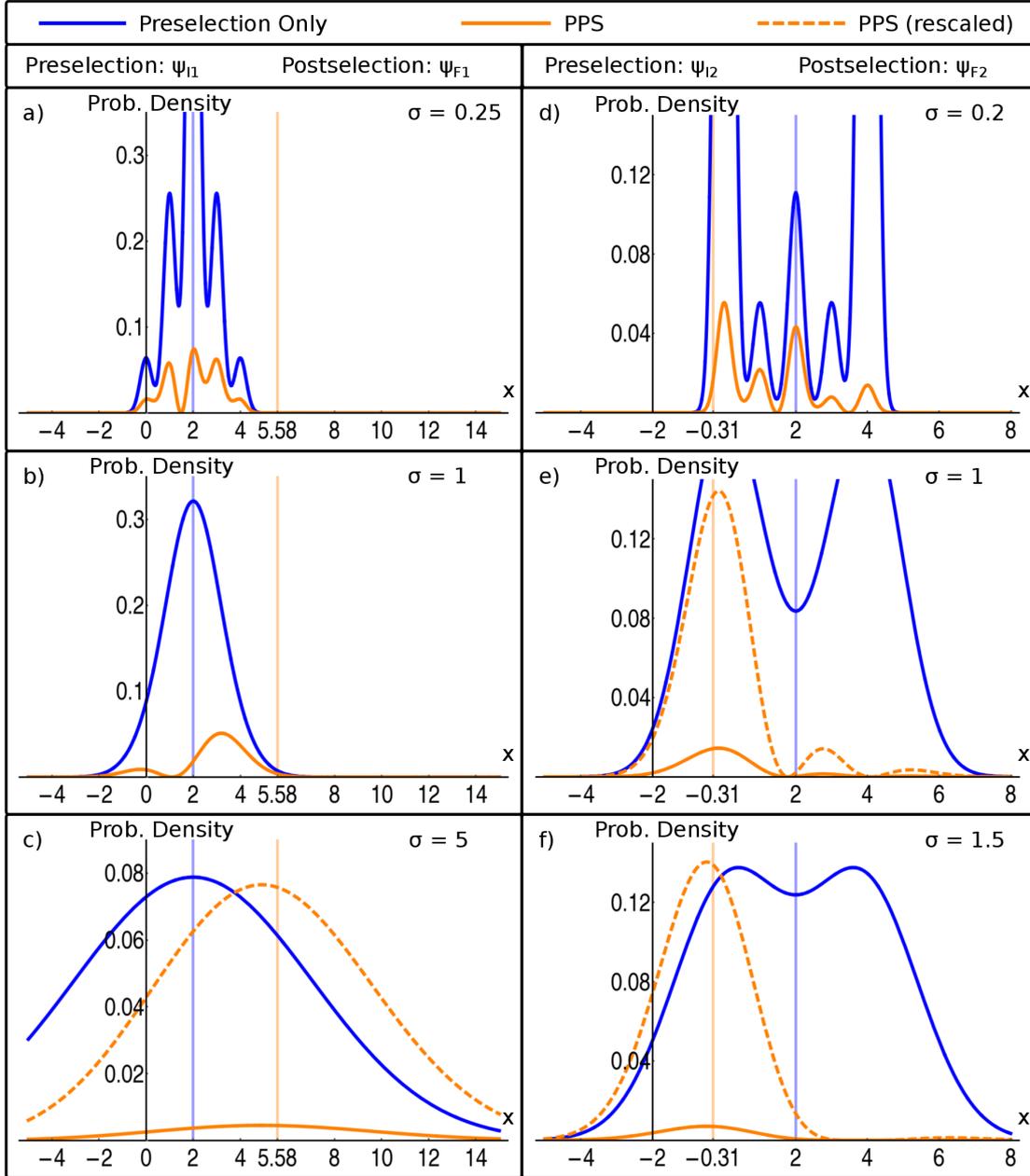
Figure 3.2.: Probability or intensity profiles in x-direction of the final pointer states for different types of measurements. The figures on the left (a-c) depict the first PPS pair and the figures on the right (d-f) the second pair. For each of the state configurations three different values of σ are presented. In addition to the non-postselected (blue) and postselected (orange) profiles, in Figures c), e) and f) the postselected pointer state is also printed with a rescaling factor (dashed, orange) to better illustrate its shape.

state. For $\sigma = 0.2$ in graph d) both measurements can still be considered to be strong. However, as can be seen in graphs e) and f) for larger standard deviations, the postselected pointer profile approaches the initial Gaussian profile faster than the non-postselected profile. While in graph f) the former represents in good approximation a Gaussian distribution centered close to the weak value of -0.31, in the profile without postselection the two peaks corresponding to different eigenvalues can still be distinguished. This illustrates the independence of the conditions for weak interaction and weak measurement.

Furthermore, the six figures illustrate how in the case of the postselected profiles (orange) the five peaks start to interfere for increasing σ. It can be seen that for larger σ the pointer intensity is reduced at positions far from the weak values, and increases around them. Another aspect that is shown is the strong reduction of overall intensity by the postselection. As the weak measurement becomes weaker and the pointer resembles a Gaussian distribution centered around the weak values more and more, the postselection probability decreases. The effective postselected profile can only be modified by decreasing the intensity at certain positions and never by adding intensity because the postselection is a filtering process. Therefore, only when the initial uncertainty of the pointer reaches out far enough into the region of the weak values, it becomes possible to create the corresponding pointer profiles through interference of the eigenvalue components with very low effective intensity.

4. Direct State Tomography

The following chapter deals with procedures for quantum state tomography based on the concept of weak values and measurements, pursuing a twofold goal. One concern is the introduction of the concept of direct state tomography, which relies on weak measurements. In this context the basic principles and procedures are delineated alongside a discussion of the Gaussian beam as the most common type of pointer. At the same time the second aim of the chapter is realized, which consists in the explicit description of the tomography experiment performed in the course of this thesis.

4.1. Qubit Tomography

The discussion of quantum tomography, eventually presented in this section, is founded on an initial introduction of the relevant qubit system alongside its principal realization in polarization states.

4.1.1. Qubit Model of Polarization

The qubit system, which is the subject of the tomography procedures presented in this chapter, is realized in the physical property of polarization, with which it shares all important structural characteristics. Therefore, the presentation of qubits, begins with a brief outline of the physical nature of polarization, which is subsequently generalized to the abstract description of the polarization degree of freedom as a quantum system.

Electromagnetic Waves

As an electromagnetic phenomenon, light satisfies a set of partial differential equations denoted as the *Maxwell equations*, which can be expressed as [35, 76, 77]

$$\vec{\nabla} \times \vec{H} = \varepsilon_0 \frac{\partial \vec{E}}{\partial t}, \qquad\qquad \vec{\nabla} \times \vec{E} = -\mu_0 \frac{\partial \vec{H}}{\partial t},$$
$$\vec{\nabla} \cdot \vec{E} = 0, \qquad\qquad\qquad \vec{\nabla} \cdot \vec{H} = 0,$$

for the electric $\vec{E}(\vec{r}, t)$ and magnetic fields $\vec{H}(\vec{r}, t)$ in free space and the constants ε_0 and μ_0 denoted as *electric permittivity* and *magnetic permeability* of free space. These equations imply another relation for $\vec{E}$ and $\vec{H}$ with [76, 77]

$$\nabla^2 \vec{E} - \varepsilon_0 \mu_0 \frac{\partial^2 \vec{E}}{\partial t^2} = 0, \tag{4.1}$$

which is known as the electromagnetic *wave equation* for the electric field. Exactly the same relation holds for the magnetic field $\vec{H}$.

The simplest solutions to the wave equation are *plane waves* of the form [35, 76–78]

$$\vec{E}(\vec{r}, t) = \vec{E}_0 e^{-i(\vec{k}\vec{r} - \omega t)}, \tag{4.2}$$

$$\vec{H}(\vec{r}, t) = \vec{H}_0 e^{-i(\vec{k}\vec{r} - \omega t)} \tag{4.3}$$

with the *wavevector* $\vec{k}$, the field amplitudes $\vec{E}_0$ and $\vec{H}_0$ and the angular frequency ω. The wavevector represents the spatial direction of propagation of the wave and is related to the wavelength λ with $|\vec{k}| = \frac{2\pi}{\lambda}$ [76–78]. Applying the Maxwell equations to these solutions yields the condition that in free space $\vec{k}$, $\vec{E}_0$ and $\vec{H}_0$ have to be mutually orthogonal. Consequently the oscillations of the two fields lie in a plane perpendicular to the direction of propagation and the plane wave represents a *transverse electromagnetic* ("TEM") wave [76].

The energy flow of the electromagnetic wave is expressed by the *Poynting vector* $\vec{S}$, which is defined as [35, 76, 77]

$$\vec{S} := \vec{E} \times \vec{H}. \tag{4.4}$$

The intensity I of the wave is consequently defined as time average of the modulus of the Poynting vector. For the plane waves the intensity becomes [76, 77]

$$I := \langle |\vec{S}| \rangle_t = \frac{1}{2} c \varepsilon_0 |\vec{E}_0|^2, \tag{4.5}$$

which shows the proportionality of the intensity to the absolute squared amplitude of the electric field.

Polarization

For any form of transverse waves propagating in three dimensional space, it is possible to define the concept of *polarization*. This is made possible by the existence of 2-dimensional space in which the system can oscillate. For TEM waves the polarization is defined as the "time course of the *direction* of the electric-field vector" [35, 76]. In general this course is elliptical and the light has *elliptical polarization*. Special cases of polarization correspond to degenerate forms of this ellipse, namely

a line and a circle with corresponding *linear* and *circular polarization* [35, 76, 78]. *Unpolarized* light is characterized by random changes of polarization so that no definitive polarization direction can be assigned [77, 78].

To express the polarization formally, it is possible to employ the description by *Stokes parameters* or alternatively the *Jones vector* [76, 78]. While the Jones vector formalism can only be applied to polarized light, the Stokes parameters describe any type of full or partial polarization. The Jones vector $\vec{J}$ is a two dimensional vector in complex space, which is defined as [78]

$$\vec{J} := \begin{pmatrix} E_x \\ E_y \end{pmatrix}, \tag{4.6}$$

where E_x and E_y denote the components of the electric field perpendicular to the propagation direction z. In general E_x and E_y are complex numbers with a relative phase. Any global phase of the two components is irrelevant for the description of polarization because the wave character implies a global oscillation in any case.

Because of the linearity of the Maxwell equations and the wave equation, any sum of solutions is again a valid solution [76, 78]. Any superposition of electromagnetic waves can therefore be regarded as a single effective wave. In particular, the superposition of two plane waves $\vec{E}_1(\vec{r}, t)$ and $\vec{E}_2(\vec{r}, t)$ with equal $\vec{k}$ and ω can be expressed as

$$\vec{E}_1(\vec{r}, t) + \vec{E}_2(\vec{r}, t) = (\vec{E}_1^{(0)} + \vec{E}_2^{(0)})e^{-i(\vec{k}\vec{r} - \omega t)}, \tag{4.7}$$

which represents a new plane wave with the field amplitude $\vec{E}_R = \vec{E}_1 + \vec{E}_2$. Employing the Jones vector formalism the polarization $\vec{J}_R$ of the superposition becomes

$$\vec{J}_R = \begin{pmatrix} E_R^{(x)} \\ E_R^{(y)} \end{pmatrix} = \begin{pmatrix} E_1^{(x)} + E_2^{(x)} \\ E_1^{(y)} + E_2^{(y)} \end{pmatrix} = \vec{J}_1 + \vec{J}_2. \tag{4.8}$$

This illustrates that the superposition of two polarized plane waves results in a new plane wave that has also a well defined polarization, which can be simply expressed by the sum of the Jones vectors representing the initial polarizations [76, 78].

In consequence, it is possible to express any polarization as a superposition of two basis states. The classification of polarizations presented above, alongside with the spatial direction of the standard coordinate system, implies three natural pairs of orthogonal polarizations, which constitute the three standard bases [78]. For linear polarizations, which are characterized by a real phase relation between the x and y components of the polarization, there exist two natural basis sets. The first set consists of *horizontal* and *vertical* polarizations $\{\vec{J}_H, \vec{J}_V\}$ and the

second one of *diagonal* or *plus* and *antidiagonal* or *minus* polarizations $\{\vec{J}_P, \vec{J}_M\}$. The corresponding Jones vectors are defined as [76, 78]

$$\vec{J}_H = \begin{pmatrix} 1 \\ 0 \end{pmatrix}, \ \vec{J}_V = \begin{pmatrix} 0 \\ 1 \end{pmatrix}, \ \vec{J}_P = \frac{1}{\sqrt{2}} \begin{pmatrix} 1 \\ 1 \end{pmatrix}, \ \vec{J}_M = \frac{1}{\sqrt{2}} \begin{pmatrix} 1 \\ -1 \end{pmatrix}. \qquad (4.9)$$

The third natural basis consists of *right* and *left circular polarizations* $\{\vec{J}_R, \vec{J}_L\}$, which are characterized by a phase difference of $\frac{\pi}{2}$ and consequently defined as [76, 78]

$$\vec{J}_R = \frac{1}{\sqrt{2}} \begin{pmatrix} 1 \\ i \end{pmatrix}, \ \vec{J}_L = \frac{1}{\sqrt{2}} \begin{pmatrix} 1 \\ -i \end{pmatrix}, \qquad (4.10)$$

where the definition in [78] is opposite. All other polarizations can be expressed as superpositions of these pairs.

Qubits

The Jones vector formalism represents the polarization in a two dimensional complex vector space, which implies a possible relation to 2-dimensional quantum systems. Such quantum system represent the simplest kind of quantum systems and are generally denoted as *quantum bits* or *qubits*. A qubit is represented by a 2-dimensional Hilbert Space with the principal orthonormal basis states $|0\rangle$ and $|1\rangle$ [29, 35]. This constitutes an analogy to the classical bit, which can have the values 0 or 1. Contrary to a classical bit, however, a qubit system can be also in different states $|\psi\rangle$ than these basis states, namely in all normalized superpositions [29, 35]

$$|\psi\rangle = \alpha|0\rangle + \beta|1\rangle, \qquad (4.11)$$

with $|\alpha|^2 + |\beta|^2 = 1$.

As is immediately clear from the Jones formalism the polarization of light represents one of the possible physical realizations of a qubit system [33, 35]. The polarization bases expressed as Jones vectors $\{\vec{J}_H, \vec{J}_V, \vec{J}_P, \vec{J}_M, \vec{J}_R, \vec{J}_L\}$ can be identified in a straight forward way with the kets $\{|H\rangle, |V\rangle, |P\rangle, |M\rangle, |R\rangle, |L\rangle\}$. The principal qubit basis is thereby identified with the basis $\{|H\rangle, |V\rangle\}$ as $|H\rangle := |0\rangle$ and $|V\rangle := |1\rangle$.

This quantum mechanical representation of polarization facilitates the attribution of polarization not only to electromagnetic waves but also to single photons [76]. In this context the polarized light wave can be seen as an ensemble of photons sharing the same polarization, where each polarized photon represents an instance of a qubit system with a pure quantum state. The quantum mechanical algebra of vector spaces reproduces consistently all properties of polarization in the quantum mechanical description, most notably single photon interference effects [76]. At the same time the relation of electrical field amplitude to intensity, translates to the relation of wavefunction to probability density [35]. Employing the density operator formalism, it is even possible to represent partially polarized or unpolarized states as incoherent superpositions.

Bloch Sphere

For single qubit systems there exists a very useful graphic representation on the *Bloch sphere*, which is based on the fact that it is possible to represent the rotation group on the 2-dimensional complex space of qubits as discussed in subsection 2.2.2. An arbitrary pure state $|\psi\rangle$ of a qubit can be parametrized by the real parameters θ and φ as [29]

$$|\psi\rangle = \cos\frac{\theta}{2}|0\rangle + e^{i\varphi}\sin\frac{\theta}{2}|1\rangle = \cos\frac{\theta}{2}|H\rangle + e^{i\varphi}\sin\frac{\theta}{2}|V\rangle. \qquad (4.12)$$

An interpretation of these parameters as spherical coordinates on a unit sphere entails an association of qubit states with locations on the sphere as expressed in Fig. 4.1.
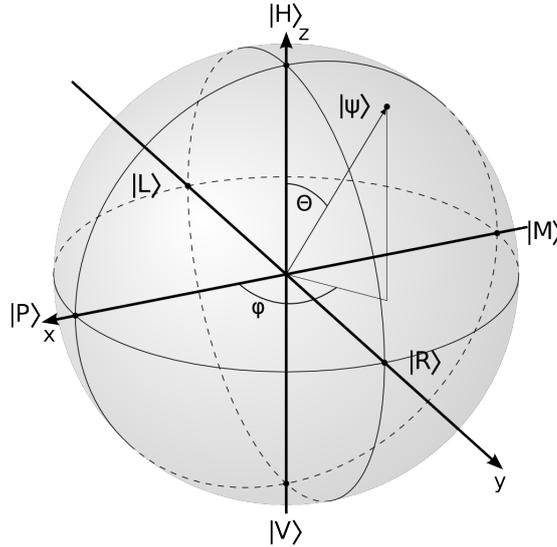
Figure 4.1.: Bloch Sphere with pure state $|\psi\rangle$ defined by the angles θ and φ. The three principal bases of polarization are identified with the three coordinate directions x, y and z. In this representation the "orthogonality" in the Hilbert Space is not equivalent to geometrical orthogonality and orthogonal quantum states lie on opposite sides of the sphere.

It should be noted that a full rotation about $\Delta\theta = 2\pi$ of the state $|\psi\rangle$ formulated above returns the system to the same location on the sphere but the resulting quantum state is $-|\psi\rangle$ and a rotation about 4π would be necessary to arrive at the exact same expression for the qubit state. While the two quantum states are effectively identical, because as mentioned in subsection 2.2.1, quantum states actually correspond to rays in Hilbert space, this property nevertheless reflects the fact that the group $SO(3)$ is only locally isomorphic to $SU(2)$ [30].

The mapping of qubit states onto three dimensional real space illustrates very well the representation of the rotation group in two dimensional complex space with the Pauli matrices as generators of state rotation. In the mapping employed in this work, the polarization states $\{|P\rangle, |M\rangle\}$ represent the eigenbasis $\{|+\rangle_x, |-\rangle_x\}$ of $\hat{\sigma}_x$, $\{|R\rangle, |L\rangle\}$ the eigenbasis of $\hat{\sigma}_y$ and $\{|H\rangle, |V\rangle\}$ the eigenbasis of $\hat{\sigma}_z$. A rotation about the angle α around axis $\vec{n}$ with $\|\vec{n}\| = 1$ can be expressed as [33, 35]

$$\hat{U} = e^{i\alpha\vec{n}\vec{\sigma}}, \tag{4.13}$$

where $\vec{\sigma}$ consists of the three Pauli matrices. This unitary operator corresponds to a rotation of a quantum state in the Bloch sphere picture.

In the density operator representation any qubit state $\hat{\rho}$ can be decomposed into a superposition of operators in the form [29, 33, 35, 74]

$$\hat{\rho} = \frac{\mathbb{1} + \vec{r}\vec{\sigma}}{2}, \tag{4.14}$$

where $\vec{r}$ is a real valued vector in three dimensional space with $\|\vec{r}\| \leq 1$, which is denoted as the *Bloch vector*. It holds that $\|\vec{r}\| = 1$ if and only if $\hat{\rho}$ is a pure state [29]. This enables the most general definition of the Bloch sphere, where each possible qubit state is uniquely represented by a corresponding point $\vec{r}$ inside the Bloch sphere with pure states lying on the surface. Because of the structural similarity to qubits, there exists a similar representation of polarization on the *Poincaré sphere*. With exception of the explicit geometrical mapping of the states, the two expressions are structurally completely equivalent and the Bloch sphere effectively represents a rotated Poincaré sphere [35].

4.1.2. Tomography Procedures

After the introduction of the polarization qubit as the relevant object system, in this subsection the tomography procedure related to weak measurements is presented and compared to conventional procedures, which employ standard measurement procedures. Both theories are presented in the context of their specific application to qubits.

Conventional Tomography

Conventional *quantum state tomography* ("QST") reconstructs the density operator $\hat{\rho}$ of an ensemble of identical systems by performing a set of measurements on different incompatible observables [71, 79]. The procedure aims to record the probabilities of different outcomes of these strong projective measurements and approximates them through relative frequencies for measurements on a number of ensembles. Because the measurement observables are incompatible, QST can perform only one type of measurement on a single system and therefore requires

a certain minimal ensemble size, to make any claims about the relevant quantum state [23].

There exists a "direct analogy" between the QST for single qubits and the measurement of polarization states, which employs the Stokes formalism [80]. In the latter a set of four intensity measurements on light of constant intensity is employed, three of which correspond to projection measurements on one of the eigenstates of the natural polarization bases mentioned in the previous subsection. The fourth measurement just measures the overall intensity of the light, which corresponds to a projection on the identity operator. In the formalism of quantum mechanics the four measured intensities $\{n_0, n_1, n_2, n_3\}$ can be expressed with probabilities multiplied by a proportionality factor $\mathcal{N}$ as [80]

$$n_0 = \frac{\mathcal{N}}{2}\mathrm{tr}(\hat{\rho}) \qquad\qquad n_1 = \mathcal{N}\mathrm{tr}(\hat{\rho}\hat{\Pi}_P)$$
$$n_2 = \mathcal{N}\mathrm{tr}(\hat{\rho}\hat{\Pi}_R) \qquad\qquad n_3 = \mathcal{N}\mathrm{tr}(\hat{\rho}\hat{\Pi}_H),$$

where the $\{\hat{\Pi}_H, \hat{\Pi}_P, \hat{\Pi}_R\}$ denote projectors onto the corresponding polarization states $\{|H\rangle, |P\rangle, |R\rangle\}$. From these intensities the Stokes parameters $\{S_0, S_1, S_2, S_3\}$ are calculated with [80]

$$S_0 = 2n_0, \quad S_1 = 2(n_1 - n_0), \quad S_2 = 2(n_2 - n_0), \quad S_3 = 2(n_3 - n_0). \qquad (4.15)$$

The density matrix $\hat{\rho}$ of the polarization state can then be written as a decomposition into Pauli matrices as [79, 80]

$$\hat{\rho} = \frac{1}{2}\sum_{j=0}^{3}\frac{S_j}{S_0}\hat{\sigma}_j, \qquad (4.16)$$

where $\hat{\sigma}_0 := \mathbb{1}$.

The same procedure can be employed to reconstruct the state of any qubit system with projections into the eigenstates of the corresponding observables $\{\sigma_x, \sigma_y, \sigma_z\}$. In particular, it is possible to measure the common polarization of single photons, where the intensity measurements are replaced by determination of frequencies of photon measurements [80]. The parameter $S_0 = \mathcal{N}$ in this case represents the normalization of these frequencies to relative frequencies, which approximate the relevant probabilities of quantum mechanical measurement.

For multi-qubit systems, represented as states in a product space of single qubit spaces, a generalized form of this procedure can be used. The n-qubit density matrix can be expressed as [80, 81]

$$\hat{\rho} = \frac{1}{2^n}\sum_{j_1,j_2,\ldots,j_n=0}^{3}\frac{S_{j_1,j_2,\ldots,j_n}}{S_{0,0,\ldots,0}}\sigma_{j_1}\otimes\sigma_{j_2}\otimes\cdots\otimes\sigma_{j_n} \qquad (4.17)$$

with the n-qubit Stokes parameters $S_{j_1, j_2, \ldots, j_n}$. These $4^n - 1$ parameters are calculated from $4^n - 1$ measured relative frequencies, which are normalized employing the parameter $S_{0,0,\ldots,0} = \mathcal{N}$. Alternatively, the coefficients $\frac{S_{j_1, j_2, \ldots, j_n}}{S_{0,0,\ldots,0}}$ can be expressed as elements of the *correlation tensor* T, which is defined with [81]

$$T_{j_1, j_2, \ldots, j_n} := \text{tr}(\rho \sigma_{j_1} \otimes \sigma_{j_2} \hat{\otimes} \ldots \otimes \sigma_{j_n}). \tag{4.18}$$

The calculation of multi-qubit Stokes parameters in standard QST represents an inversion problem for a $4^n \times 4^n$ matrix, which means that the measurement and postprocessing effort scales exponentially with the number of qubits n [24, 37, 81, 82]. For this reason various techniques have been developed to reduce the number of necessary measurements and required postprocessing in cases where additional information about the state is available [82]. Furthermore, there exist scenarios where a QST has a specific goal, as the detection of entanglement in the relevant state without the necessity of a complete reconstruction. It has been shown that in such cases the number of measurements, which are necessary to make a definitive statement, can be reduced significantly by choosing a suitable subset of only a few measurements [81].

A fundamental problem of QST is the emergence of "unphysical states", which are represented by density operator with negative eigenvalues. As discussed in subsection 2.2.1, the eigenvalues of density operators correspond to probabilities in a certain basis representation of the state and therefore operators with negative eigenvalues cannot be regarded as valid physical states. Due to the fundamental quantum shot noise, especially measurements employing small ensemble sizes exhibit a non-negligible probability of producing such unphysical operators. This motivates a series of reconstruction methods, which try to estimate the physical state that generated the measurement results with the highest probability [38, 83]. The employment of such methods, however, increases the postprocessing effort even more. Furthermore, as has been shown in [84], common state reconstruction schemes, like *maximum likelihood* or *least square optimization*, suffer from systematical errors and represent therefore a somewhat biased state reconstruction.

Concept of Direct State Tomography

Using weak measurements, it is possible to devise an alternative and fundamentally different tomography scheme, where measurements of two non-commuting observables are performed on the same quantum system. In so called *direct state tomography* ("DST") a weak measurement of one observable, which disturbs the object system only slightly, is followed by a strong measurement of the other observable [23–25, 38, 71, 73, 79]. All results gained in the former measurement are consequently divided into subensembles conditioned on different kinds of successful postselection. It should be noted that the meaning of "direct" in the context

of tomography is different from "direct measurements" as introduced in subsection 3.1.2. DST employs the usual indirect measurement for the weak part of the procedure.

The basic principle of DST for single qubits can be illustrated by decomposing a pure polarization state into corresponding weak values for the simplest case of a postselection onto a single final state. An arbitrary qubit state $|\psi\rangle$ can be written in the basis $\{|H\rangle, |V\rangle\}$ as [23, 24, 38, 73]

$$
\begin{aligned}
|\psi\rangle = & \langle H|\psi\rangle|H\rangle + \langle V|\psi\rangle|V\rangle \\
= & \frac{\langle \psi_F|\psi\rangle}{\langle \psi_F|H\rangle} \frac{\langle \psi_F|\hat{\Pi}_H|\psi\rangle}{\langle \psi_F|\psi\rangle}|H\rangle + \frac{\langle \psi_F|\psi\rangle}{\langle \psi_F|V\rangle} \frac{\langle \psi_F|\hat{\Pi}_V|\psi\rangle}{\langle \psi_F|\psi\rangle}|V\rangle,
\end{aligned}
\tag{4.19}
$$

where $\hat{\Pi}_H = |H\rangle\langle H|$, $\hat{\Pi}_V = |V\rangle\langle V|$ and $|\psi_F\rangle$ denotes the postselection state. For a choice of postselection $|\psi'_F\rangle$ that is *unbiased* with respect to the measurement basis with $\langle \psi'_F|H\rangle = \langle \psi'_F|V\rangle$, as for example $|\psi'_F\rangle = |P\rangle$, the expression simplifies to [23, 24, 38, 73]

$$
|\psi\rangle = \frac{\langle \psi'_F|\psi\rangle}{\sqrt{2}} \left(\frac{\langle \psi'_F|\hat{\Pi}_H|\psi\rangle}{\langle \psi'_F|\psi\rangle}|H\rangle + \frac{\langle \psi'_F|\hat{\Pi}_V|\psi\rangle}{\langle \psi'_F|\psi\rangle}|V\rangle \right).
\tag{4.20}
$$

A measurement in the basis $\{|H\rangle, |V\rangle\}$ is represented by the observable $\hat{\sigma}_z$ and the corresponding weak value σ_w is defined as

$$
\sigma_w := \frac{\langle \psi'_F|\hat{\sigma}_z|\psi\rangle}{\langle \psi'_F|\psi\rangle},
\tag{4.21}
$$

which implies [24, 38, 71]

$$
\frac{\langle \psi'_F|\hat{\Pi}_H|\psi\rangle}{\langle \psi'_F|\psi\rangle} = \frac{1 + \sigma_w}{2}, \quad \frac{\langle \psi'_F|\hat{\Pi}_V|\psi\rangle}{\langle \psi'_F|\psi\rangle} = \frac{1 - \sigma_w}{2}.
\tag{4.22}
$$

In conclusion the initial qubit state $|\psi\rangle$ can thus be expressed as

$$
|\psi\rangle = \mathcal{N} \left(\frac{1 + \sigma_w}{2}|H\rangle + \frac{1 - \sigma_w}{2}|V\rangle \right),
\tag{4.23}
$$

where $\mathcal{N}$ is a suitable normalization. Thus, the measurement of a single complex weak value allows the determination of both complex coefficients of the pure state.

In the context of the usual procedure of weak measurements, DST corresponds to a scenario where the preselection state is unknown and the measurement of weak values for a known postselection state allows a direct calculation of the complex state coefficients or respectively the entries of the density matrix [23, 24, 38, 71]. The real and imaginary parts of the weak value are obtained by measuring different pointer observables. In the most simple case of the linear regime of

weak measurements these quantities are simply proportional to the position and momentum shifts of the pointer system.

Apart from DST there also exists the concept of *quantum state estimation* for PPS systems, where both preselection and postselection states are not known and have to be estimated [85]. The latter, however, describes a very different problem and lies outside the scope of this thesis.

DST for Mixed Qubit States

After the general description of DST a formal derivation of the weak value dependent expression for a potentially mixed preselection state $\hat{\rho}$ is presented. For a pure postselection state $|\psi_F\rangle$ the weak value σ_w of the operator $\hat{\sigma}_z$ is defined as [26, 71, 73]

$$\sigma_w := \frac{\langle\psi_F|\hat{\sigma}_z\hat{\rho}|\psi_F\rangle}{\langle\psi_F|\hat{\rho}|\psi_F\rangle}, \tag{4.24}$$

which simplifies to the usual definition from eq. (3.44) for a pure preselection. A calculation analogous to the one presented in subsection 3.2.2 for pure preselection states, shows that in the case of mixed preselection the pointer shifts in the linear response regime have exactly the same dependence on the respective weak values as in the pure case [26, 49, 73]. The experimental strategy for the tomography of mixed qubits is the same as for pure qubits, in the sense that the corresponding weak values are extracted from the position and momentum values of the pointer state.

Because the density matrix of a qubit consists of more than 2 parameters, a single complex weak value does not suffice to determine a general qubit state. Therefore, instead of a filtering, the postselection consists in a complete strong measurement which projects onto both eigenstates of a second incompatible observable $\hat{B}$ and keeps all results [71, 73]. Effectively, this constitutes two distinct weak values, each of which is defined with respect to a different postselection state. In analogy to the formula for the pure qubit case, the density matrix is consequently expressed in dependence on the projector weak values $(\Pi_j^m)_w$ with [73, 79]

$$(\Pi_j^m)_w := \frac{\langle b_m|\hat{\Pi}_j\hat{\rho}|b_m\rangle}{\langle b_m|\hat{\rho}|b_m\rangle}, \tag{4.25}$$

where the lower index denotes the projection operator $\hat{\Pi}_j = |a_j\rangle\langle a_j|$ onto an eigenstate of the weak measurement obsevable $\hat{A}$ and the upper index the respective postselection state $|b_j\rangle$, which is an eigenstate of observable $\hat{B}$.

Using this definition, an element $\langle a_m|\hat{\rho}|a_j\rangle$ of the density operator in the measurement basis can be expressed as [73, 79]

$$
\begin{aligned}
\langle a_m|\hat{\rho}|a_j\rangle &= \sum_k \langle a_m|\hat{\rho}|b_k\rangle\langle b_k|a_j\rangle \\
&= \sum_k \langle b_k|\hat{\rho}|b_k\rangle \frac{\langle b_k|a_j\rangle}{\langle b_k|a_m\rangle} \frac{\langle b_k|\hat{\Pi}_m\hat{\rho}|b_k\rangle}{\langle b_k|\hat{\rho}|b_k\rangle} \\
&= \sum_k \langle b_k|\hat{\rho}|b_k\rangle \frac{\langle b_k|a_j\rangle}{\langle b_k|a_m\rangle}(\Pi_m^k)_w,
\end{aligned}
\tag{4.26}
$$

where the summation is performed over all eigenstates of the postselection. While here this result is obtained for a qubit system, the dimensionality of the object was of no importance for the derivation and in fact formula (4.26) is valid for any finite dimensional quantum system. The quantities, which have to be determined by measurements, are the postselection probabilities $\langle b_k|\hat{\rho}|b_k\rangle$ of the undisturbed initial state, as well as of course the weak values $(\Pi_m^k)_w$, which consist of a real and an imaginary part. In consequence $2N^2 + N$ real numbers have to be measured in this scheme for an single object system of dimensionality N, which implies a scaling of the measurement effort with N^2. It should be emphasized that in this case the number N refers to the number of dimensions of a single quantum system and not to the number of qubit systems n in conventional mulit-qubit tomography as discussed above.

In the case of a qubit object system with a weak measurement in the basis of $\hat{\sigma}_z$ and a postselection in the eigenstates of $\hat{\sigma}_x$, the full density matrix $\hat{\rho}$ of the preselection state in the basis of $\hat{\sigma}_z$ can be expressed as [24]

$$
\hat{\rho} = \begin{pmatrix} p_P(\Pi_H^P)_w + p_M(\Pi_H^M)_w & p_P(\Pi_H^P)_w - p_M(\Pi_H^M)_w \\ p_P(\Pi_V^P)_w - p_M(\Pi_V^M)_w & p_P(\Pi_V^P)_w + p_M(\Pi_V^M)_w, \end{pmatrix},
\tag{4.27}
$$

where the undisturbed postselection probabilites are defined as $p_P := \langle P|\hat{\rho}|P\rangle$ and $p_M := \langle M|\hat{\rho}|M\rangle$. Just as in the case of the pure qubit state it would suffice to measure the complex weak value σ_w with respect to both postselection states $|P\rangle$ and $|M\rangle$ to determine the respective projector weak values. Additionally, the probabilities p_P and p_M would have to be measured as well, which means that in summary the measurement of 6 real quantities is required to determine the unknown preselection qubit state in this procedure. It should be also noted that the expression presented in equation eq. (4.27) does not rely on any approximations and the quality of state determination depends only on the precision of the 6 values mentioned above.

A different and very general approach to DST, which should be also at least briefly mentioned, is the formalism formulated in [57]. The latter describes the weak interaction with a immediate pointer measurement similar to the scenario

discussed in subsection 3.2.3 as a POVM measurement on the object system. The weakness of the interaction allows an approximation of the POVM operators as linearly disturbed unity operators, which facilitates the inference of the initial quantum state from the joint probability distribution of the pointer measurements. The discussion presented in this thesis however, focuses on the exact expression form eq. (4.27).

Evaluation of DST

The main advantage of DST is the experimental and calculational simplicity reflected in eq. (4.26). Generally it is possible to determine the unknown quantum state from the measurement results with a much smaller postprocessing effort compared to QST [24, 37, 38, 86]. In contrast to QST, DST requires no global state reconstruction at all and the entries of the density matrix are obtained separately or "locally" through analytical calculation in real time [24, 71, 87]. Furthermore, the simultaneous gain of information about two complementary observables, which is reflected in the complex valued weak value, usually entails simpler experimental setups [37, 73, 86]. Therefore, DST is especially suitable for the tomography of high dimensional quantum states, where the complexity of the systems prohibits a practical application of conventional QST. Such measurements of high dimensional systems were successfully implemented in [25], where a 27-dimensional orbital angular momentum state was measured and in [87], where a DST together with a *compressed sensing* technique was employed to determine a 192-dimensional spatial wavefunction.

Apart from the mentioned advantages, however, DST as presented above also exhibits a series of disadvantages. For instance, the large uncertainty of the weak measurement entails the necessity of a large amount of measurement runs, which causes DST to be far less efficient than QST [37, 79, 87]. As discussed in chapter 3, a certain minimal amount of ensembles has to be measured to determine the weak value with sufficient precision in the linear pointer response regime. In consequence a DST, which aims to extract the weak values through linear pointer shifts, usually requires several orders of magnitude more measurement runs than a comparable QST [37, 87].

If the interaction strength ϵ is increased, the amount of necessary ensembles is reduced but as eq. (3.65) shows this causes the linear approximation to break down. In fact even for a small ϵ, suitable combinations of pre- and postselection will result in very large weak values, which will also invalidate the approximations of the linear regime [37, 38, 86]. As most DST schemes rely on a weak value measurement through linear relation to pointer shifts, they consequently exhibit a fundamental bias, which causes systematical errors in the state determination especially for states that are orthogonal or almost orthogonal to some postselection states [24, 37, 38, 79, 86].

Additionally to the approximation encountered in the measurement of the weak value, approaches to DST usually employ also a second approximation. The undisturbed postselection probabilities $\langle b_n | \hat{\rho} | b_n \rangle$, as formulated in eq. (4.26), are a universal part of most DST schemes [23, 24, 57, 73, 79]. However, they represent additional unknown quantities, which would have to be measured by postselecting the unknown quantum state without any interaction. Therefore, it is common to approximate them with the already accessible probabilities of postselection $\langle b_n | \hat{\rho}' | b_n \rangle$ for states $\hat{\rho}'$, which are weakly disturbed by the interaction. Because there is always some backaction of the weak interaction on the object system, the probability $\langle b_n | \hat{\rho}' | b_n \rangle$ is not exactly equal to $\langle b_n | \hat{\rho} | b_n \rangle$ for a finite interaction strength ϵ [23, 54, 57, 73]. Nevertheless, all approaches mentioned above approximate the postselection probabilities, assuming a negligible change due to a very weak interaction.

Qubit Weak Values

To conclude the discussion of DST for qubits, a parametrization of pure qubit weak values is presented. Recalling eq. (4.12), a polarization qubit can be expressed as

$$|\psi\rangle = \cos\frac{\theta}{2}|H\rangle + e^{i\varphi}\sin\frac{\theta}{2}|V\rangle, \tag{4.28}$$

where the parameters θ and φ correspond to angles on the Bloch sphere. For the postselection state $|P\rangle = \frac{1}{\sqrt{2}}(|H\rangle + |V\rangle)$ and observable $\hat{\sigma}_z$ the weak value σ_w of a pure preselected qubit becomes [88]

$$\sigma_w = \frac{\langle P|\hat{\sigma}_z|\psi\rangle}{\langle P|\psi\rangle} = \frac{\cos\frac{\theta}{2} - e^{i\varphi}\sin\frac{\theta}{2}}{\cos\frac{\theta}{2} + e^{i\varphi}\sin\frac{\theta}{2}} \tag{4.29}$$

As proposed in [24], the ability to perform weak tomography for pure qubits can be demonstrated by measuring the weak values of states lying on circles on the Bloch Sphere, which coincide with the 3 principal planes denoted as XY, YZ and ZX. For all pure states lying in the XY-plane, it holds that $\theta = \frac{\pi}{2}$, which implies a weak value dependence only on φ with

$$\sigma_w^{XY} = \frac{1 - e^{i\varphi}}{1 + e^{i\varphi}} = -i\tan\frac{\varphi}{2} \in \mathbb{C}. \tag{4.30}$$

In the same manner it is possible to calculate the weak values for states in the YZ-plane $(\varphi = \frac{\pi}{2})$ as

$$\sigma_w^{YZ} = \frac{\cos\frac{\theta}{2} - i\sin\frac{\theta}{2}}{\cos\frac{\theta}{2} + i\sin\frac{\theta}{2}} = e^{-i\theta}, \tag{4.31}$$

and for states in the YZ-plane $(\varphi = 0)$ as

$$\sigma_w^{ZX} = \frac{\cos\frac{\theta}{2} - \sin\frac{\theta}{2}}{\cos\frac{\theta}{2} + \sin\frac{\theta}{2}} = -\tan\frac{\tilde{\theta}}{2} \in \mathbb{R}, \tag{4.32}$$

75

with $\tilde{\theta} := \theta - \frac{\pi}{2}$.

As can be seen from eq. (4.30) and eq. (4.32), the modulus of the weak values corresponding to these planes has a similar form of angular dependence and can take arbitrary values from $[0, \infty[$. However, while the weak values from XY-plane are strictly imaginary, the states from the ZX-plane imply strictly real weak values. The weak values corresponding to the YZ-plane have a constant modulus of 1 and an arbitrary complex phase. To faithfully determine an initial pure qubit state, the DST procedure as presented in eq. (4.23) must be able to determine the weak values formulated above as exactly as possible from the measurements performed on the pointer system.

4.2. Gaussian Beam as Pointer

As presented in chapter 3, the defining characteristic of weak measurements is the pointer state after weak interaction and postselection. Therefore, the next segments are dedicated to an in-depth analysis of the pointer system used in most weak experiments so far, namely the Gaussian beam.

4.2.1. Physical Properties

In the following subsection the properties of the Gaussian beam are discussed on the foundation of a short description of the basic principle of a laser.

Laser Modes

The acronym "LASER" denotes the process of *Light Amplification by Stimulated Emission of Radiation* [77]. A schematic sketch of a typical laser oscillator is presented in Fig. 4.2.
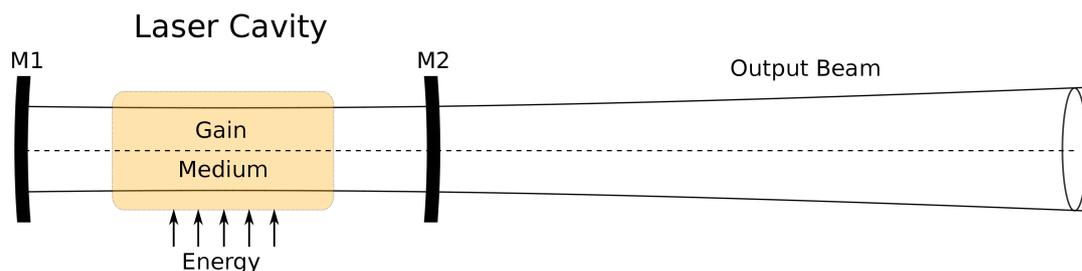
Figure 4.2.: Laser cavity with gain medium. The energy constantly pumped into the gain medium is emitted via stimulated emission into the light field inside the cavity. While mirror $M1$ has a high reflectivity, mirror $M2$ is partially transmitting, which allows a portion of the light to leave the resonator. For a similar figure see [77]

The main components consist of two mirrors forming an optical *Fabry-Perot resonator* or *cavity* with a *gain medium* inside [76–78]. The geometry of the cavity allows only specific types of resonant standing waves, which are denoted as the *modes* of the resonator. While one of the mirrors is highly reflective to minimize losses, the other mirror has a non-vanishing transmission coefficient and continuously transmits a fraction of the intensity of the resonating modes. At the same time energy is continuously delivered or *pumped* into the gain medium. As a consequence the atoms of the medium are elevated into excited states, and successively decay back into lower energy states emitting the energy in form of light into the cavity. This process, however, does not happen randomly. The presence of the light field inside the cavity *stimulates* emission of light with the same phase,

polarization and direction, which means that the same modes are continuously amplified, compensating for the losses through the partially transmitting mirror [77, 78]. With the addition of further filtering mechanisms, it is possible to attain the emission of a single well defined spatial mode with a small divergence and a very narrow frequency spectrum, which corresponds to a large coherence length [76–78].

In a typical laser cavity with spherical mirrors the possible modes can be represented as *Hermite-Gaussian* TEM_{mn} modes denoted by the two integer indices m and n [76–78]. Corresponding to the shape of the mirrors, all Hermite-Gaussian modes share the same parabolic phase dependence, where the surfaces of equal phase are denoted as *wavefronts* or *phasefronts*. The particular modes differ, however, in the numbers of nodes in their intensity profiles in x and y direction, which are represented by the two indices m and n. The field amplitude $E_{mn}(x, y)$ of a general TEM_{mn} mode can be written as [76, 77]

$$E_{mn}(x, y, z) = E_0 \frac{w_0}{w(z)} H_m\left(\sqrt{2}\frac{x}{w(z)}\right) H_n\left(\sqrt{2}\frac{y}{w(z)}\right) e^{-\frac{x^2+y^2}{w^2(z)}} e^{-ik\frac{x^2+y^2}{2R(z)}} e^{i\varphi(z)},$$
(4.33)

where H_n denotes the *Hermite polynomial* of order n and $\varphi(z)$ an additional z-dependent phase factor. The z-dependent values R and w represent the radius of the phasefront curvature and the characteristic transverse beam size called *waist*, with $w_0 := w(0)$, respectively.

Gaussian Beam

The most commonly used laser mode is the TEM_{00} mode also known as the *Gaussian beam*, which has many useful properties [76–78]. Employing eq. (4.33) with $m = n = 0$, the complex amplitude of the Gaussian Beam E_G can be written as [76]

$$E_G(x, y, z) = E_0 \frac{w_0}{w(z)} e^{-\frac{x^2+y^2}{w^2(z)}} e^{-ik\frac{x^2+y^2}{2R(z)}} e^{-i(kz-\zeta(z))}.$$
(4.34)

The particular shape of the Gaussian beam is governed by the wavelength $\lambda = \frac{2\pi}{k}$ and the waist w_0 at $z = 0$. These two parameters determine the characteristic length $z_R := \frac{\pi w_0^2}{\lambda}$, which is denoted as the *Rayleigh range* [76, 78]. The z-dependence of the parameters w, R and ζ can then be expressed in relation to z_R with [76, 78]

$$w(z) = w_0 \sqrt{1 + \left(\frac{z}{z_R}\right)^2},$$
(4.35)

$$R(z) = z \left[1 + \left(\frac{z_R}{z}\right)^2\right],$$
(4.36)

$$\zeta(z) = \arctan \frac{z}{z_R}.$$
(4.37)

The parameter ζ represents the *Guoy phase* and expresses a phase retardation of π, which the beam acquires traveling from $z = -\infty$ to $z = \infty$ in comparison to a plane wave or a spherical wave [76]. In Figure Fig. 4.3 a cross section in the xz-plane through a Gaussian beam is depicted.
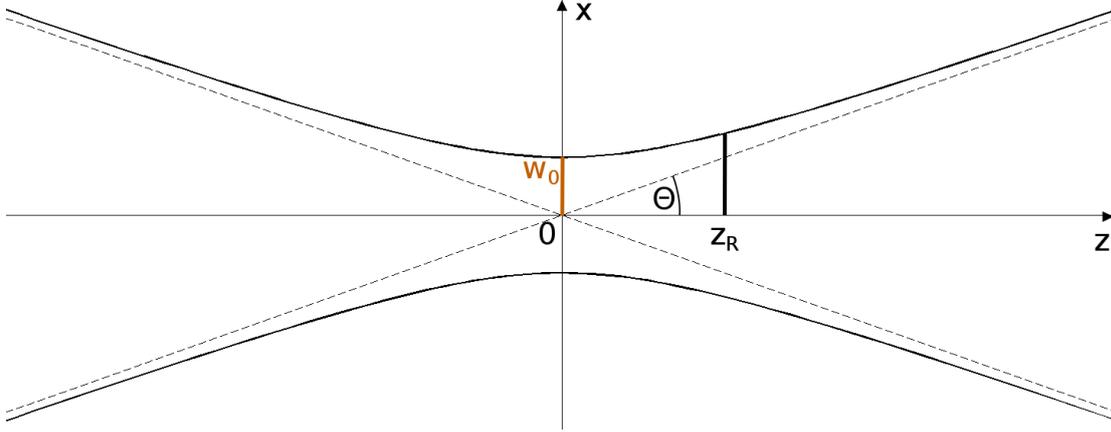
Figure 4.3.: Gaussian beam with waist w_0 in focus $z = 0$ and waist $w_{z_R} = \sqrt{2}w_0$ at $z = \pm z_R$. For $|z| \to \infty$ the beam diverges with the angle 2θ. Similar figures can be found in [76, 78]. The thick curved lines represent the waist of the beam.

As can be seen in the graphic the parameters are defined in such a way that a longitudinal position of $z = 0$ corresponds to the focus of the beam with the minimal waist w_0. For $z = z_R$ the waist of the beam is increased to $w(z_R) = \sqrt{2}w_0$. In the regions $|z| \gg z_R$ the waist is approximately linear in z and diverges on a cone described by the half angle $\theta_0 = \frac{\lambda}{\pi w_0}$ [76, 78]. The ratio of wavelength to beam waist in the focus thus determines the divergence of the beam. The radius of curvature at the focus $z = 0$ goes to infinity, which corresponds to flat phasefronts without any curvature. For $|z| \gg z_R$ the radius scales linearly with z and consequently the wavefront approximate the wavefronts of a spherical wave [76]. At $z = z_R$ the wavefront reaches its maximum curvature with a minimal radius of $R(z_R) = 2z_R$.

Transverse Wavefunction

The formulation of the spatial field amplitude of the Gaussian beam in eq. (4.34) enables the derivation of a transverse spatial wavefunction of the photons in the mode at longitudinal position z. Because the complex amplitude can be written as a product of the amplitudes in x and y direction, it is sufficient to formulate the one dimensional wavefunction $\phi_z(x)$ with

$$\phi_z(x) = \left(\frac{2}{\pi w_z^2}\right)^{\frac{1}{4}} e^{-\frac{x^2}{w_z^2}} e^{-ik\frac{x^2}{2R_z}}, \tag{4.38}$$

where all global phases were neglected and a suitable normalization was chosen with $\int_{-\infty}^{\infty} |\phi_z(x)|^2 \, dx = 1$. In the expression above the index z indicates a z-dependence of the corresponding quantities. The full transverse wavefunction Φ_z at longitudinal position z can be written as the product of the x and y wavefunctions with $\Phi(x, y) = \phi_z(x)\phi_z(y)$. The quantum states of the two spatial dimensions are thus separable and uncorrelated, which enables a separate evaluation.

A calculation of the position expectation value $x_0 := \langle \hat{x} \rangle$ and the standard deviation Δx for the one dimensional wavefunction yields

$$x_0 = 0, \quad \Delta x = \frac{w_z}{2}, \tag{4.39}$$

which allows a reparametrization with $\Delta_z := \frac{w_z}{2}$. The wavefunction then becomes

$$\phi_z(x) = \left(\frac{1}{2\pi \Delta_z^2} \right)^{\frac{1}{4}} e^{-\frac{x^2}{4\Delta_z^2}} \, e^{-ik\frac{x^2}{2R_z}}, \tag{4.40}$$

which exactly resembles the Gaussian pointer distribution introduced in chapter 3, except of course the quadratic phase term. Thus, in the focus plane with $z = 0$ the transverse spatial wavefunction of the photons in the TEM_{00} mode is represented by a standard Gaussian profile. Furthermore, the calculation of the standard deviation shows that the phase term does not influence the variance of the wavefunction, which only depends on the waist w_z.

The other set of relevant quantities are the respective expectation value $p_0 := \langle \hat{p}_x \rangle$ and standard deviation Δp in momentum space, which are calculated to

$$p_0 = 0, \quad \Delta p = \frac{\hbar}{w_0} = \frac{\hbar}{2\Delta_0}. \tag{4.41}$$

In contrast to the position uncertainty which increases as the beam travels away from the focus plane, the momentum uncertainty stays constant. A Gaussian beam therefore only saturates the uncertainty with $\Delta x \, \Delta p = \frac{\hbar}{2}$ in the focus plane.

Another quantity that is important to evaluate in the context of weak measurements is the covariance of position and momentum $c_{xp} = \text{Re}\left[\langle \hat{x}\hat{p}_x \rangle \right]$ as defined in chapter 3. Calculating the covariance in the case of the Gaussian beam yields

$$c_{xp} = -\frac{\hbar}{2} \frac{z}{z_R}, \tag{4.42}$$

which clearly shows that outside the focal plane there exists a correlation between the position and the momentum of the Beam. Furthermore, the magnitude of the covariance becomes arbitrarily large as z goes towards $\pm\infty$.

Fourier Optics

As demonstrated in subsection 2.2.2 the momentum wavefunction $\tilde{\psi}(p)$ can be obtained by a Fourier transform of the wavefunction $\psi(x)$ in position space. Therefore, to determine the momentum expectation value $\hat{p}_x$ the Gaussian Beam after

weak interaction and postselection has to be transformed. In optics there exist two principal implementations of such a Fourier transform, the *far-field* Fourier transform and the Fourier transform via a lens [76].

In the context of the theory of *Fraunhofer diffraction* it is possible to formulate the distribution of the complex amplitude $g(x, y)$ at a large enough distance $z = d$ as the Fourier transform of the field amplitude $f(x, y)$ at $z = 0$ [76, 78]. This description employs an approximation, which is valid for an initial amplitude confined to a circle with radius r_I with $\frac{r_I^2}{\lambda d} \ll 1$ and for the final amplitude confined to a circle with radius r_F, which fulfills the same restriction [76]. For a larger distance d, the regions, which are faithfully transformed, get larger and a full Fourier transform is realized in the far-field with $d \to \infty$. The complex amplitude in the far-field is then proportional to the Fourier transformed initial amplitude $\tilde{f}(k_x, k_y)$ with a parametrization as [76]

$$g(x, y) \propto \tilde{f}\left(\frac{x}{\lambda d}, \frac{y}{\lambda d}\right). \tag{4.43}$$

The other method of optical Fourier transform employs a lens with focal length $f > 0$. A lens of this type Fourier transforms the amplitude in the front focal plane into its back focal plane. The result is a proportionality relation between the two focal planes, which resembles the equation above for the far-field case [76].

The increasing correlation between position and momentum for a Gaussian beam in free space can be seen as a representation of this transformation. As the beam distance from the focus gets larger, the spatial distribution starts to resemble the momentum distribution more and more. Because of the large distance d and the huge waist due to the divergence, a measurement of the beam in the far-field is highly impractical. Therefore, in experimental setups the momentum space is accesses via a Fourier lens [24, 38].

4.2.2. Pointer Response

After establishing a description of the physical properties of the Gaussian beam, it is possible to evaluate this specific type of pointer in the context of the theory of weak measurements.

Exact Shifts

In the following paragraphs, a calculation of the exact shifts δx and δp in position and momentum space after a PPS measurement is presented. The expressions are formulated for an interaction represented by the qubit observable $\hat{\sigma}_z$ characterized by the weak value σ_w. The weak value is constituted by arbitrary pre- and postselection states $|\psi_I\rangle$ and $|\psi_F\rangle$, which are parametrized as

$$|\psi_I\rangle := \alpha|H\rangle + \beta|V\rangle, \quad |\psi_F\rangle := \gamma|H\rangle + \delta|V\rangle. \tag{4.44}$$

4. Direct State Tomography

Consequently the weak value can be written as

$$\sigma_w = \frac{\langle \psi_F | \hat{\sigma}_z | \psi_I \rangle}{\langle \psi_F | \psi_I \rangle} = \frac{\alpha \gamma^* - \beta \delta^*}{\alpha \gamma^* + \beta \delta^*}. \tag{4.45}$$

Continuing from the formulation of the final pointer state $|\Phi_F\rangle$ after postselection as expressed in eq. (3.37), the final pointer state in the case of a $\hat{\sigma}_z$ interaction becomes

$$|\Phi_F\rangle = \mathcal{N} \left(\alpha \gamma^* |\Phi_{+\epsilon}\rangle + \beta \delta^* |\Phi_{-\epsilon}\rangle \right) \tag{4.46}$$

with the normalization coefficient $\mathcal{N} = (|\alpha \gamma^*|^2 + |\beta \delta^*|^2 + 2\mathrm{Re}\left[\alpha \beta^* \gamma^* \delta \langle \Phi_{-\epsilon} | \Phi_{+\epsilon} \rangle\right])^{-\frac{1}{2}}$. The expectation value of a pointer observable $\hat{q}$ can thus be calculated as

$$\langle \hat{q} \rangle_F = \frac{|\alpha \gamma^*|^2 \langle \Phi_{+\epsilon} | \hat{q} | \Phi_{+\epsilon} \rangle + |\beta \delta^*|^2 \langle \Phi_{-\epsilon} | \hat{q} | \Phi_{-\epsilon} \rangle + 2\mathrm{Re}\left[\alpha \beta^* \gamma^* \delta \langle \Phi_{-\epsilon} | \hat{q} | \Phi_{+\epsilon} \rangle\right]}{|\alpha \gamma^*|^2 + |\beta \delta^*|^2 + 2\mathrm{Re}\left[\alpha \beta^* \gamma^* \delta \langle \Phi_{-\epsilon} | \Phi_{+\epsilon} \rangle\right]}. \tag{4.47}$$

The relevant quantities, which need to be evaluated for the calculation of the expectation value shifts, are $\langle \Phi_a | \hat{x} | \Phi_b \rangle$ and $\langle \Phi_a | \hat{p}_x | \Phi_b \rangle$. Employing the analysis presented in (A.1.2) the expectation values can be expressed as

$$\langle \hat{x} \rangle_F = \frac{\epsilon \left(|\alpha \gamma^*|^2 - |\beta \delta^*|^2 \right) - 2\epsilon \mathrm{Im}\left[\alpha \beta^* \gamma^* \delta\right] \frac{z}{z_R} e^{-\frac{\epsilon^2}{2\Delta_0^2}}}{|\alpha \gamma^*|^2 + |\beta \delta^*|^2 + 2\mathrm{Re}\left[\alpha \beta^* \gamma^* \delta\right] e^{-\frac{\epsilon^2}{2\Delta_0^2}}}, \tag{4.48}$$

$$\langle \hat{p}_x \rangle_F = \frac{\frac{\hbar \epsilon}{\Delta_0^2} \mathrm{Im}\left[\alpha \beta^* \gamma^* \delta\right] e^{-\frac{\epsilon^2}{2\Delta_0^2}}}{|\alpha \gamma^*|^2 + |\beta \delta^*|^2 + 2\mathrm{Re}\left[\alpha \beta^* \gamma^* \delta\right] e^{-\frac{\epsilon^2}{2\Delta_0^2}}}. \tag{4.49}$$

A substitution of the weak value expressions derived in (A.2.1) yields the final exact expressions for the pointer shifts with

$$\langle \hat{x} \rangle_F = \frac{\epsilon \mathrm{Re}\left[\sigma_w\right] - \epsilon \mathrm{Im}\left[\sigma_z\right] \frac{z}{z_R} e^{-\frac{\epsilon^2}{2\Delta_0^2}}}{1 - \frac{1}{2}(1 - |\sigma_w|^2)(1 - e^{-\frac{\epsilon^2}{2\Delta_0^2}})}, \tag{4.50}$$

$$\langle \hat{p}_x \rangle_F = \frac{\frac{\hbar \epsilon}{2\Delta_0^2} \mathrm{Im}\left[\sigma_z\right] e^{-\frac{\epsilon^2}{2\Delta_0^2}}}{1 - \frac{1}{2}(1 - |\sigma_w|^2)(1 - e^{-\frac{\epsilon^2}{2\Delta_0^2}})}. \tag{4.51}$$

The two formulas describe the dependence of the Gaussian beam pointer on the weak value of the system for interactions of arbitrary strength ϵ. An expansion in orders ϵ confirms that they exactly match the approximations for the linear regime of weak measurements (3.51) and (3.53). In the case of the position shift it is necessary to employ the covariance for the Gaussian beam calculated in eq. (4.42). Furthermore, this results agree with the explicit expression for the

position shift in the case of a Gaussian profile calculated in [26], which, however, does not consider the z-dependent curvature.

The quadratic phase term in eq. (4.38), which is responsible for the correlation, has its origin in the manner in which the pointer evolves propagating through space. This evolution increases the dependence of the shift on the imaginary part of the weak value, which is initially only present in the momentum shift. For $|z| \rightarrow \pm\infty$ the position shift is totally dominated by the imaginary part of the weak value, which exactly corresponds to the far-field Fourier transform into the momentum space.

Interaction Regimes

For a real weak value σ_w increasing from 0 to ∞, the response of the Gaussian pointer in the focus plane with $z = 0$ is presented in Fig. 4.4 according to eq. (4.50).

As can be seen from Fig. 4.4 the linear approximation of the shifts eventually breaks down in all cases, when the magnitude of the weak value becomes too large [26, 49, 61, 89]. In the case of purely imaginary weak values, the same behavior is expected in momentum space. For a certain weak value a maximal displacement of the pointer is achieved and $|\langle \hat{x} \rangle_F|$ begins to drop towards 0 with further increasing weak values [26, 49]. A calculation of the gradient of the exact expressions (4.50) and (4.51) yields the extremal shifts $\{\delta x_{ex}, \delta p_{ex}\}$ and the corresponding weak values $\sigma_w^{(x,ex)}, \sigma_w^{(p,ex)}$ depending on the parameter $\frac{\epsilon}{\Delta}$ with

$$\delta x_{ex} = \pm \frac{\epsilon}{\sqrt{1 - f(\epsilon)}} \qquad\qquad \delta p_{ex} = \pm \frac{\frac{\hbar\epsilon}{2\Delta_0^2} e^{-\frac{\epsilon^2}{2\Delta_0^2}}}{\sqrt{1 - f(\epsilon)}}$$

$$\sigma_w^{(x,ex)} = \pm \sqrt{\frac{1 + f(\epsilon)}{1 - f(\epsilon)}} \qquad\qquad \sigma_w^{(p,ex)} = \pm i \sqrt{\frac{1 + f(\epsilon)}{1 - f(\epsilon)}},$$

where $f(\epsilon) := e^{-\frac{\epsilon^2}{\Delta_0^2}}$. These expressions agree with the extremal shifts calculated in [70]. For $\epsilon > 0$ these extremes always exist and always correspond to weak values outside of the spectrum of eigenvalues $[-1, 1]$ with $\frac{1+f(\epsilon)}{1-f(\epsilon)} > 1$, $\forall \epsilon > 0$.

In Fig. 4.4 the estimation of the validity of the linear regime provided in eq. (3.65) is confirmed and the approximation appears valid for $|\sigma_w| \leq 0.1 \frac{\Delta}{\epsilon}$. However, as can be seen in Fig. 4.5, where the region of small real weak values with $|\sigma_w| < 1$ is presented, for sufficiently large $\frac{\epsilon}{\Delta}$, the linear approximation is also incorrect in the case of small weak values.

The latter behavior is caused by the non-vanishing expression $1 - |\sigma_w|^2$ in the denominators of the eqs. (4.50) and (4.51) for $|\sigma_w| \ll 1$. This constitutes a

Mean x-Position: δx / ε
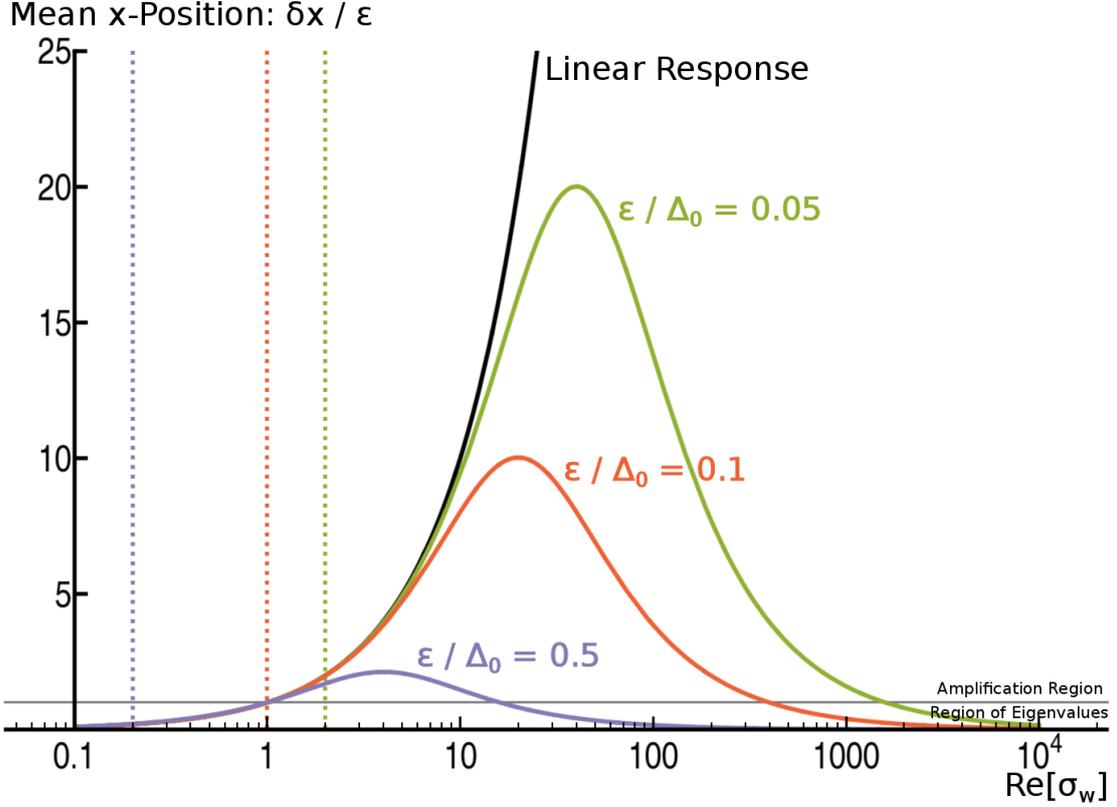
Figure 4.4.: Mean values of pointer position for strictly real weak values and three different interaction strengths $\frac{\epsilon}{\Delta_0}$. For comparison also the approximate linear response of the pointer is plotted as well. The dashed lines represent the values where the weak values are exactly one order of magnitude smaller than the boundaries given by the condition for weak measurements, so that $0.1\frac{\Delta_0}{\epsilon} = |\sigma_w|$. The horizontal line at $\frac{\delta x}{\epsilon} = 1$ denotes the boundary of the amplification region with pointer shifts beyond the range of eigenvalues $[-1, 1]$.

violation of the other condition for the linear response eq. (3.63), which in the case of $\hat{A} = \hat{\sigma}_z$ can be expressed as

$$\frac{\epsilon}{\Delta} \ll |\sigma_w|. \tag{4.52}$$

The region where the shift of the pointer exceeds the range of the eigenvalues $[-1, 1]$ is denoted as the *amplification region*. Considering Fig. 4.4, it can be seen that for sufficiently small interaction parameters $\frac{\epsilon}{\Delta}$, there exists a considerable overlap between the amplification region and the linear response regime. This property is used in weak amplification techniques, which will be briefly presented below.

As mentioned in subsection 4.1.2, the role of the pointer shifts in tomography is the determination of weak values and the unavoidable breakdown of the ap-
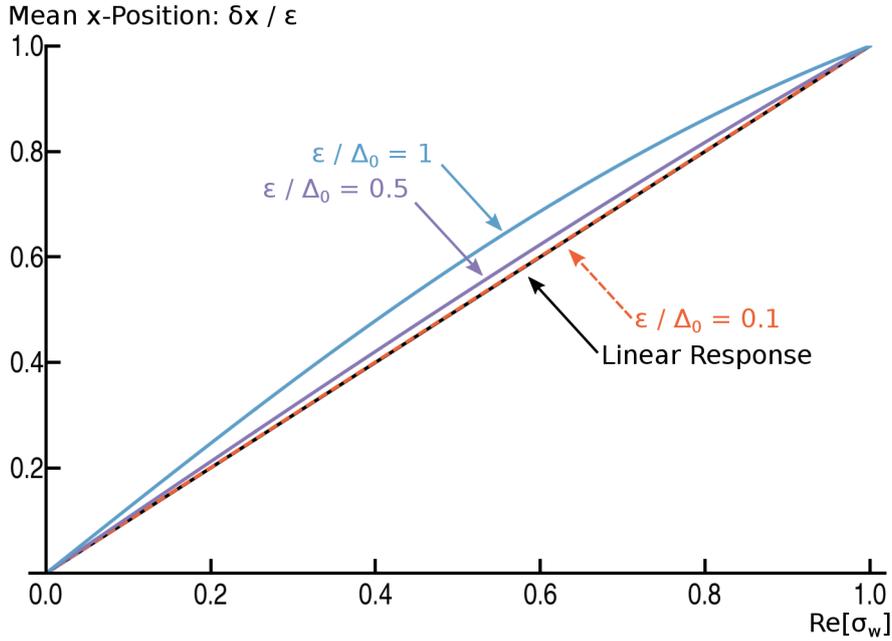
Figure 4.5.: Mean values of pointer position for small real weak values $\sigma_w \in [0, 1]$ and three different interaction strengths $\frac{\epsilon}{\Delta_0}$. The curve for $\frac{\epsilon}{\Delta_0} = 0.1$ is dashed to make it distinguishable from the linear response curve.

proximation for a subset of states causes a bias in procedures relying on the linear regime. In Fig. 4.6 the probability distribution for qubit weak values is given for the case of postselection onto $|P\rangle$ and random pure preselection states equally distributed over the surface of the Bloch sphere.

The low probability of finding a weak value outside of a relatively small interval around 0, validates the assumptions that in the case of qubits, large weak values will be sufficiently rare and most unknown states will be determined with good precision. If the pointer response is well known as in the case of the Gaussian pointer presented in this work, it is possible to reduce the bias in state determination even further by inverting the functional dependence of the shifts on the weak values, thus gaining precise expressions for the determination of the latter from the shifts. This approach, however, is limited by the fact that the pointer response curve as presented in Fig. 4.4 is not injective over the whole region of weak values. While the precision of the state determination could be increased by considering the exact response curve up to the maximum, the shifts caused by the very rare larger weak values would be falsely attributed to lower ones.

Another approach, which aims to remove the bias of DST, is the introduction of *coupling-deformed pointer observables* as presented in [79, 86]. The basic principle of the latter is to avoid the measurement of usual observables as $\hat{x}$ or $\hat{p}_x$, and to modify the measurement apparatus instead in such a way that effectively
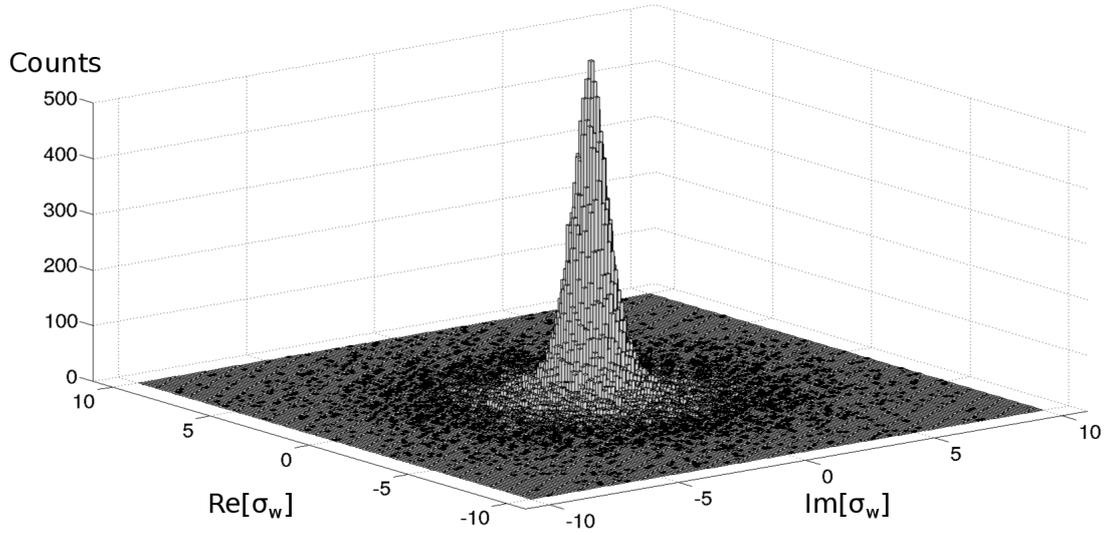
Figure 4.6.: Distribution of weak values for qubits obtained via a Monte-Carlo simulation of 10^5 random initial qubit states, equally distributed over the Bloch-sphere. As can be seen, large moduli of weak values are very improbable and most initial states imply weak values with moduli in the range $[0, 5]$. Similar diagrams for random pre- and postselection can be found in [88].

a different type of measurement is realized. An exact knowledge of the pointer response behavior for the usual observables allows a precise definition of the new coupling deformed observables, which cause a linear pointer response ideal for the purpose of DST. As the authors claim, the necessary experimental modification is small and a huge advantage lies in the possibility to introduce a stronger inter-action leading to a higher efficiency of the DST [79, 86]. In this work however, a different procedure based on the inversion of the exact pointer response expressions is presented below, which allows the precise and unbiased reconstruction of arbitrary pure qubit states.

Exact DST Procedure

In contrast to DST procedures for qubits that include mixed states as expressed in eq. (4.27), the tomography of pure qubits does not require two distinct types of postselection. For the determination of the unknown state the measurement of a single complex weak value is sufficient as described in eq. (4.23). Therefore, a second measurement result provided by another measurement with a different postselection is redundant and can be used in cases where the first measurement is imprecise. In the scheme proposed in [24] the probability factors $\langle \psi_F | \hat{\rho} | \psi_F \rangle$ from eq. (4.27), which scale the contribution of the respective weak value according to

the probability of successful postselection, filter the incorrect measurement results obtained for close to orthogonal postselection. While this approach mitigates the greatest part of the error, some bias is still left because of the reliance on linear approximations for the pointer shifts and the approximation for the undisturbed postselection probability as discussed in subsection 4.1.2.

The approach presented in this thesis also proposes the conduction of a second postselection on a state orthogonal to the first postselection. In the case of the postselection states $|P\rangle$ and $|M\rangle$, the pointer response for an initial qubit state in the ZX-plane of the Bloch sphere, parametrized by the angle θ, is presented in Fig. 4.7.
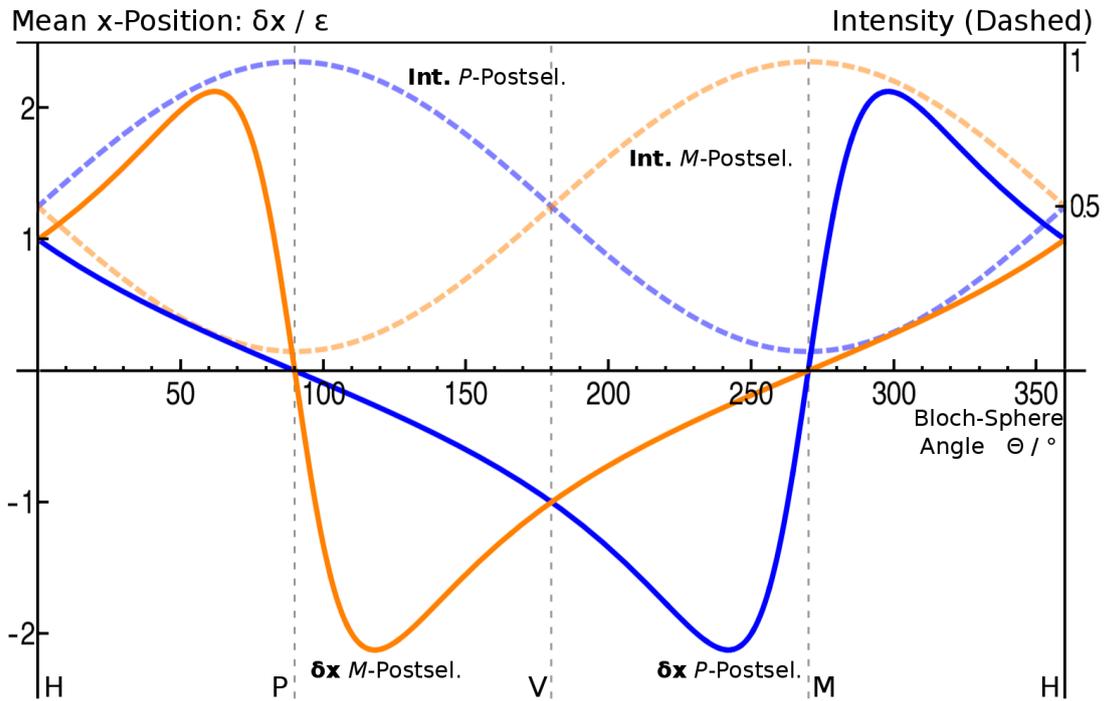
Figure 4.7.: Shifts of mean pointer x-position in dependence of Bloch sphere angle θ of the initial state. The solid lines represent the shifts for P- (blue) and for M-postselection (orange). The dashed lines signify the postselection probabilities, which are proportional to the measured intensities. The vertical lines mark the positions of the principal polarization states on the horizontal axis of the diagram. For P-postselection the intensity is higher in the region $\theta \in [0, 180°]$, in which the response curve is fully invertible and vice versa for M-postselection.

The diagram illustrates that in the region with $\theta \in [0, 180°]$, where one of the response curve for M-postselection is not injective the curve for the P-postselection can be inverted and vice versa for $\theta \in [180°, 360°]$. An exact tomography procedure would thus compare the probabilities of the two postselections and choose the one that yielded the higher postselection probability for the state determination.

4. Direct State Tomography

As presented in detail in (A.2.2), in this Boolean scheme the two kinds of postselections lie on opposite sides of the Bloch sphere and effectively divide the latter into two halves. Only states from the region closer to the respective postselection state are determined from the data acquired using this particular postselection. It has been calculated above that the maximal pointer shift and thus the point until which the response curve can be inverted, lies always in the region of amplification and corresponds to a weak value outside the range of eigenvalues. As also presented in (A.2.2), preselection states, for which such weak values are obtained, are located in the half of the Bloch sphere that is opposite to the postselection state as well. This is also confirmed by the formulas for the qubit weak values on the three principal Bloch planes as presented in eq. (4.30), (4.31) and (4.32).

Combining the equations (4.50) and (4.51) and keeping only solutions corresponding to response regions without amplification yields

$$\sigma_w = \mathcal{A}_\sigma\Big(\langle x\rangle_F, \langle \hat{p}_x\rangle_F\Big)\, e^{i\varphi_\sigma\big(\langle x\rangle_F, \langle \hat{p}_x\rangle_F\big)}, \tag{4.53}$$

with the explicit form of the functions $\mathcal{A}_\sigma$ and φ_σ calculated explicitly in (A.2.3). The expression (4.53) represents an exact analytical formula for the calculation of weak values from measured shifts of Gaussian pointers. Successively the corresponding weak values can be inserted into eq. (4.23) or a similar formula for the case of postselection into $|M\rangle$ to calculate the unknown state. Together with the Boolean decision scheme based on the amount of postselection probability they constitute an exact and unbiased state determination scheme via weak measurements.

Weak Amplification

Although the procedure of weak amplification has a different purpose than QST, the methods share the same dependence on pointer systems and therefore the basics of this experimental method are briefly discussed at this point. Contrary to QST in the experimental scenario of high precision metrology the unknown quantity is not a quantum state but rather the interaction between two systems, which can be parametrized by the interaction parameter ϵ [26, 38, 90, 91]. Considering one of the systems as the object system in a well known preselection state and the other system as the pointer, ϵ can usually be determined from the measured pointer shift. A reorganization of eq. (3.30) yields

$$\epsilon = \frac{\delta x}{\langle \hat{A}\rangle} \tag{4.54}$$

with the measured pointer shift δx and the expectation value of operator $\hat{A}$ depending on the preselection state of the object system and the interaction observable $\hat{A}$. In principle, employing this relation, it is possible to measure arbitrarily

weak interactions if the properties of the object and pointer systems are well known.

For ideal measurement devices the uncertainty in the determination of δx due to statistical shot noise can be reduced by a high enough number of measurements as discussed in subsection 3.1.3. However, usually there exist technical restrictions denoted as *technical noise*, which limit the resolution of the measurement on the pointer [90–92]. In general any experimental implementation of a pointer measurement has a lower resolution limit δ, which cannot be overcome , no matter how many measurement runs are conducted. In such a case, as already proposed in [4], the introduction of a postselection, which constitutes a large weak value A_w in the object system, can amplify the pointer shift above the technical resolution limit, allowing a measurement of the interaction strength [9, 38, 90–93]. The necessary magnitude of the weak value can be estimated employing eq. (3.52) as

$$\delta x > \delta \quad \Rightarrow \quad \text{Re}\,[A_w] > \frac{\delta}{\epsilon}. \tag{4.55}$$

This expression is only valid in the linear response regime and it has to be made sure that the effective process still constitutes as weak measurement, which, however, can be easily accomplished by tuning the pointer uncertainty Δx so that condition (3.65) is fulfilled.

While this method allows experimental sensitivity beyond the usual measurement resolution, it should be noted that it has the same dependence on statistical noise as an unamplified measurement. In fact, in the case of an ideal pointer measurement the larger shift is exactly balanced by the lower number of statistics due to filtering postselection [38, 58, 90–92, 94]. Therefore, the method of weak amplification provides neither an advantage nor a disadvantage if the major source of experimental errors is quantum statistical noise. Still a certain benefit of weak amplification lies in the fact that the same resolution is obtained with just a fraction of measurement events, which can be useful if the detection device cannot accommodate arbitrarily large measurement frequencies [38, 70]. If, however, technical noise is a limiting factor on the measurement resolution, weak amplification can increase the resolution by several orders of magnitude and thus represents a very useful experimental technique as has been demonstrated in various experiments [22, 91–93, 95].

In this context it should be noted that in the exact tomography scheme presented above, only the unamplified response region is employed. It is generally difficult to combine tomography methods with weak amplification because of the unavoidable breakdown of injectivity in the region of large weak values. However, considering a scenario with dominant technical noise, an arbitrary number of ensembles and an adjustable postselection, it is possible to devise a tomography scheme that incorporates the benefits of weak amplification. In this procedure the postselection is carefully varied until it is possible to measure a pointer shift

in an invertible regime. In consequence, it is possible to extract the weak value from the amplified pointer shift, which allows the subsequent calculation of the coefficients of the unknown pointer state, knowing of course, which postselection state was set.

4.3. Tomography Experiment

The introduction of polarization qubits as the object system alongside suitable procedures for their tomography and the subsequent account of the properties of a Gaussian beam pointer in the previous sections are now complemented by the presentation of the tomography experiment conducted during this thesis.

4.3.1. Description of Experiment

The presentation of the experiment begins with a short overview over the experimental setup together with a brief discussion of the relevant optical components.

Basic Principle

The aim of the experiment is to demonstrate the ability of DST for pure polarization qubits by reproducing the experimental procedure presented in [24]. Similar to the approach in the original experiment, the idea is to prove the performance of the procedure by faithfully measuring the polarization state of the pure states on the principal axes of the Bloch sphere as parametrized in section 4.1. Because of the analytical relation between the pointer response curves, the corresponding weak values and the complex state coefficients, it is in fact sufficient to demonstrate a successful measurement of the expected pointer response curves for the set of polarizations mentioned above. After it has been shown that the pointer system behaves as expected and that this behavior is measurable with sufficient accuracy, a tomography procedure would simply consist in the reversal of this measurement process with a succeeding calculation of the respective state coefficients or density matrix. With this experimental setup both the original procedure for mixed state presented in [24], and the exact DST procedure presented above would be possible to realize.

The pointer system employed in this DST is the one dimensional horizontal spatial degree of freedom of photons, denoted as the x-direction. Object and pointer system thus represent different degrees of freedom of the same particles, which means that the direct destructive pointer measurement has to be conducted after the postselection. The measured pointer observables are position $\hat{x}$ and momentum $\hat{p}_x$ with momentum as the generator of the interaction. The interaction operator is $\hat{\sigma}_z$, which implies that the polarization is correlated with a translation of the spatial wavefunction in x-direction. It should be noted that such an experimental configuration in the context of weak measurements was already used in the first realization of weak measurements in [21], however, without the measurement of the momentum of the pointer.

4. Direct State Tomography

Setup

In Fig. 4.8 the experimental setup is presented.
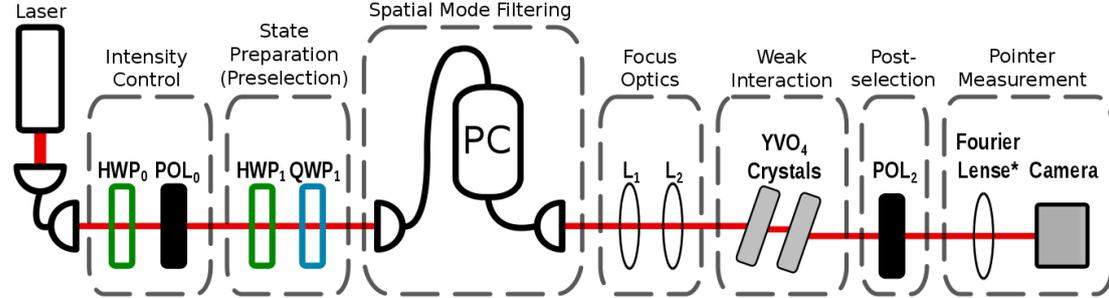
Figure 4.8.: Experimental setup for the DST experiment. The half wave plate HWP_0 rotates the polarization leaving the first fiber, to vary the amount of intensity passing through the V-polarizer (POL_0). The two wave plates HWP_1 and QWP_1 are used to rotate the V-polarization state into an arbitrary different pure polarization state, which represents the preselection. After the spatial mode filtering in the second fiber along with the polarization compensation provided by the compensator (PC), the beam is coupled out into the region of interaction, where it is focused on the camera employing the two lenses L_1 and L_2. The weak interaction is created by two YVO_4 crystals and the successive postselection is provided by the P-polarizer (POL_2). Eventually the position distribution is measured on the camera without the Fourier lens, which is subsequently inserted into the setup for a measurement of pointer momentum.

The laser light is collected into a fiber and diverted to the intensity control region, where it is coupled out having acquired some random polarization. The following half wave plate rotates the polarization, which changes the amount of intensity transmitted by the subsequent V-polarizer as long as the initial polarization is not circular. This combination of waveplate and polarizer therefore effectively constitutes a method to gradually tune the intensity of the beam. A combination of another half wave plate and a quarter wave plate is used to rotate the vertically polarized state to an arbitrary pure state on the Bloch sphere as described below. In this way, the preselection state is prepared and the rest of the setup is designed not to change this polarization state anymore until the weak measurement.

The beam is coupled into another fiber to restore the shape of the mode, which is necessarily disturbed by the preceding optical components. However, the fiber performs a random rotation of polarization and therefore additional polarization compensation is required. As presented below, the latter is achieved by the mechanical polarization compensator and the set of subsequent crystals, which are primarily used to perform the weak interaction.

The restored Gaussian beam is coupled out of the fiber, focused by a pair of lenses and directed onto a second set of crystals, which apply the weak interaction. By displacing the H and V components of the polarization by different amounts in x-direction, these crystals weakly correlate the polarization with the position of the photons. After postselecting with another P-polarizer, the spatial probability distribution of the beam is measured. For this position measurement the beam is focused on the camera, which allows to measure the real part of the weak value without any contribution from the imaginary part. To measure the momentum distribution a third lens is positioned in such a way that its front focal plane coincides with the camera position of the position measurement. A measurement of the spatial distribution at the back focal plane with the camera consequently measures the Fourier transform of the initial distribution, which corresponds to the momentum.

From these intensity distributions the position and momentum expectation values in x-direction are calculated, which allow the determination of the pointer response curves. Subsequently, the theoretical models for the pointer response are fitted onto the data to demonstrate the measurement of the expected pointer response for the prepared preselection states.

Laser System

The employed laser system consists of a *grating stabilized* laser diode. In the *external cavity method* a certain wavelength of the emitted light is selected and reflected back into the resonator to stimulate the amplification of a narrow wavelength spectrum [96, 97]. This *feedback* can be accomplished by different setups, one of which is the *Littrow configuration*, which uses a *blazed grating* to selectively reflect the first diffraction order of a certain wavelength back into the source [78, 96, 97]. The blazing of the grating, which consists in a sawtooth profile on the grating surface, shifts the maximum of intensity from the $0th$ order to a different order of diffraction for a particular wavelength [78, 98].

A part of the remaining intensity leaves the resonator by diffraction in other orders and is coupled into an optical fiber. Such a setup effectively constitutes the filtering of a very small wavelength range in the resonator [96, 97]. The employed laser diode thus emits approximately monochromatic light with a wavelength of about 805 nm.

Fibers and Couplers

Optical fibers are cylindrical optical waveguides consisting of a transparent cylindrical core enclosed by transparent cladding. Because the refraction index n_1 of the core is higher than the refraction index n_2 of the cladding, light falling on the core-cladding boundary under an angle large enough is reflected totally, which enables a guided light propagation with very few losses [76, 78, 99]. Only light

which enters the fiber with an angle of incidence with the fiber axis smaller than the critical angle $\theta_C = \arcsin(\frac{n_2}{n_1})$ is guided through the fiber. Furthermore, the fiber cannot be curved too much or the condition for total reflection breaks down as well [76, 99].

Light in fiber propagates in the form of light modes, each of which maintains its spatial distribution [76, 99]. If the core diameter of the fiber is small enough, only the fundamental mode is guided and the fiber is denoted as a *single mode* fiber in contrast to *multi mode* fibers, which allow the simultaneous propagation of several distinct modes. Since the fundamental mode in fibers resembles the Gaussian TEM_{00} mode, a single mode fiber can be used to restore a distorted Gaussian beam [76]. Because of the relatively small waist of the beam in the single mode fiber, standardized *fiber couplers* are used to couple light into and out of optical fibers. Couplers consist of a mount to fix the fiber and a lens that is used to focus or collimate the highly dispersive beam leaving or coming into the fiber.

Due to random stress and imperfections the propagation of polarized light through a usual single mode fiber results in a random rotation of the polarization [76]. Using a polarization compensator, which induces additional controlled mechanical stress, in principle it is possible to vary this polarization rotation until the fiber effectively conserves the polarization state. Such a procedure, however, involves a process of random trial and error and is not very time efficient. Therefore, in experimental reality, it is much more practical to use the mechanical polarization compensator only to achieve a conservation of polarization for two states of a linear polarization basis and use an additional device to compensate for the remaining phase difference, which the fibers still introduces between the two basis states. This phase compensation in the experiment is achieved by the pair of birefringent crystals after the fiber as will be presented below.

Waveplates

The operating principle of *wave plates* or *wave retarders* consists in the introduction of an additional phase between two orthogonal components of linear polarization for a specific wavelength [76, 78]. While *half wave plates* introduce a phase of π and thus can be used to rotate the axis of linear polarization, *quarter wave plates* introduce a phase of $\frac{\pi}{2}$ enabling a conversion from linear to circular polarization. However, the action of waveplates on general elliptically polarized light is more complex and can be described by certain transformation matrices [35, 76]. For the configuration employed in the state preparation of this setup, which consists of a half wave plate acting on a linear polarization followed by a quarter wave plate, the transformation matrix $\hat{T}$ can be expressed as $\hat{T}(\theta_H, \theta_Q) = \hat{T}_Q(\theta_Q) \cdot \hat{T}_H(\theta_H)$, where $\hat{T}_H$ and $\hat{T}_Q$ denote the transformations induced by the single waveplates and θ_H and θ_Q the corresponding rotation angles of the waveplates with respect

to the horizontal polarization direction. The unitary transformation matrices of the waveplates can be expressed in the $\{|H\rangle, |V\rangle\}$ basis as [35]

$$\hat{T}_H(\theta_H) := \begin{pmatrix} \cos(2\theta_H) & \sin(2\theta_H) \\ \sin(2\theta_H) & -\cos(2\theta_H) \end{pmatrix}, \tag{4.56}$$

$$\hat{T}_Q(\theta_Q) := \begin{pmatrix} \cos^2(\theta_Q) - i\sin^2(\theta_Q) & (1+i)\cos(\theta_Q)\sin(\theta_Q) \\ (1+i)\cos(\theta_Q)\sin(\theta_Q) & \sin^2(\theta_Q) - i\cos^2(\theta_Q) \end{pmatrix}. \tag{4.57}$$

It should be noted that the matrices in [35] are formulated for a different definition of the circular polarizations, which means that the matrix $\hat{T}_Q$ is conjugated.

For an initial vertical polarization $|V\rangle$ all linear polarizations $|\psi_L\rangle$ in the ZX-plane of the Bloch sphere can be obtained by removing the quarter wave plate and simply rotating the half wave plate with $|\psi_L\rangle = \cos(2\theta'_H)|H\rangle + \sin(2\theta'_H)|V\rangle$, where $\theta'_H := \theta_H - \frac{\pi}{4}$. With the rotation angle $\theta''_H := -\theta_H + \frac{\pi}{4}$ of the half wave plate, an introduction of the quarter wave plate at angle $\theta_Q = 0$ entails the state $|\psi_{YZ}\rangle = \cos(2\theta'_H)|H\rangle + i\sin(2\theta'_H)|V\rangle$, which corresponds to states in the YZ-plane. Eventually states $|\psi_{XY}\rangle = \frac{1}{\sqrt{2}}(|H\rangle + \exp(i4\theta'''_H)|V\rangle)$ on the XY-plane can be obtained by turning the quarter wave plate to $\theta_Q = \frac{\pi}{4}$, with $\theta'''_H := -\theta_H - \frac{\pi}{8}$. The combination of the two waveplates, therefore, allows the preparation of all pure qubit states described in subsection 4.1.2 necessary for the evaluation of the tomography procedure.

Polarizers

Devices that allow the filtering of a single well defined polarization states are denoted as *polarizers*. There exist a range of possible principles for the implementation of polarizers, such as selective absorption (*dichroism*), reflection, scattering and birefringence, which all have to exhibit an asymmetry with the respect to the relevant polarization and the component orthogonal to it [78]. The polarizers employed in this experiment are dichroic polarizers with a coating of identically oriented prolate silver particles, which absorb photons that exhibit a certain linear polarization [100]. By rotating the polarizer it is therefore possible to use it as a polarization filter for arbitrary linear polarizations.

Focusing Procedure

As can be seen from the explicit expression for the pointer position (4.50) there is always a contribution of the imaginary part of the weak value to the position expectation value for all longitudinal z-positions of the Gaussian beam with $z \neq 0$. Therefore, the experimental strategy is to focus the beam onto the camera in order to assure an undisturbed measurement of the real part of the weak value. This is realized by a pair of plano-convex lenses, each with a focal length of 20 cm as presented in Fig. 4.9.
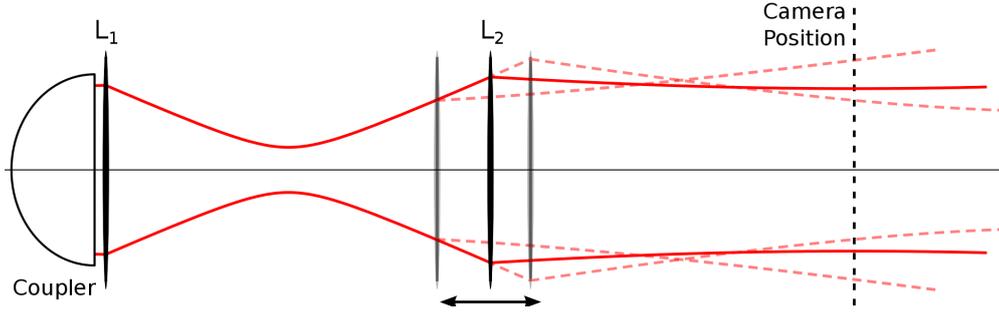
Figure 4.9.: Schematic focusing procedure of the Gaussian beam onto the camera using the lenses L_1 and L_2 with focal lengths of 20 cm. Lens L_2 is gradually displaced until the focal plane of the beam coincides with the camera position. The solid red line represents the desired scenario while the dashed lines correspond to not-optimal lens positions.

The exact positioning of the focal plane onto the camera is achieved by weak measurement. In the case of the employed P-postselection, the preselection states $|R\rangle$ and $|L\rangle$ imply the strictly imaginary weak values $-i$ and i, as can be seen from eq. (4.30) or eq. (4.31). Therefore, for a position measurement in the focal plane, there should be no difference in the expectation value of the pointer positions δx_R and δx_L for these states. Only for $z \neq 0$ such a difference $\delta x_z := \delta x_R - \delta x_L$ will be observable. Using eq. (4.50) it is possible to express the z-dependence of the position difference δx_z as

$$\delta x_z = 2\epsilon \frac{z}{z_R} e^{-\frac{\epsilon^2}{2\Delta_0^2}} = 2\epsilon \frac{z}{z_R} e^{-\frac{2\epsilon^2}{w_0^2}}. \tag{4.58}$$

To focus the beam, lens L_1 and the camera are placed on fixed positions while lens L_2 is moved until the position difference δx_z as measured on the camera disappears. Based on the resulting distance between lens and focal plane of approximately 37.5 cm and on the measured beam waist of about 760 μm it is possible to estimate the variation of δx_z induced by a displacement of lens L_2, as presented in Fig. 4.10.

In comparison to the estimated values, Fig. 4.11 contains the measured values of δx_z. The approximately linear progression of the position differences is reproduced well by the data. However, the slope of the fit to the measured values and the slope of the calculated linear approximation differ by a factor of approximately 2.45. While the reason for this discrepancy is unclear, some possible explanations will be discussed in subsection 4.3.3. Nevertheless the procedure allows to identify a location of lens L_2, which entails the coincidence of camera position and focal plane.
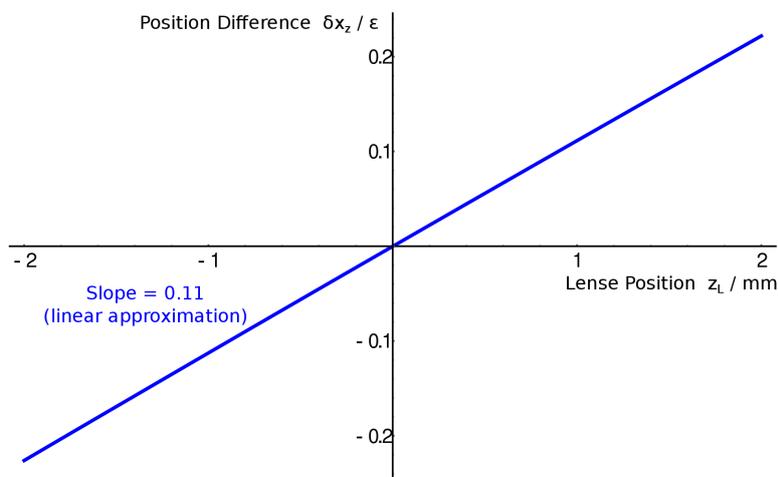
Figure 4.10.: Expected differences in mean position for R- and L preselection for a displacement of lens L_2. The differences are expressed as multiples of the interaction strength ϵ and show an approximately linear dependence on the z-position of the lens close to the focal plane. As the focal plane is moved beyond the camera and consequently z changes its sign, also the sign of the difference δx_z is switched. It should be noted that the calculation is complicated by the fact that a change in the position of lens L_2 affects several parameters such as the Rayleigh range, the z-position of the focal plane and the distance between lens and camera.
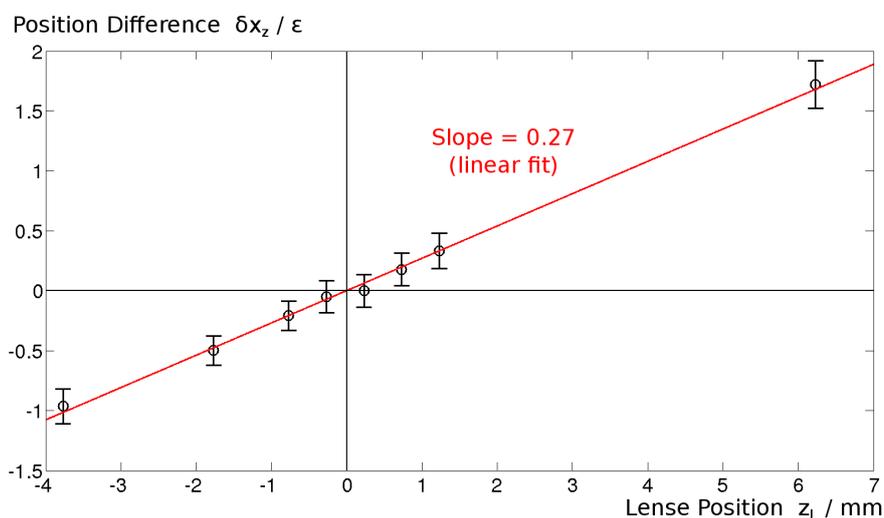
Figure 4.11.: Measured differences δx_z in mean position for R- and L preselection for a displacement of lens L_2. While it is possible to confirm the estimated linear dependence of δx_z on the displacement of lens L_2, the measured slope is approximately 2.45 times larger than in the estimation as presented in Fig. 4.10.

97

Pointer Measurement

The camera employed to measure the intensity distributions of the Gaussian beam, which are proportional to the probability distribution of the pointer state, is a *WinCamD* CMOS camera manufactured by *DataRay* [101]. It has an active area of 6.7 *cm* × 6.7 *cm* and a resolution of 1 *Mpixel*. For the determination of the mean beam position in x-direction, the intensity distribution is averaged over the y-direction, which gives rise to a one-dimensional beam profile as presented in Fig. 4.12. To determine the mean value of this profile, a Gaussian function is fitted onto the distribution after a background subtraction has been performed. For this correction simply the lowest intensity value is subtracted from every data point as was also done in the original experiment [24].
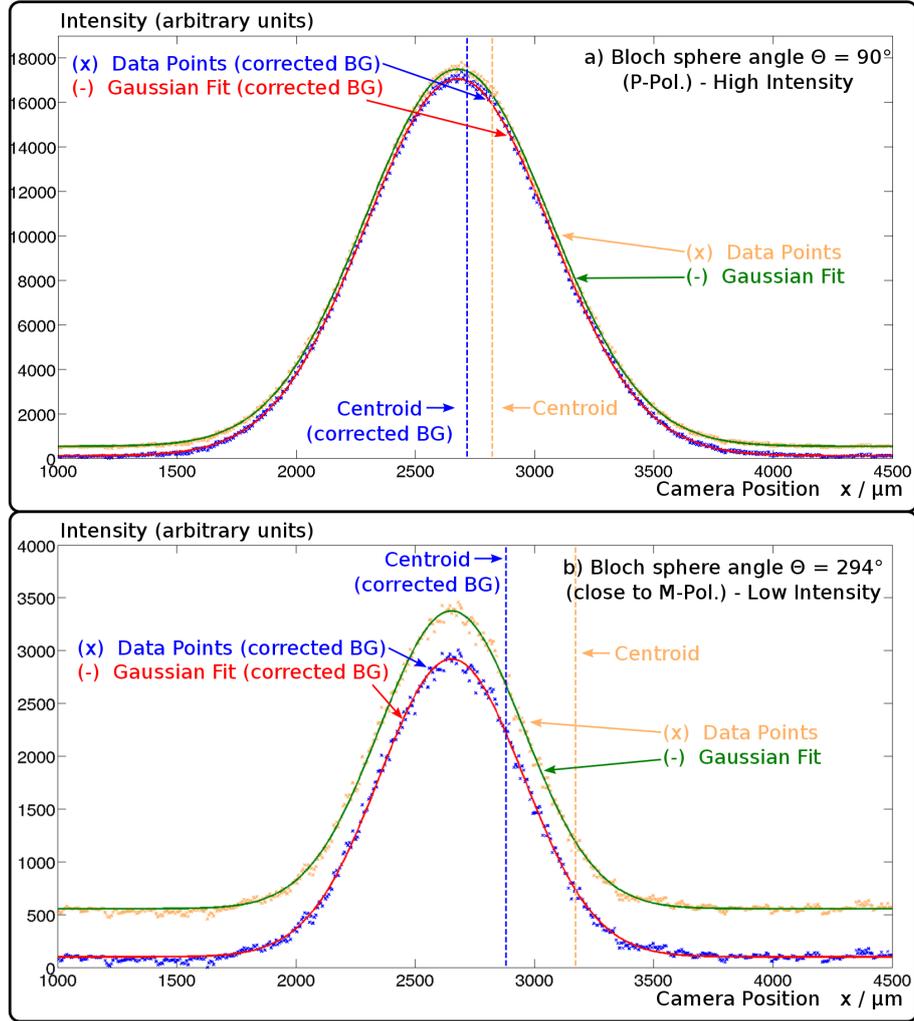
Figure 4.12.: Determination of mean values from intensity profiles. The two depicted intensity profiles represent extreme cases, as for profile a) the measured intensity is maximized with a preselection state that is equal to the P-postselection and profile b) corresponds to an almost orthogonal preselection state $|\psi\rangle = \cos\frac{\theta}{2}|H\rangle + \sin\frac{\theta}{2}|V\rangle$ with $\theta \approx 294°$, which entails a much smaller overall intensity after postselection. The robustness of the fit of a Gaussian distribution to additional background is demonstrated and no significant change can be observed if the background is corrected. In contrast, the centroid of the distribution is heavily dependent on the background, especially in the case of low signal intensity. For the measurements performed in this thesis the method of a Gaussian fit with additional background subtraction was employed with errors corresponding to the confidence intervals of the fit parameters for the x-position of the fitted profile.

4.3.2. Birefringent Crystals

Birefringent crystals represent a critical component of the experiment as they perform the weak measurement interaction and are furthermore employed to correct for the polarization rotation in the mode filtering fiber as discussed above. An analysis of their complex properties is presented below.

Optically Anisotropic Media

It is possible to characterize materials with respect to the spatial dependence of their optical properties. Because solid matter with a crystal structure has well defined spatial axes, there exist cases when the optical properties of the crystal vary corresponding to the spatial directions. In the latter case such materials are denoted as *optically anisotropic crystals* in contrast to *isotropic* crystals with spatially independent optical properties [76, 78, 102].

In a medium the Maxwell equations presented in section 4.1 change their form, relating the electric and magnetic fields not directly to each other, but rather to the corresponding *flux densities*, where $\vec{D}$ denotes the *electric flux density* or *electric displacement field* and $\vec{B}$ the *magnetic flux density* [76, 78]. The electric and therefore also optical properties of a medium can be characterized by the relation of $\vec{D}$ to the electrical field $\vec{E}$. In an optically isotropic medium the two fields have a linear relation with $\vec{D} = \varepsilon \vec{E}$, where ε is the *electric permittivity* of the medium. In an optically anisotropic medium, however, the relationship is more complex and expressed by the *electric permittivity tensor* $\hat{\varepsilon}$, with $D_j = \sum_m \hat{\varepsilon}_{jm} E_m$ [76, 78].

The form of the permittivity tensor depends on the choice of coordinates and it is always possible to find coordinate directions, which imply a diagonal form of the tensor. These directions are denoted as the *principal axes* of the medium, to each of which corresponds a certain value of electric permittivity $\hat{\varepsilon}_{jj}$. Consequently it is possible to calculate separate refractive indices n_j for each of the principal axes with $n_j = \frac{\hat{\varepsilon}_j}{\varepsilon_0}$, where ε_0 is the permittivity of free space already encountered in the context of the Maxwell theory of light. Optical properties of media can be characterized by the relations of these three indices.

In the case of three equal indices of refraction, the permittivity tensor is effectively equal to a constant and the medium is optically isotropic. If exactly two of the indices are equal, the medium possesses a single axis with a different index denoted as the *optical axis* and is therefore described as *uniaxial*. Eventuallly if all three indices differ, the medium is called a *biaxial* medium [76, 78, 102]. Uniaxial media can be distinguished by the relation of the single refraction index n_E denoted as the *extraordinary*, to the pair of equal indices integrated into a single *ordinary* index of refraction n_0. The *Yttrium orthovanadate* crystals (YVO_4) employed in this experiment are uniaxial crystals. Their refraction indices can be ascertained employing the empirical *Sellmeier equations*, which allow a calcu-

lation of the refraction index from empirically determined *Sellmeier coefficients* in dependence on the wavelength [99]. For Sellmeier coefficients provided by the manufacturer [103] and the employed wavelength of 805 nm the two refractive indices can be calculated to $n_0 = 1.97$ and $n_E = 2.18$. Because the extraordinary refraction index n_E is larger than the ordinary n_0, the crystals are denoted as a *positive* unixial medium [76, 78].

Double Refraction

The existence of a spatial direction with an extraordinary refractive index in uni-axial crystals entails a different refraction behavior for different orientations of the electric field, denoted as *birefringence* or *double refraction* [76, 78]. In consequence, the crystal acts differently on certain polarization states, depending on the orientation of the polarization with respect to the optical axis. A certain orientation of the optical axis defines a linear polarization basis with one component definitely orthogonal to the axis and the other potentially non-orthogonal. In fact only in the case, where the direction of light propagation coincides with the direction of the optical axis, both polarization components are necessarily orthogonal to the optical axis. In the general case, however, only one of the components is completely orthogonal and therefore effectively experiences an isotropic medium characterized by the ordinary index of refraction n_0 [76, 78]. Consequently the part of beam with the latter polarization is denoted as the *ordinary beam*. The other part of the beam, denoted as the *extraordinary beam* experiences in general an unusual refraction behavior, which depends on the angle between the direction of propagation and the direction of the optical axis [76, 78].

The standard refraction of an optical beam at a boundary plane separating two media characterized by different indices of refraction n_1 and n_2 is given by Snell's law as [76, 78, 99]

$$n_1 \sin(\theta_1) = n_2 \sin(\theta_2), \tag{4.59}$$

where the angles θ_1 and θ_2 denote the angles of incidence and emergence with respect to the normal direction of the plane. Passing from the medium of a smaller index to a medium with a larger index, the beam is thus refracted towards the normal vector and vice versa. It should be noted that while the refraction of the ordinary beam always agrees with the law of Snell, this is in general not the case for the extraordinary beam [76, 78, 102]. Only if the latter is exactly parallel to the optical axis, it is possible to describe its refraction behavior by the standard refraction law, employing the extraordinary refraction index n_E.

The YVO_4 crystals employed in this experiment are flat cuboids with a thickness of approximately 300 μm and an optical axis that coincides with the front plane of light incidence. Therefore, to achieve an interaction in the basis $\{|H\rangle, |V\rangle\}$, there exist two possible orientations of the crystals suitable for the experiment as presented in Fig. 4.13.
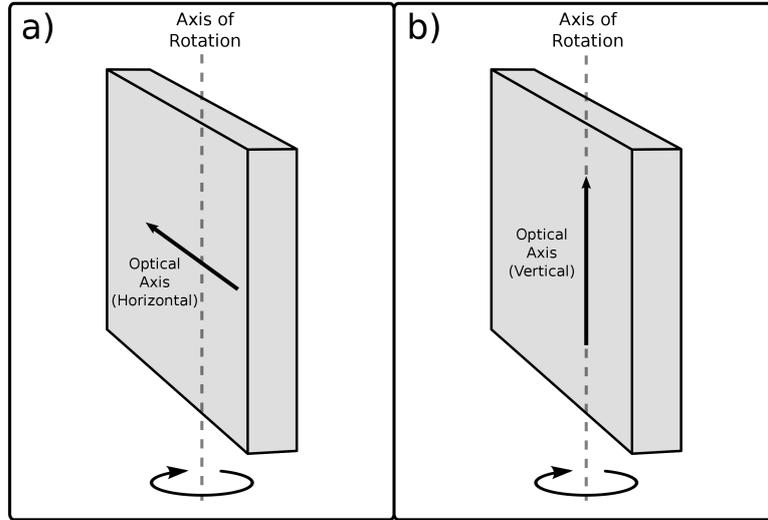
Figure 4.13.: Possible orientations of the optical axis in a YVO_4 crystal, corresponding to a discrimination of polariazation states with respect to the $\{|H\rangle, |V\rangle\}$ basis. While the optical axis lies always in the front plane of the crystal, in case a) it is parallel to the rotation axis and in case b) perpendicular to the latter.

While in case a) the V-component is orthogonal to the optical axis and therefore constitutes the ordinary beam with the H-component as the extraordinary beam, the situation is opposite in case b). However, there exists also another crucial difference between the two possible orientations of the crystals. Because the optical axis in case b) coincides with the axis of rotation, the extraordinary V-component remains always parallel to the optical axis, which means that even though it represents the extraordinary beam it still obeys Snell's law of refraction as stated above. In case a) the optical axis is rotated along with the crystal, which entails that the extraordinary H-component has an intermediate direction with respect to the optical axis.

The reason for unusual behavior of the extraordinary beam in the case where it is neither orthogonal nor parallel to the optical axis, lies in the fact, that the propagation direction in the standard refraction law is defined according to the direction of wavevector of the beam $\vec{k}$ [76, 78]. However, in the case of an anisotropic medium the direction of beam propagation represented by the Poynting vector does not coincide with the wavevector, if the beam experiences a combination of two different refraction indices [76, 78]. Consequently the beam travels at an oblique angle with its wavefronts. The refraction of the wavefronts obeys Snells law with a modified refraction index inside the medium $n(\theta)$, which lies between

the values of the ordinary and the extraordinary indices and can be calculated as [76]

$$\frac{1}{n^2(\theta)} = \frac{\cos^2(\theta)}{n_0^2} + \frac{\sin^2(\theta)}{n_E^2},$$ (4.60)

where θ denotes the angle between the wavevector and the optical axis. At the same time, the direction of the Poynting vector is rotated away from the wavevector towards the optical axis by an angle ρ, which can be expressed as [104]

$$\rho(\theta) = \theta - \arctan\left(\left(\frac{n_0}{n_E}\right)^2 \tan(\theta)\right).$$ (4.61)

In the case of crystal orientation a), this property leads to a smaller effective deflection for the extraordinary beam even though it experiences the larger refraction index, as will be presented below.

Beam Displacement

For symmetry reasons both the ordinary and the extraordinary component recover their old directions of propagation after leaving the crystal. The consequence of the double refraction is therefore a different displacement of the two polarization components of the beam [21, 102]. If the displacement is small enough compared to the waist of the Gaussian beam, it constitutes the intended weak interaction between the polarization object system and the spatial pointer.

Preselecting the states $|H\rangle$ and $|V\rangle$, the setup is used for a beam position measurement without postselection. In Fig. 4.14 the measured beam displacement of the differently oriented YVO_4 crystals for several crystal rotation angles is presented alongside theoretical models.

Except for the extraordinary beam in the case of the horizontal orientation of the optical axis a), theoretical models based on the Snell law were fitted onto the measured data. In the other case the displacement of the extraordinary beam was modeled employing eqs. (4.60) and (4.61).

The measured behavior shows good agreement with the theoretical models. Because both crystal orientations cause a greater displacement of the V-component, even though in one case it represents the ordinary and in the other the extraordinary beam, it is necessary to rotate both crystals in the same direction to avoid a compensation. In Fig. 4.15 the effective separation of the beam components is illustrated schematically. While both beams accumulate a common spatial offset, the relevant quantity is the separation of the polarization components, which effectively constitutes the weak interaction.
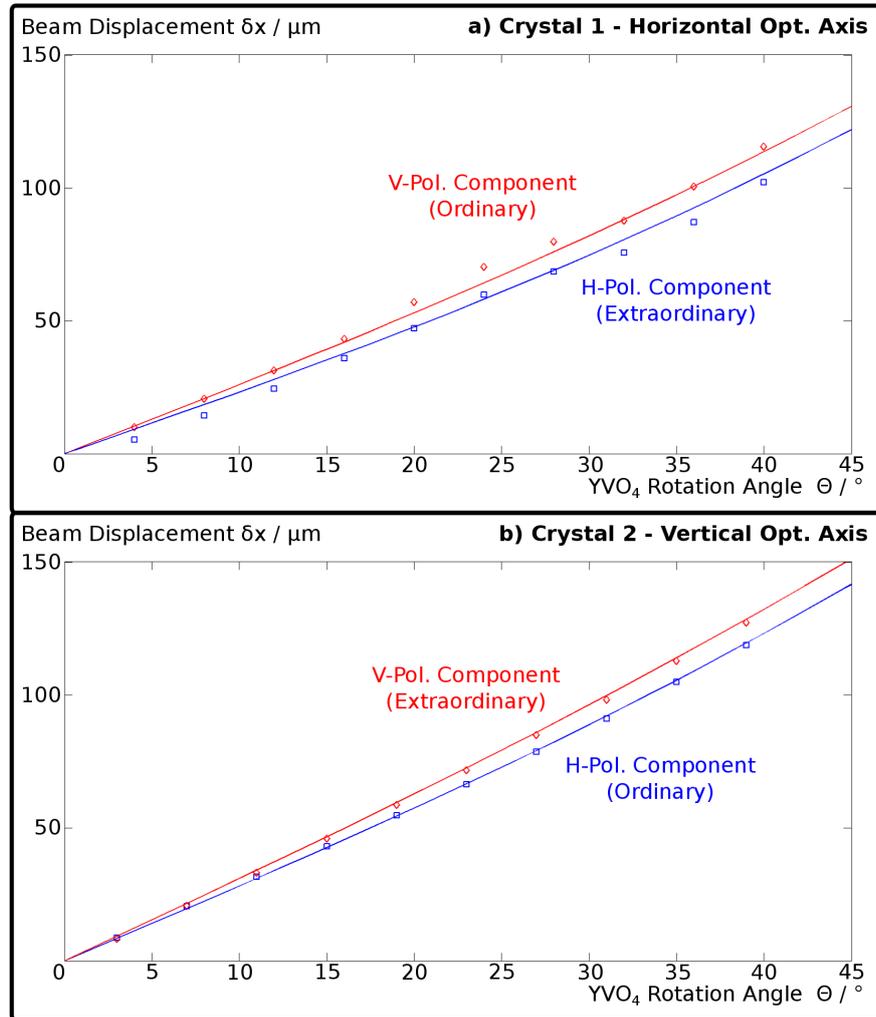
Figure 4.14.: Measured beam displacements induced by the two YVO$_4$ Crystals with horizontal (a) and vertical (b) orientation of optical axes. The squares and rhombs represent measured values and the lines the theoretical models. In both cases the V-component of polarization is displaced by a greater amount. In graph a) for angles 20, 25 and 30 a distortion effect can be seen in the values for the V-component, which might be caused by a deformation of the beam profile originating from stains or dirt on the crystal. Furthermore, the fact that at an angle of 0 there is no overlap of the two components in case a), might be explained by an imperfect cut of the crystal, where the optical axis is not perfectly parallel to the incident plane. In consequence a walk off of the extraordinary component can be observed even for a crystal rotation of 0.
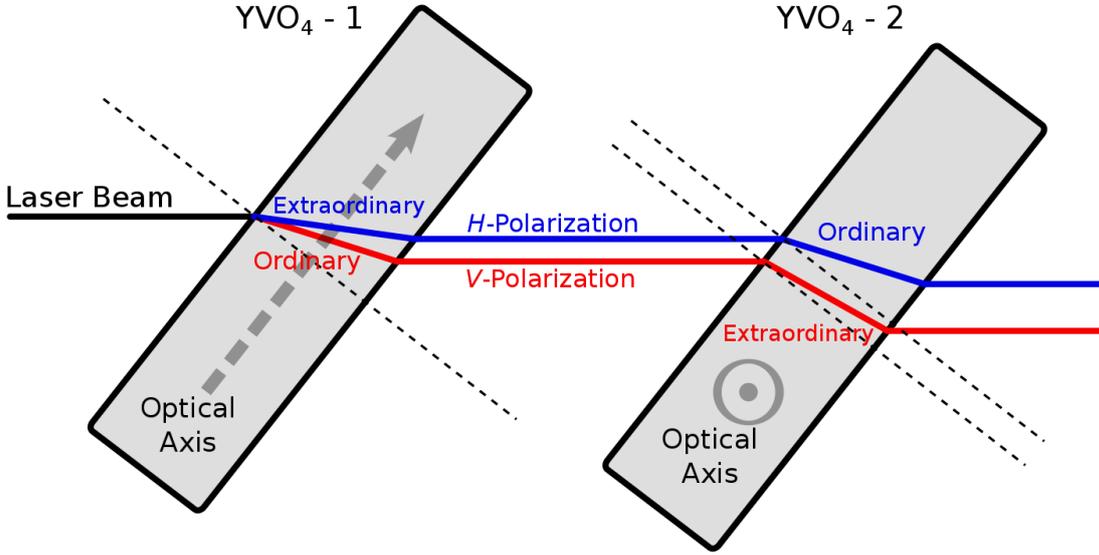
Figure 4.15.: Schematic beam propagation through interaction crystals, as seen from above. While in crystal 1 the optical axis lies in the horizontal plane and consequently the H-polarization component experiences extraordinary refraction behavior, for crystal 2 the V-polarization component represents the extraordinary beam. However, in the latter case the refraction of the extraordinary beam obeys Snell's law because the optical axis is parallel to the polarization direction.

Phase Shift

As mentioned above in the context of the compensation of polarization rotation in the fiber, the birefringent YVO_4 crystals do not only cause a beam displacement but a shift in phase as well. Because the two beam components experience different refractive indices, they effectively cover a different optical pathlength $l_{\mathrm{eff}} = n_j l_j$, when traveling the length l_j through the crystals [76, 78, 99]. In Fig. 4.16 the calculated geometrical lengths, alongside the effective pathlengths of the two polarization components, are plotted for the case of a vertically oriented optical axis.

As becomes clear in Fig. 4.16, the small ratio of wavelength λ to crystal thickness d entails a pathlength difference of several wavelengths, which also implies a phase difference $\Delta\varphi$ of several periods. Therefore, the interaction effectively disturbs the preselection polarization if the relation $\Delta\varphi = \pm m 2\pi$ with $m \in \mathbb{N}$ is not fulfilled. As shown in Fig. 4.17, however, for large enough rotation angles the phase difference between the beam components is much more sensitive to small angular rotations than the beam displacement.

Consequently, it is possible to fine tune the phase difference by slightly rotating one of the crystals after a suitable angle for the desired amount of beam separation
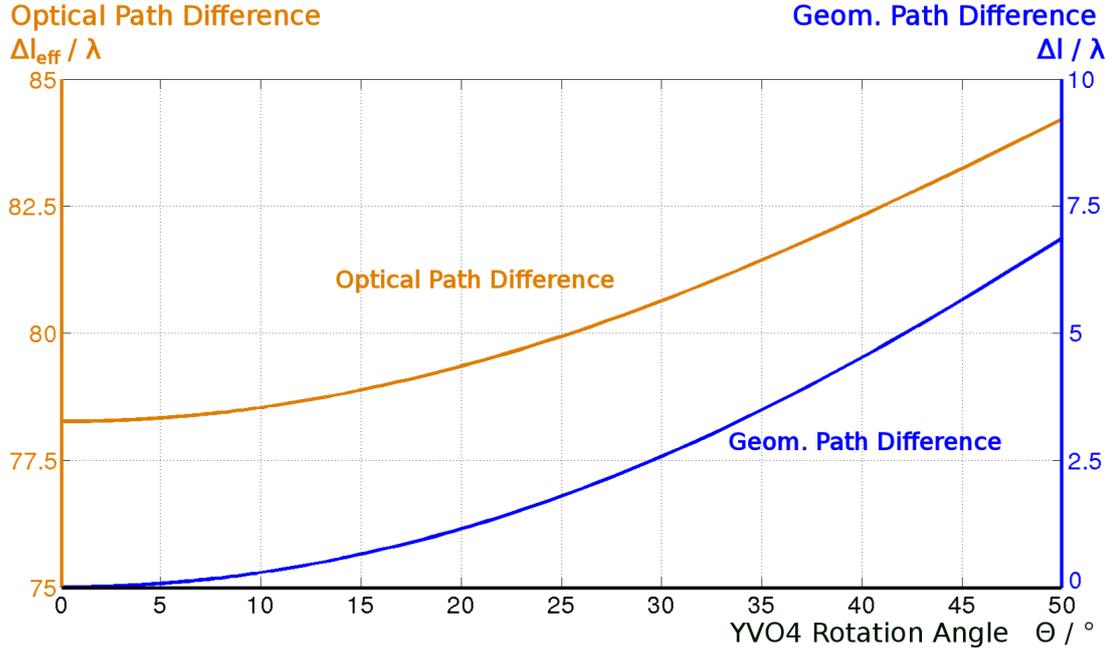
Figure 4.16.: Optical (orange) and geometrical (blue) pathlength differences between the ordinary and extraordinary component for a single YVO_4 crystal with a vertically oriented optical axis in dependence on the angle θ between crystal and incident beam. The crystal has a thickness of 300 μm and the differences in pathlength are given in multiples of $\lambda = 805 \; nm$.

has been found. This ensures the correct phase relation between the weakly separated H- and V-components upon postselection.

Concerning the difference in pathlength, another beneficial effect of the opposite orientation of the respective crystal axes of the two crystals stems from the fact that the absolute path difference as presented in Fig. 4.16 is at least partly compensated when the beam successively passes through both crystals. Because both of them have approximately the same thickness and the geometrical path lengths of the H- and V-polarized components are approximately equal, the overall difference in optical pathlength is reduced as different components experience the larger refractive index in the two crystals. In this way, an absolute pathlength difference above the coherence length of the laser can be avoided.
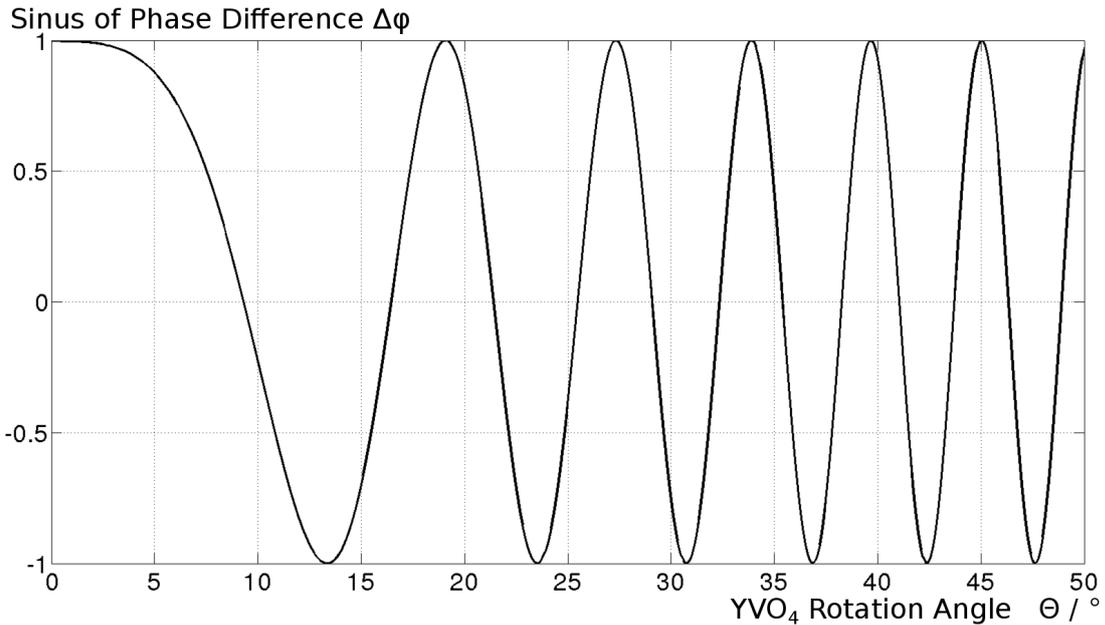
Figure 4.17.: Sinus of calculated phase shift $\Delta\varphi$ between H- and V-polarization components of beam, induced by passage through YVO_4 crystal with a thickness of 300 μm for a wavelength of 805 nm. The phase shift is plotted in dependence on the angle θ between crystal and incident beam.

4.3.3. Evaluation of Experiment

In conclusion of the description of the tomography experiment, the results of the weak measurements are presented. While the data agree with the predictions under most aspects, also some fundamental discrepancies have been observed, which will be discussed as well.

Pointer Position

In Fig. 4.18 the measured pointer position response curves for preselection states on the principal planes of the Bloch sphere are presented. In the case of XZ-plane there is a discrepancy between the theoretical prediction for the validity range of the linear response regime and the measured mean position values. While the shape of pointer response fits very well to the expected curve, it implies an effective beam waist that is smaller than the measured waist by a factor of 15.6. The origin of this phenomenon is unclear and possible explanations will be discussed below.

Apart from this single inconsistency, however, the three curves are in good agreement with the theoretical predictions. For pure preselection states from the YZ-plane, a cosine shape is expected with extreme displacements for H- and V-polarizations and no displacement for R- and L-polarizations. In fact, the
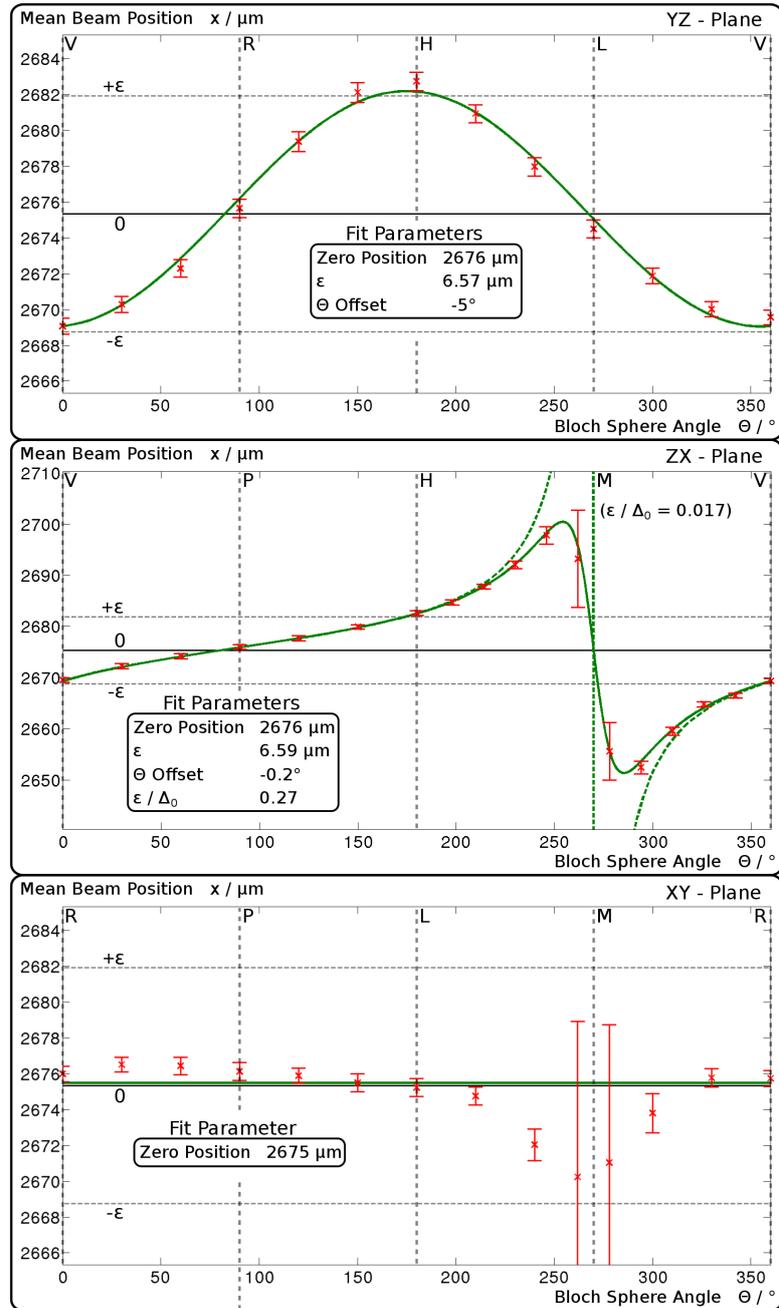
Figure 4.18.: Measured pointer response curves in position space. The green lines represent fits of the theoretical predictions to the measured data points (red), where each point is weighted with its inverse error. The values of zero displacement and ϵ are calculated by averaging over the values determined by the three fits. In the case of ZX-plane the additional dashed green line represents the expected response corresponding to a smaller value of $\frac{\epsilon}{\Delta_0}$.

vanishing position difference of the latter states was used to identify the correct camera position in the first place. The cosine shape resembles a pointer response without postselection, as the imaginary phase between the components prohibits any interference effects between the two components for a measurement in the focal plane with $z = 0$. Consequently the intensity after postselection is constant for all preselection states, which is reflected in the equal errors of all data points from the YZ-plane.

In the unamplified region of the ZX-plane, the pointer response shows also the expected behavior with H- and V-polarization data points at the same positions as in the case of the YZ-plane. Furthermore, as expected the P data point exhibits no displacement and the fit also implies zero displacement in the case of M-polarization, which could not be measured due to a very low intensity. However, in the amplified region the displacement of the mean values of the pointer is much smaller than implied by the measured values of ϵ and Δ_0, even under consideration of the larger error due to low signal intensity.

For the measurement in the XY-plane no pointer displacement is expected at all, as these preselection states imply strictly imaginary weak values as presented in subsection 4.1.2. This property is confirmed very well by the data. However, for data points close to the M-preselection even small deviations from these symmetrical amplitudes are amplified by the postselection, which explains the relatively large displacements in this region. This sensitivity is also reflected in the large slope of the approximately linear pointer response curve in the ZX-plane close to M-polarization.

Pointer Momentum

Unfortunately the employed procedure was not suited to measure the momentum distribution. The reason for this is the relatively large beam waist in the focal plane where the position measurement is performed, which entails a Fourier transformed profile with a very small waist $w_{FT} < 50\ \mu m$. In consequence, the shifts in momentum space are also reduced proportionally and it is not possible to resolve them with the camera employed in this setup. The experiment could be improved by a reduction of the beam waist in the focal plane, which could be achieved by a replacement of the second lens used in the focus procedure by a lens with a smaller focal length. This would result in a larger beam diameter in the Fourier plane as presented in Fig. 4.19.

Discrepancies between Experiment and Theoretical Predictions

Two fundamental discrepancies between the theoretical calculations and the measured data have emerged in the course of the experiment. The first problem consists in unexpectedly large position shifts for imaginary weak values, which
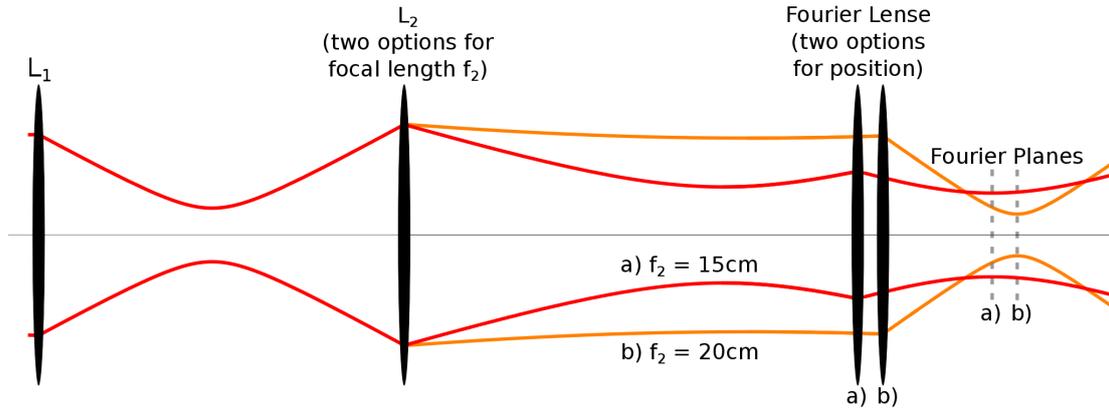
Figure 4.19.: Schematic illustration of the improvement of momentum measurement through modification of the focus procedure. While a reduction of the focal length f_2 of lens L_2 to 15 cm (a), entails a smaller beam waist for the position measurement, the waist in the Fourier plane becomes larger than in the case of $f_2 = 20$ cm (b).

have been measured outside the focal plane of the beam as described in subsection 4.3.1 and presented in Fig. 4.10 and Fig. 4.11. The second is the breakdown of the linear response for much smaller weak values than expected as illustrated in Fig. 4.18.

Both phenomena cannot be explained by the formalism as described in this thesis and consequently it must be assumed that some physical factors have not been yet described correctly. A hint to the source of a possible problem might be the fact that in the original experiment [24] it has been emphasized that the phasefront of the beam also has to be approximately flat in the region of interaction. Therefore, in the original experiment the beam is also focused on the quartz crystal, which applies the interaction. In the case of the experiment performed in this thesis the phasefront is also approximately flat in the region of interaction as it lies close to the focal plane ($\Delta l \approx 20$ cm) compared to the Rayleigh length ($z_R \approx 2.25$ m) but no additional focusing of the beam is performed.

Another effect that was compensated in the original experiment but neglected in the present one, are internal reflections in the crystal, which add additional intensity at x-positions that are further displaced from then the main beam [24]. Therefore, the authors employ an additional iris onto which the beam focused again to filter out the additional reflected beams. Such internal reflections could disturb the measurement especially in the case of almost orthogonal postselection, where the intensity of the main signal is heavily reduced. In contrast, for components that undergo internal reflections in the crystal, the separation between the H- and V-components increases, which reduces the interference effects of the

postselection. In the similar experiment [21], where also a quartz crystal was employed, internal back-reflections are also mentioned as a problem.

A different explanation, which seems only relevant to the reduced pointer displacements for large weak values from the ZX-plane, could be a fault in the determination of the mean pointer position. While in this thesis the latter was determined by fitting a Gaussian profile onto the intensity distribution as presented in Fig. 4.12, this method is expected to fail for weak values with sufficiently large moduli, for which the pointer distribution no longer represents a single Gaussian as discussed in section 3.3. In the latter cases it would be necessary to measure the mean of the distribution by a calculation of the centroid instead of a Gaussian fit. However, as illustrated in Fig. 4.20, the ratio of signal to background, which was achieved in this experiment was not sufficient to allow significant centroid measurements for low signal intensities. This could have been improved by increasing the power of the laser.
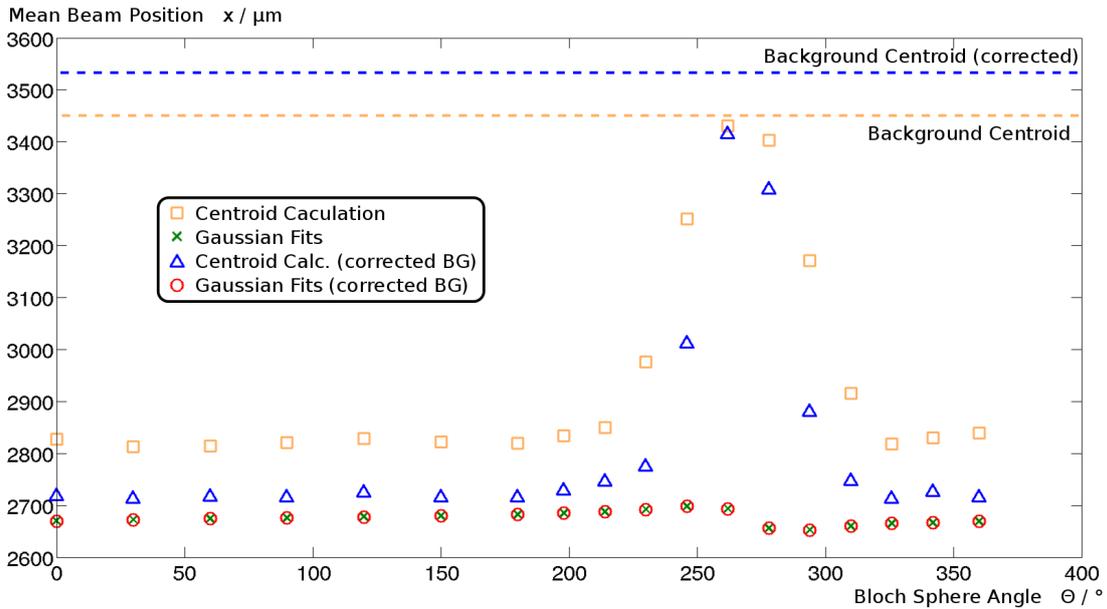
Figure 4.20.: Pointer response for different kinds of mean value determination. The measured mean position values correspond to preselection states from the ZX-plane of the Bloch sphere. Both kinds of Gaussian fits (red and green) yield very similar values even for small signal intensities in the region of almost orthogonal postselection with $\theta \approx 270°$. In contrast, the centroid values converge to the centroid of the background for low signal intensities.

At this point it does not seem to be clear, how these possible explanations are related to the two deviating effects that where measured in the course of the experiment. While it is possible that the two are related and point to a single property that has not been captured correctly in the theoretical description, they

might also have different causes. It is also possible that some completely different effect, which has not been described in this thesis, might be responsible for the discrepancies.

As the reason for the reduced amplification of the pointer response is unknown, it is difficult to conclude whether a DST procedure could be realized with the present setup. If the only discrepancy between observed and predicted pointer behavior is a different effective position uncertainty, which implies an amplification breakdown at smaller weak values, then it should be possible to conduct the tomography under consideration of this modified parameter. However, it might be the case that the phenomenon responsible for the discrepancy also affects the form of the pointer response for states outside the three measured plains of the Bloch sphere. In these cases the validity of the inversion formula (4.53) is not assured and a definitive statement about the validity of the DST procedure cannot be given as long as the origin of the discrepancy is not understood. In any case the procedure is not complete without a measurement of the momentum shift, which is absolutely necessary for the determination of states with the DST schemes described here. Only if additional information about the phase relation between the $|H\rangle$ and $|V\rangle$ components of the initial state is available, it is possible to make statements about this state based only on a position measurement of the pointer.

5. The Meaning of Weak Values

The final chapter is dedicated to the discussion of the meaning of weak values in quantum mechanics. It aims to give an overview over the origins and motivations of the most common interpretations and controversies regarding weak values and measurements. In this context also a minimal and non-controversial definition of the concept is given. Eventually also a set of theoretical proofs for a basic property of weak measurements is given alongside a possible interpretation and a proposal for an experimental confirmation.

5.1. Interpretation of Weak Measurements

In the following section the most important elements of the interpretational controversy surrounding the concept of weak values are delineated.

5.1.1. Time-Symmetrical Quantum Mechanics

As the inception of the concept of weak values lies in the time-symmetrical formulation of quantum mechanics, the discussion of the interpretation of weak values begins with an presentation of this approach. Subsequently the emergence of counterfactual claims is described and illustrated in the context of the three box problem.

Two-State Vector Formalism

The concept of time-symmetrical quantum mechanics was first introduced by Aharanov, Bergmann and Lebowitz in [5] alongside the concept of pre- and postselected measurments as already mentioned in chapter 3. As was pointed out by ABL, most of the laws of classical physics are time-symmetric or in other words "form invariant under time reversal" [5]. A comparison with quantum mechanics discloses that the standard quantum mechanical evolution, as expressed by the Schrödinger equation, shares this property and in fact describes reversible and deterministic processes. It is only the reduction of the wavefunction introduced by the measurement postulates, which constitutes an irreversible process, thus breaking the time symmetry for quantum mechanics [5, 53, 62, 64]. The addition of a time-asymmetric component to otherwise symmetrical laws might vindicate

the consideration, whether this asymmetry is a fundamental property of the theory or a contingent feature, which simply depends on the standard perception of time [27, 62].

It is possible to identify the concept of the quantum state itself as the source of the time-asymmetry because in its preparation it is defined by a complete measurement in the past, which yielded a reduction into the particular state [27]. In contrast, a future measurement is fundamentally undetermined as long as an incompatible observable is measured. Therefore, it might be feasible to reformulate the theory by introducing a state determination that is related to past and future in a symmetrical way. In consequence, an additional set of conditions is introduced, which is regarded as providing additional information about a quantum state at an earlier point in time [27, 66, 69, 105]. Such a concept is of course incompatible with standard quantum mechanics, where a pure quantum state is considered as the complete description of the system and no structures are provided that would allow the conditioning of measurements on this state on the future. Nevertheless, it was proposed [62, 66], to regard pre- and postselected quantum systems as physical systems to which two sets of boundary conditions can be attributed. The resulting ensembles, which are determined by past and future conditions in a symmetrical way, allow for a completely time symmetric formulation of quantum measurement at least for the time interval between pre- and postselection [62, 67].

The formalism introduced to represent time-symmetric quantum ensembles employs two quantum states to represent a physical system determined by two sets of conditions and is therefore denoted as the *two-state vector formalism* ("TSVF"). A two-state vector is expressed as [27, 62, 66]

$$\langle \psi_F | \; | \psi_I \rangle, \tag{5.1}$$

where $|\psi_I\rangle$ represents the "forward evolving" state, which is determined by measurements performed in the past (preselection) and $|\psi_F\rangle$ the "backward evolving" state determined by measurements performed in the future (postselection). This formulation of a physical state in dependence of two quantum states eventually motivates a range of claims, which are not element of the standard quantum mechanical description as will be discussed below.

System in between Measurements

The time-symmetric approach to quantum mechanics represented by the TSVF, identifies the ABL formula (3.38) as the relevant description for measurements of pre- and postselected systems. The ABL rule is introduced in subsection 3.2.1 as the conditioned probability of measuring the outcome a_j for a potentially degenerate observable $\hat{A}$ defined as $\hat{A} = \sum_j a_j \hat{\Pi}_j$ with the projectors $\{\hat{\Pi}_j\}$. In the standard description the initial quantum state $|\psi_I\rangle$ is interpreted as the state

that is strongly measured and the subsequent postselection $|\psi_F\rangle$ constitutes as second projective measurement of the resulting state. From the perspective of TSVF, however, the interpretation of the ABL formula is symmetric with respect to the two conditions of pre- and postselection, which is in agreement with the formal symmetry of the expression under exchange of the two states. Thus, the formula is interpreted as a new kind of time symmetric measurement postulate, which is valid for pre- and postselected ensembles and allows statements about measurement outcomes between these two defining conditions [27, 62].

As long as the interpretation of the ABL formula is factual and thus considers measurements $\hat{\Pi}_j$ that are actually carried out, it is unproblematic and in complete agreement with the predictions of standard quantum theory [67, 106]. In fact, even the contextuality of the formalism is not controversial if the measurements are actually performed. For two observables $\hat{A}$ and $\hat{B}$ with different sets of projectors into the corresponding eigenspaces, the summed postselection probability in the denominator may be different, even if both sets of projectors contain $\hat{\Pi}_j$. In consequence the ABL formula may yield different probabilities for a measurement of the value corresponding to $\hat{\Pi}_j$ for the two observables. This difference is not paradoxical because each observable provides different possibilities for the reduction of the initial state, which may possess very different overlaps with the postselection state [10, 20]. Therefore, the overall conditional probability changes not because the actual measurement of the value corresponding to $\hat{\Pi}_j$ has different probabilities for the two observables, but rather because the sets of alternative states are different.

As discussed above, the knowledge of a quantum state in standard quantum mechanics allows the formulation of statements about the outcomes of future measurements on the system. From the perspective of a time-symmetrized approach it might appear equally legitimate to "reverse the projection postulate" and to formulate claims about the outcomes of past measurements that could have been carried out before the postselection [67, 106]. Statements of the latter kind are usually denoted as *counterfactual* claims [107]. These are, however, at odds with the usual interpretation of quantum mechanics, where the state after the measurement is in a fundamentally undetermined superposition of basis states of another incompatible observable. Consequently it is impossible to attribute any distinct eigenvalue of the second measurement observable to the state before the measurement is factually carried out implying a state reduction. In other words, the notion of *histories* or *trajectories* does not exist in standard quantum mechanics [12, 64, 67]. In contrast, counterfactual theories effectively imply an *epistemic* interpretation of the quantum state, which regards the wavefunction as a representation of incomplete knowledge of the system that can be complemented with additional information provided by the postselection state as proposed in [5, 52, 75]. This is opposed to an *ontic* view, which attributes physical reality to the quantum state as it constitutes a complete description of physical systems

5. The Meaning of Weak Values

[42, 108]. However, the consequence of the ontic interpretation is the necessity of a reduction postulate, which can be avoided in epistemic approaches. While it is far beyond the scope of this thesis to discuss the diverse field of considerations about the question what a quantum state represents, the presented notions might facilitate a discussion of the role of weak values in counterfactual interpretations as presented below. In the successive segment, however, the transition from a factual use of the ABL rule to a counterfactual application will be explicated on the basis of a common example.

Three Box "Paradox"

The so called "three box paradox" or "three box problem" represents an important example, which is often discussed in the context of the time-symmetrical formulation of quantum mechanics with PPS ensembles [11, 13, 20, 27, 66, 68, 105, 109]. In this example the "three boxes" are respresented by an orthonormal basis of a 3-dimensional Hilbert space, denoted as $\{|1\rangle, |2\rangle, |3\rangle\}$, with $|1\rangle$ corresponding to the particle "being in box 1" and so on. The state of this PPS system is described by the two state vector $\langle\psi_F|\ |\psi_I\rangle$ with the two states

$$|\psi_I\rangle = \frac{1}{\sqrt{3}}(|1\rangle + |2\rangle + |3\rangle), \quad |\psi_F\rangle = \frac{1}{\sqrt{3}}(|1\rangle + |2\rangle - |3\rangle). \tag{5.2}$$

According to the time-symmetric approach, the results of measurements performed on the three box system between pre- and postselection have to be calculated via the ABL rule. Because of the contextuality of the ABL formula, however, it is not enough to specify a single projector, but instead a complete eigendecomposition of a well-defined observable on the three box system [26]. For this particular discussion of the three box example, the observables $\hat{A}$, $\hat{B}$, $\hat{C}$ and $\hat{D}$ are considered, with

$$\begin{aligned}
\hat{A} &:= \alpha|1\rangle\langle 1| + \beta\left(|2\rangle\langle 2| + |3\rangle\langle 3|\right), \\
\hat{B} &:= \alpha|2\rangle\langle 2| + \beta\left(|1\rangle\langle 1| + |3\rangle\langle 3|\right), \\
\hat{C} &:= \alpha\left(|1\rangle\langle 1| + |2\rangle\langle 2|\right) + \beta|3\rangle\langle 3|, \\
\hat{D} &:= \alpha|1\rangle\langle 1| + \beta|2\rangle\langle 2| + \gamma|3\rangle\langle 3|,
\end{aligned} \tag{5.3}$$

where α, β and γ denote different eigenvalues. It should be noted that the identification of measurement outcomes with eigenvalues rather than final states in the following discussion is motivated by the aim to express different projector decompositions of the measurements. This corresponds to the description of indirect measurement, where different states associated with the same eigenvalue are correlated with the same pointer state and therefore not distinguished by the measurement interaction.

For a measurement of observable $\hat{A}$, the ABL rule yields a probability of 1 to measure the eigenvalue α, which is interpreted as "finding the particle in box 1" [27, 66]. In the same manner, a measurement of observable $\hat{B}$ implies that the particle "is" also with certainty in box 2. As a "paradoxical" result it is concluded, that in the case of this PPS system, the particle is both in box 1 and box 2 with certainty. Furthermore, a measurement of observable $\hat{C}$ yields the eigenvalue α only with probability of $\frac{4}{5}$, which suggests that the particle might not be found in the boxes when they are measured in combination. Eventually, the context dependence of the ABL formula is demonstrated, when observable $\hat{D}$ is measured and the probability of "finding the particle in box 1" or "finding it in box 2" is only $\frac{1}{3}$. Although both the measurement of observable $\hat{A}$ and $\hat{D}$ contain the space of state $|1\rangle$ as a non-degenerate eigenspace and the same projective measurement with the projector $|1\rangle\langle 1|$ is carried out, the probabilities given by the ABL rule for a measurement of value α are different.

While this results might appear surprising at first glance, in the factual case they are in perfect agreement with the standard formulation of quantum mechanics as already discussed above. A standard projective measurement of observables $\hat{A}$, $\hat{B}$ and $\hat{C}$ will cause a reduction of the preselection state into one of two alternatives, one of which is orthogonal to the postselection. Consequently, the conditional probability of the non-orthogonal outcome alternative becomes 1. In the case of a measurement of observable $\hat{D}$, all resulting states after the projective measurement have the same postselection probability and therefore all of them are identified as potential outcomes by the ABL formula. Employed in this way, the ABL formula represents a method to calculate probabilites of measurement outcomes in pre- and postselected systems that is consistent with the standard theory of quantum measurement [11].

If the predictions of the ABL rule are, however, extended to counterfactual scenarios, they become highly problematic. The statement that the pre- and postselected particle "is in both boxes simultaneously" effectively identifies ensembles that are fundamentally distinct from the perspective of standard quantum mechanics. A measurement of observable $\hat{A}$ separates the initial preselected ensemble in a superposition state of three boxes into two subensembles, one of which collapsed into the state $|1\rangle$ and the other in the state $\frac{1}{\sqrt{2}}(|2\rangle - |3\rangle)$. A projective measurement of observable $\hat{B}$ yields a subensemble in state $|2\rangle$ and another in state $\frac{1}{\sqrt{2}}(|1\rangle - |3\rangle)$. Thus, from the perspective of standard quantum mechanics the different measurements correspond to two complete distinct scenarios and an identification of the ensemble in state $|1\rangle$ after the measurement of observable $\hat{A}$ and the ensemble in state $|2\rangle$ after the measurement of observable $\hat{B}$ is not warranted [11, 65, 67, 109]. As one critic remarks pointedly,

> "... arguing that the system is in two different states at the same time is no more meaningful than to use the same piece of plasticine to make

first a ball, then a cube, and later argue that a body can be round and
cubic at the same time." [20]

5.1.2. Weak Values as Measurement Outcomes

While in the previous subsection the implications of the TSVF are discussed
without reference to weak values, the role of the latter in the context of these
controversies is presented in the following paragraphs.

Weak Values as Average Values

Despite the problematic nature of counterfactual claims as demonstrated in the
discussion of the three box example presented above, it has been proposed [12,
27, 57–59, 63, 72, 75] that it is possible to experimentally proof such claims by
performing weak measurements, which do not disturb the system significantly and
thus effectively provide information about counterfactual scenarios. Thus, in these
approaches weak measurements are seen as factual observations of counterfactual
scenarios [11, 15]. In this context the property of weak values to be potentially
arbitrarily large or even complex, invites certain highly non-standard conclusions
as presented below.

As pointed out in [11, 15], such an employment of weak measurements effec-
tively compares the meaning of weak values as outcomes of weak measurements
to the meaning of expectation values as mean outcomes of standard quantum
measurements. This interpretation is denoted as the "realistic, straightforward
interpretation" ("RSFI") of weak values [11]. In fact a range of expressions of
this kind can be found in the relevant literature as for example the claim that a
set of weak measurements allows the determination of an "accurate mean value
for the observable of interest" [72], the proposal of "determining the mean value
[...], as a weak value" [110] or simply the treatment of weak values as "conditioned
expectation values" [64], as already presented in section 3.2. The assertion of the
"measurement" of a "spin component of 100" for a spin-$\frac{1}{2}$ from [4] also represents
an instance of this controversial identification of weak values and expectation
values, as was already pointed out in the earliest of criticisms [6, 7, 9].

One consequence of this equal treatment are claims about the measurements
of unusual values that imply "several peculiar phenomena that occur in between
measurements" [59]. Furthermore, weak measurements as an experimental real-
izations of counterfactual statements, are regarded as allowing the introduction
of the concept of quantum trajectories or similar statements about the "past of
quantum particles" [12, 57, 72, 75, 110, 111]. The fact that the weak value of an
observable for a certain pre- and postselected ensemble could be measured in a
direct pointer response, is used as a basis to attribute this value to the observable
and treat the weak value in the same way as the expectation value of an usual pre-
selected ensemble. This approach consequently allows counterfactual statements

about the trajectories of photons passing through double slits [72] or the path of particles traveling through an interferometer [12, 13]. An explicit example of such epistemic conclusions is presented below, when the three box problem is revisited from the perspective of weak measurements.

Weak Three Box Measurement

In the following the claim that weak measurements "explain" the three box "paradox" is illustrated. As proposed in [12, 13], the weak probing of the particle's presence in the boxes is conducted via weak interactions described by the three projectors $\hat{\Pi}_1 = |1\rangle\langle 1|$, $\hat{\Pi}_2 = |2\rangle\langle 2|$ and $\hat{\Pi}_3 = |3\rangle\langle 3|$. Calculating the corresponding weak values $\hat{\Pi}_w^{(j)}$, which are defined as

$$\hat{\Pi}_w^{(j)} := \frac{\langle\psi_F|\hat{\Pi}_j|\psi_I\rangle}{\langle\psi_F|\psi_I\rangle}, \tag{5.4}$$

where $|\psi_I\rangle$ and $|\psi_F\rangle$ are the usual three box pre- and postselection states, yields that $\hat{\Pi}_w^{(1)} = \hat{\Pi}_w^{(2)} = 1$ and $\hat{\Pi}_w^{(3)} = -1$. These weak values are then interpreted in connection to a novel form of weak "number operators" that signify the presence of particles, including the unusual statement of a particle number of $-N$ in box 3 [27].

Furthermore, it is possible to measure all three of these weak values simultaneously when three successive weak measurements are performed. In fact, in the limit of a sufficiently weak interaction the shifts caused by a series of arbitrary weak measurements simply add up without changing the shape of the pointer distribution. This is seen as a suggestion that weak measurements are able to probe properties of a PPS system, which it possesses simultaneously. Because it is even possible to measure weak values corresponding to complementary observables simultaneously in this manner, it is argued that weak measurements can reveal the values of non-compatible observables at the same time [46, 62, 67]. The latter property is denoted as the "sum rule" of weak measurements.

In modified versions of the three box scenario nested interferometers are considered, which can be described by the two-state vectors [12, 13]

$$\langle\psi_F| = \frac{1}{2}\left(\langle 1| + i\langle 2|\right) + \frac{1}{\sqrt{2}}\langle 3| \qquad \frac{1}{2}\left(|1\rangle + i|2\rangle\right) + \frac{1}{\sqrt{2}}|3\rangle = |\psi_I\rangle, \tag{5.5}$$

$$\langle\psi_F| = \frac{1}{\sqrt{3}}\left(\langle 1| + i\langle 2| + \langle 3|\right) \qquad \frac{1}{\sqrt{3}}\left(|1\rangle + i|2\rangle + |3\rangle\right) = |\psi_I\rangle, \tag{5.6}$$

respectively. In both examples, the fact that the weak value measurements of the projectors $\hat{\Pi}_1$ and $\hat{\Pi}_2$ are non-zero, while the weak value of the projector $\hat{\Pi}_1 + \hat{\Pi}_2$ vanishes, is used to conclude that the path of quantum particles through the interferometers did not consist of a "set of continuous trajectories" [13].

Thus, the weak values that can be obtained from weak measurements on three or more dimensional systems of this type are seen as the basis for claims about the state of PPS systems between the two conditioning projections in the past and the future. Because the weak values can be obtained with an arbitrarily weak interaction, they are regarded as a genuine property of the system, which only depends on the pre- and postselection states and not on the factual conduction of a strong projective measurement.

Weak Values as Relative Amplitudes

The controversial claims in the context of weak measurements can be unraveled if the identification of weak values with expectation values is critically analyzed. While this identification is usually grounded on the similar linearity in the pointer response as already presented in subsection 3.2.2, there are no formal reasons that would justify the treatment of a weak measurement on equal grounds as the standard measurement of an observable [7, 9, 11, 15]. This fact is even conceded by proponents of epistemic interpretations of weak values [107]. What is overlooked in accounts that treat weak values as usual measurement outcomes is the fact that the procedure of weak measurement is fundamentally distinct from the standard quantum measurements, where the interaction is used to resolve the eigenstates of the observables in the pointer response and a consecutive pointer measurement has the function of identifying the corresponding probability distribution [7, 20]. The pointer response in the standard sense of measurements is thus just a means to measure probabilites. In the concept of weak measurements, this pointer response is used to obtain the measurement value in a fundamentally different way, which is of course also possible for a standard expectation value, which can be directly measured from a shifted pointer distribution even if the eigenstates are not resolved. However, it follows by no means from the formalism of quantum mechanics that the weak value obtained from such a measurement of a pointer shift has any direct relation to the expectation value of the particular pre- and postselected subensemble [11].

While in general there is no formal connection between weak values and usual expectation values of observables, there exists a clear relation between the complex amplitudes of the wavefunction in the basis of the weak measurement and the corresponding weak values. This relation is the foundation of DST and has been presented in detail in chapter 4. Instead of an identification with standard outcomes of measurements it seems therefore more justified to regard weak values as "relative probability amplitudes" as presented in [11, 20]. As discovered in [4], PPS ensembles exhibit the property that it is possible to measure these relative probability amplitudes, denoted as "weak values", directly from the pointer response. This makes it possible to measure the coefficients of the wavefunction in a novel and useful way. All further claims about the meaning of these quantities

appear unwarranted if one considers that weak measurements simply probe the quantum state in between pre- and postselection [20, 73].

Therefore, considering the three box example with weak measurements, it is no surprise that both box states can be weakly measured simultaneously as they are both in superposition in the preselection state. From the formal point of view, this does not in any way entail the conclusion that the particle is in both boxes at once and the simultaneous measurement of both weak values rather allows the statement that the system is in a superposition state, which can potentially be reduced into one of the box states [20]. As discussed above, the former type of claims might be natural from the point of view of a time-symmetrized theory, but should be differentiated from standard expressions as "expectation values" or "measurement outcomes".

In the same sense it is to be understood that DST measures incompatible observables at the same time. The weak measurement indeed provides information about both observables but only in the sense in which the knowledge of a wavefunction would provide the same information [20, 73]. Consequently it is also not surprising and in complete agreement with standard quantum theory that large pointer shifts can emerge, which can even affect complementary pointer observables in the case of complex weak values [7, 11, 20]. As presented in subsection 3.2.3 in detail, they can be seen as a consequence of interference effects, which arise when the pointer states corresponding to the eigenstates of the measurement observable are weighted with the complex coefficients of pre- and postselection. In the same way it is possible to explain the effects attributed to weak traces or trajectories.

5.2. Weak Values as Weak Eigenvalues

While a RSFI of weak values appears highly problematic, it is still possible to draw a realistic interpretation of weak values from a very particular perspective. Below, the basic concept of such an approach is delineated alongside a subsequent description of a suitable experiment to confirm the postulated reality of weak value in this specific sense.

5.2.1. Operational Meaning of Pointer Response

In the following paragraphs the operational definition of physical reality is extended to the model of indirect measurement and a series of proofs are presented, which show the reality of the weak value in the sense of this definition.

Operational Definition Measurement

Apart from the RSFI discussed above, there exists also a different realistic interpretation of weak values, which, however, takes a radical *operationalist* standpoint without the reference to mean values. "Operationalism" refers to the proposition that the meaning of physical quantities is completely determined by the procedures employed to measure them [32, 112]. It can be argued [63] that historically the definition of an *element of reality* in physics has always been epistemic as expressed in the definition given by Einstein, Podolsky and Rosen in their famous paper [113]. The EPR definition is stated as:

> "If, without in any way disturbing a system, we can predict with certainty (i.e., with probability equal to unity) the value of a physical quantity, then there exists an element of physical reality corresponding to this physical quantity." [113]

Because a quantum system, which is in the eigenstate $|a\rangle$ of some observable corresponding to the eigenvalue a, will yield this eigenvalue upon measurement of that observable with certainty, the authors consequently consider the property of the system described by the eigenstate $|a\rangle$ as an element of reality [113]. As discussed in chapter 3, the pointer shifts corresponding to object systems in eigenstates of the weak interaction observable entail pointer evolutions that shift the pointer wavefunction without changing its shape. Therefore, it can be argued that elements of reality in the sense of EPR correspond to measurement results, where the shape of the pointer wavefunction is conserved. In consequence a novel definition of the concept of an "element of reality" is proposed, which explicitly relates to the change in pointer distributions caused by the interaction with the relevant object system. It is stated as follows:

"If we are certain that a procedure for measuring a certain variable
will lead to a definitive shift of the unchanged probability distribution
of the pointer, then there is an element of reality: the variable equal
to this shift." [63]

The latter definition implies the reality of weak values for the interaction regime
defined in weak measurements. As discussed in section 3.2 and expressed in
eq. (3.58), the pointer state after a weak measurement can be approximately de-
scribed by an interaction parametrized by the weak value, exactly in the same way,
in which an eigenvalue parametrizes the shift of the pointer in a usual standard
measurement. Therefore, in the very strict operational sense proposed above, this
structural similarity between the two pointer evolutions motivates the claim that
the weak value can be regarded as a real property of PPS systems, which manifests
itself upon an arbitrary interaction with other systems, as long as this interaction
is sufficiently weak [27, 63, 107].

Quantitative Analysis of Pointer States

As a quantitative confirmation of the epistemic reality of weak values in the sense
presented above, a comparison between the relevant pointer states is proposed
[114]. For this purpose three types of pointer states after interactions with object
systems described by characteristic values of different types are considered. The
first type of pointer is the result of an interaction with an object system in an
eigenstate of the measurement observable and is denoted as a "pointer associated
with an eigenvalue". A pointer state, after an interaction with an object system
described by a superposition of eigenstates and measured without postselection,
yielding the expectation value as a measurement outcome is consequently called a
"pointer associated with an expectation value". Eventually a "pointer associated
to a weak value" is considered, which interacted weakly with the object system in
a preselection state and was subsequently filtered with respect to a postselection.
Each of the pointer types can be described by a single value pertaining to the
object system, an eigenvalue, an expectation value, and a weak value.

It can be proven that in the limit of weak interactions, there exists a funda-
mentally greater similarity between the pointer coupled to an eigenvalue and the
pointer coupled to a weak value case than between the pointer coupled to an
eigenvalue and the one coupled to an expectation value if all three values are
equal. In the context of the definition of physical reality presented above, that
similarity can be regarded as a confirmation of the structural similarity between
a PPS system and a system in an eigenstate of the measurement observable in
a strictly epistemic sense [114]. The theoretical proofs for this assertion will be
presented in the next segments after the necessary formalism has been introduced.

For an interaction parametrized by the small parameter ϵ, the generator $\hat{p}$,
the initial pointer state $|\Phi_0\rangle$ and the observable $\hat{A}$ with the eigenbasis $\{|a_j\rangle\}$

corresponding to the eigenvalues $\{a_j\}$, the pointer state $|\Phi_e\rangle$ after interaction with an object system in the eigenstate $|a_k\rangle$ is simply $|\Phi_{\epsilon a_k}\rangle$ following the usual definition introduced in the context of eq. (3.13). For a preselected object system in the superposition state $|\chi_I\rangle = \sum_j \gamma_j |a_j\rangle$, with an expectation value $\langle \hat{A} \rangle = \sum_j |\gamma_j|^2 a_j$ is equal to eigenvalue a_k, the final pointer state $\hat{\rho}_{exp}$ is a mixed state with

$$\hat{\rho}_{exp} = \sum_j |\gamma|^2 |\Phi_{\epsilon a_j}\rangle \langle \Phi_{\epsilon a_j}|, \tag{5.7}$$

as presented in eq. (3.28). The pointer state $|\Phi_w\rangle$ coupled to a pre- and post-selected object system such that the weak value $A_w = a_k$ is obtained, can be expressed as

$$|\Phi_w\rangle = \frac{1}{\mathcal{N}} \langle \psi_F | e^{-i\epsilon \hat{A} \otimes \hat{p}} |\psi_I\rangle |\Phi_0\rangle \tag{5.8}$$

with pre- and postselection states $|\psi_I\rangle$ and $|\psi_F\rangle$, the normalization $\mathcal{N} = \sqrt{\langle \Phi_w | \Phi_w \rangle}$ and the notation $|a\rangle|b\rangle := |a\rangle \otimes |b\rangle$.

To show that the operational reality of the weak value is similar to that of eigenvalues, the fundamental similarity between pointer wavefunctions of the pointer coupled to the eigenvalue and to the weak value has to be confirmed [114]. As the relevant quantity to evaluate the similarity of the states, the fidelity or "overlap" is considered as defined in chapter 2. The following proof thus aims to show a fundamental difference between two fidelities $F(|\Phi_e\rangle, |\Phi_w\rangle)$ and $F(|\Phi_e\rangle, \hat{\rho}_{exp})$, which can be expressed as

$$F(|\Phi_e\rangle, |\Phi_w\rangle) = |\langle \Phi_e | \Phi_w \rangle| = \frac{1}{\mathcal{N}} \left| \langle \Phi_{\epsilon a_k} | \langle \psi_F | e^{-i\epsilon \hat{A} \otimes \hat{p}} |\psi_I\rangle |\Phi_0\rangle \right|, \tag{5.9}$$

$$F(|\Phi_e\rangle, \hat{\rho}_{exp}) = \sqrt{\langle \Phi_e | \hat{\rho}_{exp} | \Phi_e \rangle} = \sqrt{\sum_j |\gamma_j|^2 \left| \langle \Phi_{\epsilon a_k} | \Phi_{\epsilon a_j} \rangle \right|^2}. \tag{5.10}$$

Comparison of Weak Value and Eigenvalue

In order to evaluate the fidelity in the weak value case, it is instructive to expand eq. (5.9) in powers of ϵ as

$$|\langle \Phi_e | \Phi_w \rangle| = \frac{1}{\mathcal{N}} \left| \sum_n \frac{(-i)^n}{n!} \epsilon^n \langle \psi_F | \left(\hat{A} - a_k \right)^n |\psi_I\rangle \langle \hat{p}^n \rangle \right|, \tag{5.11}$$

where $\langle \hat{p}^n \rangle := \langle \Phi_0 | \hat{p}^n | \Phi_0 \rangle$. Keeping terms up to fourth order in ϵ and using the relation $A_w = a_k \in \mathbb{R}$ yields the approximate expression

$$|\langle \Phi_e | \Phi_w \rangle| \approx \frac{|\langle \psi_F | \psi_I \rangle|}{\mathcal{N}} \left| 1 - \frac{\epsilon^2}{2} \left(A_w^2 - (A_w)^2 \right) \langle \hat{p}^2 \rangle + \frac{i\epsilon^3}{6} \left(A_w^3 - 3A_w^2 A_w + 2(A_w)^3 \right) \langle \hat{p}^3 \rangle \right.$$
$$\left. + \frac{\epsilon^4}{24} \left(A_w^4 - 4A_w^3 A_w + 6A_w^2 (A_w)^2 - 3(A_w)^4 \right) \langle \hat{p}^4 \rangle \right|, \tag{5.12}$$

where A_w^n denotes the higher order weak values as defined in eq. (3.44) with $A_w^n \neq (A_w)^n$.

The normalization $\mathcal{N}$ can be expanded in the same manner which yields

$$
\frac{1}{\mathcal{N}^2} \approx |\langle\psi_F|\psi_I\rangle|^2 \left(1 - \epsilon^2 \left(\mathrm{Re}\left[A_w^2\right] - (A_w)^2\right)\langle\hat{p}^2\rangle - \frac{\epsilon^3}{3}\left(\mathrm{Im}\left[A_w^3\right] - 3A_w\mathrm{Im}\left[A_w^2\right]\right)\langle\hat{p}^3\rangle \right.
$$
$$
\left. + \frac{\epsilon^4}{12}\left(\mathrm{Re}\left[A_w^4\right] - 4A_w\mathrm{Re}\left[A_w^3\right] + 3|A_w^2|^2\right)\langle\hat{p}^4\rangle\right).
$$
(5.13)

Inserting eq. (5.13) into eq. (5.12), expanding in powers of ϵ again and keeping only terms with ϵ^4 or lower, results in the final expression for the overlap in the weak value case

$$
|\langle\Phi_e|\Phi_w\rangle| = 1 - \frac{1}{8}\left(\langle\hat{p}^4\rangle - \langle\hat{p}^2\rangle^2\right)\left|A_w^2 - (A_w)^2\right|^2\epsilon^4 + O(\epsilon^5),
$$
(5.14)

which can be rewritten as

$$
|\langle\Phi_e|\Phi_w\rangle| = 1 - \frac{1}{8}\left(\Delta(\hat{p}^2)\right)^2 (\Delta A_w)^4\epsilon^4 + O(\epsilon^5),
$$
(5.15)

where $\Delta A_w := |A_w^2 - (A_w)^2|^{\frac{1}{2}}$ is the *weak uncertainty* as defined in [62].

It is thus proven that for any pre- and postselection states, which generate some weak value, the fidelity between the pointer state following the postelection and the pointer state corresponding to an eigenvalue equal to the weak value, scales at least with order ϵ^4.

Comparison of Expectation Value and Eigenvalue

As in the weak value case this fidelity from eq. (5.9) is expanded in orders of ϵ, also in the expectation value case, which results in

$$
\sqrt{\langle\Phi_e|\hat{\rho}_{exp}|\Phi_e\rangle} \approx \left(\sum_j |\gamma_j|^2 \left|1 - i\epsilon(a_j - a_k)\langle\hat{p}\rangle - \frac{\epsilon^2}{2}(a_j - a_k)^2\langle\hat{p}^2\rangle\right|\right)^{\frac{1}{2}}
$$
$$
\approx \left(\sum_j |\gamma_j|^2 \left(1 + \epsilon^2\left(a_j^2 - 2a_ja_k + a_k^2\right)\langle\hat{p}\rangle^2\right.\right.
$$
(5.16)
$$
\left.\left. - \epsilon^2\left(a_j^2 - 2a_ja_k + a_k^2\right)\langle\hat{p}^2\rangle\right)\right)^{\frac{1}{2}}
$$

Using the relation $\langle A^n\rangle = \sum_j |\gamma_j|^2 a_j^n$ and the fundamental assumption $\langle\hat{A}\rangle = a_k$, this expression simplifies to

$$
\sqrt{\langle\Phi_e|\hat{\rho}_{exp}|\Phi_e\rangle} \approx \sqrt{1 - \epsilon^2\left(\langle\hat{p}^2\rangle - \langle\hat{p}\rangle^2\right)\left(\langle\hat{A}^2\rangle - \langle\hat{A}\rangle^2\right)}
$$
$$
\Rightarrow \quad \sqrt{\langle\Phi_e|\hat{\rho}_{exp}|\Phi_e\rangle} = 1 - \frac{\epsilon^2}{2}(\Delta p)^2(\Delta A)^2 + O(\epsilon^3).
$$
(5.17)

Contrary to the weak value case, the lowest order of scaling in the expectation value case ϵ^2 does not vanish, as long as the preselection state is not an eigenstate of $\hat{A}$ and the initial pointer state is not an eigenstate of $\hat{p}$. Thus, it can be argued that for a sufficiently weak interaction with $\epsilon \to 0$, the overlap between the pointer coupled to an eigenvalue and the pointer coupled to a weak value (5.15) is infinitely better than the overlap between the eigenvalue and the expectation value pointers (5.17). An experimental observation of these properties would confirm the operational reality of weak values as presented above.

5.2.2. Experimental Confirmation of Overlaps

The fundamentally different scaling behaviors between the three pointer states can be confirmed in a simple interferometric experiment as described below.

Principle of Setup

To measure the fidelity between the different pointer states a similar interaction principle is employed, as for the DST presented in chapter 4. While the Gaussian beam pointer is suitable without any reservations, in a dichotomic polarization object system it is impossible to prepare a superposition state that corresponds to an expectation value which is equal to one of the two eigenvalues. As proposed in [114], however, it is possible to emulate a third eigenstate with the eigenvalue 0 by the absence of any interaction. Therefore, in the proposed experiment with an interaction parametrized by the operator $\hat{\sigma}_z$ the characteristic value is chosen to be zero. The corresponding eigenvalue $a_k = 0$ is realized by the absence of interaction, the expectation value $\langle \hat{\sigma}_z \rangle = 0$ by a preselected system only with the preselection state $|\psi_I\rangle = |P\rangle$ and the weak value $\sigma_w = 0$ by using the same state as a postselection with $|\psi_F\rangle = |\psi_I\rangle = |P\rangle$.

The setup employed to measure the fidelity between the different pointer states is a *Mach-Zehnder-interferometer* as described in [78] and depicted in Fig. 5.1.

While in the reference-arm the pointer coupled to the eigenvalue is prepared by an absence of interaction, in the test-arm both the states corresponding to the expectation value and to the weak value can be created by inserting or removing the postselection polarizer. As discussed in subsection 4.3.2, it is possible to vary the interaction strength ϵ by rotating the YVO_4 crystal, which enables an analysis of the scaling behavior of the fidelities. To compensate for the intensity losses due to the postselection it is necessary to reduce the intensity in the reference-arm to equal the intensities in the two arms. The latter step effectively corresponds to the renormalization of the weak value pointer state after the projective postselection. Eventually the value of the fidelity can be measured by evaluating the intensity change in one of the output ports when the phase between the two interferometer paths is varied, as discussed below.
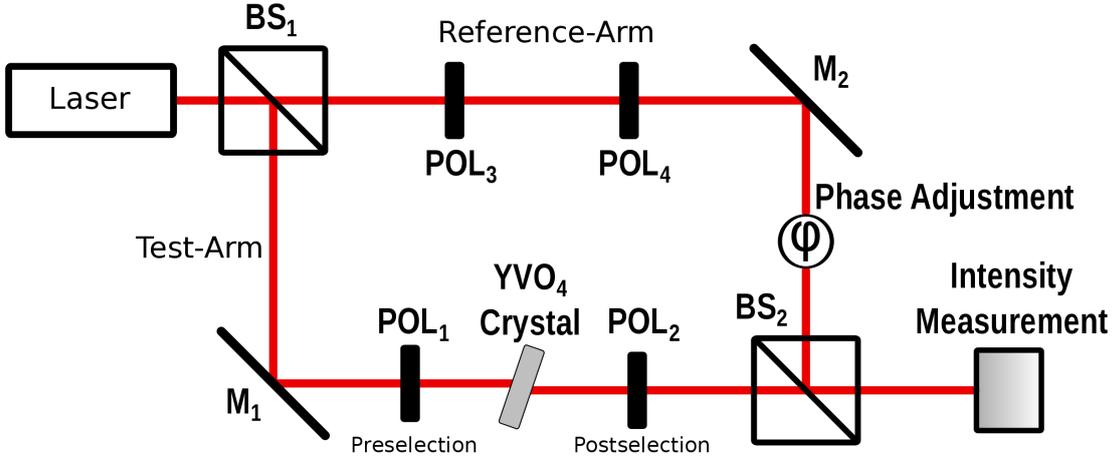
Figure 5.1.: Setup for the measurement of the fidelites for different pointer states. The beam-splitters BS_1 and BS_2 and the two mirrors M_1 and M_2 are standard elements of a Mach-Zehnder-interferometer. They are used to create two beam paths or "arms", which are overlapped again after different sets of operations have been executed in each arm. In the lower test-arm the pointer states corresponding to expectation values and weak values can be prepared with the two polarizers POL_1 and POL_2, which represent pre- and postselection and an YVO_4 crystal, which creates the weak interaction. In the upper reference-arm, where the pointer state corresponding to eigenvalue 0 is prepared, the intensity can be varied by rotating the polarizer POL_3, which changes the amount of light transmitted by the successive polarizer POL_4. For practical reasons, the polarizer POL_4 is rotated to P-polarization, just as the postselection polarizer POL_2. An additional component is used to change the phase relation between the two arms, which is necessary for the measurement of the visibility.

The expected scaling behavior of the fidelity for the Gaussian beam pointers corresponding to the object system states defined above is presented in Fig. 5.2.

Visibility as Measure for Fidelity

A fundamental difficulty appears in the case of the pointer state coupled to an expectation value, where the object system and the pointer system are in a non-separable state. Because the two systems are realized as different degrees of freedom of the same particle, it is not trivial to experimentally realize a separated projection of the mixed pointer state onto the pointer state corresponding to an eigenvalue from the reference-arm. In the experiment, however, the symmetry of the interaction allows the measurement of a quantity that is proportional to the pursued fidelity. For the comparison of the weak value and the eigenvalue this problem does not arise because in both cases the pointer state is separable from
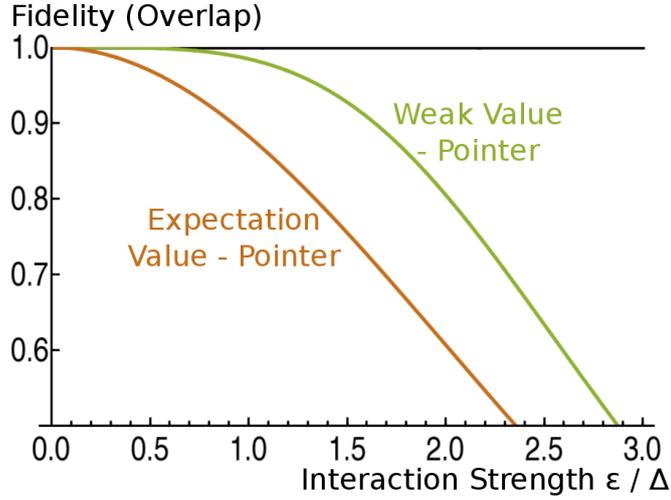
Figure 5.2.: Scaling of fidelities between the eigenvalue pointer and the pointers corresponding to the weak value and to the expectation value. The fidelity is plotted in dependence on the interaction strength $\frac{\epsilon}{\Delta}$, where Δ is the standard deviation of the Gaussian pointer profile.

the object state, and it is possible to generate the necessary overlap by simply rotating the two object states into the same polarization state.

The quantity calculated for the evaluation of the fidelity is the *visibility* $\mathcal{V}$, which is defined as [78]

$$\mathcal{V} = \frac{I_{max} - I_{min}}{I_{max} + I_{min}}, \qquad (5.18)$$

where I_{max} and I_{min} represent the maximal and minimal intensities, which are recorded when the superposition of the two states is varied between maximally constructive and maximally destructive interference by changing the phase relation between the two arms of the interferometer. The composite state $|C_e\rangle$ in the case corresponding to the eigenvalue can be written as

$$|C_e\rangle = |P\rangle \otimes |\Phi_0\rangle. \qquad (5.19)$$

In the case of the expectation the non-separable state $|C_{exp}\rangle$ becomes

$$|C_{exp}\rangle = \frac{1}{\sqrt{2}} \left(|H\rangle \otimes |\Phi_\epsilon\rangle + |V\rangle \otimes |\Phi_{-\epsilon}\rangle \right). \qquad (5.20)$$

Assuming a maximal intensity I_{max} in the case of the phase φ and consequently a minimal intensity I_{min} with the phase $\varphi + \pi$, the visibility can be expressed as

$$
\begin{aligned}
\mathcal{V} &= \frac{\||C_e\rangle + e^{i\varphi}|C_{exp}\rangle\|^2 - \||C_e\rangle - e^{i\varphi}|C_{exp}\rangle\|^2}{\||C_e\rangle + e^{i\varphi}|C_{exp}\rangle\|^2 + \||C_e\rangle - e^{i\varphi}|C_{exp}\rangle\|^2}, \\
&= \frac{4\mathrm{Re}\left[e^{i\varphi}\langle C_e|C_{exp}\rangle\right]}{4} = \mathrm{Re}\left[e^{i\varphi}\langle C_e|C_{exp}\rangle\right] \\
&= \frac{1}{2}\left(\mathrm{Re}\left[e^{i\varphi}\langle\Phi_0|\Phi_\epsilon\rangle\right] + \mathrm{Re}\left[e^{i\varphi}\langle\Phi_0|\Phi_{-\epsilon}\rangle\right]\right).
\end{aligned}
\tag{5.21}
$$

For the states used in the experiment the fidelity $F(|\Phi_e\rangle, \hat{\rho}_{exp})$ from eq. (5.9), can be reformulated to

$$
F(|\Phi_e\rangle, \hat{\rho}_{exp}) = \sqrt{\frac{1}{2}\left(|\langle\Phi_0|\Phi_\epsilon\rangle|^2 + |\langle\Phi_0|\Phi_{-\epsilon}\rangle|^2\right)}.
\tag{5.22}
$$

To relate the quantities from eqs. (5.21) and (5.22), it is necessary to assume real and strictly positive pointer wavefunctions, as it is the case with the employed Gaussian profiles. This implies $\varphi = 0$ because in the latter case a maximal intensity corresponds simply to an additive superposition of the two wavefunctions. Consequently the visibility can be expressed as

$$
\mathcal{V} = \frac{1}{2}\left(|\langle\Phi_0|\Phi_\epsilon\rangle| + |\langle\Phi_0|\Phi_{-\epsilon}\rangle|\right).
\tag{5.23}
$$

It becomes clear that it is the symmetry of the interaction with $\langle\Phi_0|\Phi_\epsilon\rangle = \langle\Phi_0|\Phi_{-\epsilon}\rangle$, which eventually allows the identification of the measured visibility with the relevant fidelity as

$$
\mathcal{V} = |\langle\Phi_0|\Phi_{\pm\epsilon}\rangle| = \sqrt{|\langle\Phi_0|\Phi_{\pm\epsilon}\rangle|^2} = F(|\Phi_e\rangle, \hat{\rho}_{exp}).
\tag{5.24}
$$

By a measurement of the visibilities under variation of the interaction strength ϵ, it is therefore possible to measure the scaling behaviors of both fidelities for the different pointer states prepared in the test-arm.

6. Conclusions

In this thesis the intricate field of weak measurement and values has been discussed. While different interpretations of the concept of weak values have been presented, no definite conclusion about their status and meaning in physics can be given at this point. It has been demonstrated how weak values emerge naturally from PPS measurements and how they manifest in linear pointer responses for interactions that satisfy suitable conditions. Furthermore, it has been discussed how the unusual pointer shifts encountered in weak measurements, emerge naturally from interference effects caused by the relation between pre- and postselection. These formal results can be captured in total by the standard formulation of quantum mechanics and while they surely present an unique way to consider quantum systems, they do not seem to introduce new physics.

If, however, the time-symmetric approach to quantum mechanics, which lies at the origin of weak values, is combined with a radical operationalist perspective on quantum measurement, the formalism of weak values seems to imply the possibility of gaining more information about physical systems than permitted by the standard quantum theory. The corresponding claims about the past of quantum particles, including such elements as negative particle numbers, have been shown to be extremely controversial and founded in a highly unusual concept of measurement outcomes. In contrast, an interpretation of weak values as relative probability amplitudes has proven a more substantial approach, which is completely consistent with the standard interpretation of quantum mechanics and is used in the procedure of direct state tomography.

While the controversy regarding the meaning of weak values is surely one of the most prominent subject of the field, the formalism of weak values can be also very useful in practical implementations, independently of the interpretation. As has been presented in this thesis, experimental techniques as direct state tomography and weak amplification have proven the usefulness of weak measurements in various applications. However, as pointed out by critics, these procedures display their potential only under very specific experimental conditions, which limits the scope of their applicability. While direct state tomography appears to be especially suited for the analysis of high dimensional quantum systems, weak amplification is only useful in scenarios with unlimited statistics and dominating technical noise. For the direct state tomography of pure qubits also an exact and unbiased boolean scheme was proposed.

The direct state tomography experiment that was reproduced in the course of this thesis could not overcome two principal discrepancies between theoretical predictions and the data. While the measured pointer response curves showed good agreement with the theory with respect to most of their properties, the linear regime of the pointer response broke down for much smaller weak values than expected. Furthermore, in the process of the calibration of the experiment a much larger contribution of imaginary weak values to the pointer shift has been observed, than was predicted by the theoretical calculations as presented in this thesis. While some possible explanations for these phenomena were discussed, no definite explanation can be given at this point.

In the context of the operational interpretation of weak values as the real properties of PPS systems, a proof for the scaling of the fidelities between different pointer states after interaction was developed. While this result surely represents an interesting property of weak measurements, it is, however, debatable what kind of interpretational conclusions it implies. Because weak measurements do not involve any empirical content, which is not included in standard quantum mechanics, the question may arise how relevant the debate about their interpretation is to physics. Even in the radically operational interpretation, the counterfactual claims about the past of particles pertain only to their weak interactions and in the case of strong measurements the time-symmetric ABL rule still contains the element of state reduction. The issue of an interpretation of weak measurements beyond the scope of standard quantum mechanics, therefore seems to be related mainly to the definition of notions as "reality" and "measurement", which are the subject of an ongoing discourse about the meaning of physical theories in general.

A. Appendix

A.1. Formulas for Gaussian Beams

A.1.1. Standard Gaussian Profile

The square-normalized Gaussian profile $F_G(x)$ is defined as

$$F_G(x) := \left(\frac{1}{2\pi\Delta^2}\right)^{\frac{1}{4}} \exp\left(-\frac{x^2}{4\Delta^2}\right), \tag{A.1}$$

with $\langle \hat{x} \rangle = \langle \hat{p}_x \rangle = 0$, $\Delta x = \Delta$ and $\Delta p = \frac{\hbar}{2\Delta}$.

A product of Gaussian profiles shifted differently in position space can be expressed as

$$F_G(x-a)F_G(x-b) = \frac{1}{\sqrt{2\pi\Delta^2}} \exp\left(-\frac{1}{4\Delta^2}\left[(x-a)^2 + (x-b)^2\right]\right)$$
$$= \frac{1}{\sqrt{2\pi\Delta^2}} \exp\left(-\frac{1}{2\Delta^2}\left(x - \frac{a+b}{2}\right)^2\right) \exp\left(-\frac{1}{8\Delta^2}(a-b)^2\right), \tag{A.2}$$

which implies the overlap

$$\int_{-\infty}^{\infty} F_G(x-a)F_G(x-b)\,\mathrm{d}x = \exp\left(-\frac{1}{8\Delta^2}(a-b)^2\right). \tag{A.3}$$

A.1.2. Curved Gaussian Profile

For the curved Gaussian profile $F_C(x)$ of a Gaussian beam defined in subsection 4.2.1 as

$$F_C(x) := \left(\frac{1}{2\pi\Delta_z^2}\right)^{\frac{1}{4}} \exp\left(-\frac{x^2}{4\Delta_z^2}\right) \exp\left(-ik\frac{x^2}{2R_z}\right), \tag{A.4}$$

with $\Delta_z := \frac{w_z}{2}$ and all z-dependent quantities signified with the index z, the overlap can be calculated as

$$\int_{-\infty}^{\infty} F_C^*(x-a)F_C(x-b)\,\mathrm{d}x = \exp\left(-\frac{(a-b)^2}{8\Delta_0^2}\right), \tag{A.5}$$

with the important identity

$$\frac{1 + (\frac{k}{2R_z})^2 w_z^4}{w_z^2} = \frac{1}{w_0^2} \quad \Leftrightarrow \quad \frac{1 + 16(\frac{k}{2R_z})^2 \Delta_z^4}{4\Delta_z^2} = \frac{1}{4\Delta_0^2}. \tag{A.6}$$

The position expectation value $\langle \hat{x} \rangle$ becomes

$$\int_{-\infty}^{\infty} x F_C^*(x-a) F_C(x-b) \, \mathrm{d}x = \left(\frac{a+b}{2} - i\frac{a-b}{2}\frac{z}{z_R} \right) \exp\left(-\frac{(a-b)^2}{8\Delta_0^2} \right), \tag{A.7}$$

with the important identity

$$\frac{kw_z^2}{2R_z^2} = \frac{z}{z_R}. \tag{A.8}$$

For the momentum expectation value $\langle \hat{p}_x \rangle$ it can be obtained that

$$\int_{-\infty}^{\infty} F_C^*(x-a)(-i\hbar\partial_x) F_C(x-b) \, \mathrm{d}x = i\hbar\frac{a-b}{4\Delta_0^2} \exp\left(-\frac{(a-b)^2}{8\Delta_0^2} \right). \tag{A.9}$$

A.2. Formulas for Qubit Weak Values

A.2.1. Reformulation of Weak Value Expressions

An arbitrary qubit weak value can be separated into real and imaginary parts with

$$\sigma_w = \frac{\alpha\gamma^* - \beta\delta^*}{\alpha\gamma^* + \beta\delta^*} = \frac{|\alpha\gamma^*|^2 - |\beta\delta^*|^2 + 2i\mathrm{Im}\left[\alpha\beta^*\gamma^*\delta\right]}{|\alpha\gamma^*|^2 + |\beta\delta^*|^2 + 2\mathrm{Re}\left[\alpha\beta^*\gamma^*\delta\right]}, \tag{A.10}$$

which implies

$$\mathrm{Re}\left[\sigma_w\right] = \frac{|\alpha\gamma^*|^2 - |\beta\delta^*|^2}{|\alpha\gamma^*|^2 + |\beta\delta^*|^2 + 2\mathrm{Re}\left[\alpha\beta^*\gamma^*\delta\right]}, \tag{A.11}$$

$$\mathrm{Im}\left[\sigma_w\right] = \frac{2\mathrm{Im}\left[\alpha\beta^*\gamma^*\delta\right]}{|\alpha\gamma^*|^2 + |\beta\delta^*|^2 + 2\mathrm{Re}\left[\alpha\beta^*\gamma^*\delta\right]}. \tag{A.12}$$

The modulus of the weak value can be rewritten as

$$|\sigma_w|^2 = \frac{|\alpha\gamma^*|^2 + |\beta\delta^*|^2 - 2\mathrm{Re}\left[\alpha\beta^*\gamma^*\delta\right]}{|\alpha\gamma^*|^2 + |\beta\delta^*|^2 + 2\mathrm{Re}\left[\alpha\beta^*\gamma^*\delta\right]} \tag{A.13}$$

and

$$1 - |\sigma_w|^2 = \frac{4\mathrm{Re}\left[\alpha\beta^*\gamma^*\delta\right]}{|\alpha\gamma^*|^2 + |\beta\delta^*|^2 + 2\mathrm{Re}\left[\alpha\beta^*\gamma^*\delta\right]}. \tag{A.14}$$

A.2.2. Foundation of Boolean Direct State Tomography Scheme

For the following proofs it is instructive to define new coordinates θ' and φ' on the Bloch sphere, with which an arbitrary qubit state $|\psi\rangle$ is parametrized as

$$
\begin{aligned}
|\psi\rangle &= \cos\frac{\theta'}{2}|P\rangle + e^{i\varphi'}\sin\frac{\theta'}{2}|M\rangle \\
&= \left(\cos\frac{\theta'}{2} + e^{i\varphi'}\sin\frac{\theta'}{2}\right)|H\rangle + \left(\cos\frac{\theta'}{2} - e^{i\varphi'}\sin\frac{\theta'}{2}\right)|V\rangle.
\end{aligned}
\tag{A.15}
$$

For a division of Bloch sphere into two half spheres with the $|P\rangle$ and $|M\rangle$ states at the poles, states with $\theta' \in]\frac{\pi}{2}, \frac{3\pi}{2}[$ lie in the "M half sphere", and the others in the "P half sphere".

The moduli of the qubit weak values $|\sigma_w^{(P)}|$ and $|\sigma_w^{(M)}|$ for P- and M-postselection can thus be expressed as

$$
|\sigma_w^{(P)}| = \left|\frac{\langle P|\hat{\sigma}_z|\psi\rangle}{\langle P|\psi\rangle}\right| = \left|\frac{e^{i\varphi'}\sin\frac{\theta'}{2}}{\cos\frac{\theta'}{2}}\right| = |\tan\frac{\theta'}{2}|
\tag{A.16}
$$

$$
|\sigma_w^{(M)}| = |\cot\frac{\theta'}{2}|.
\tag{A.17}
$$

The latter result proofs that states in the half spheres corresponding to the postselection states, always imply weak values with moduli smaller than one and vice versa.

It remains to proof that the postselection probability for states from the same half sphere as the postselection state is also higher than for states from the opposite half, which represents the basis for the boolean tomography scheme as presented in subsection 4.2.2. For a preselection state $|\psi\rangle = \alpha|H\rangle + \beta|V\rangle$ with $\alpha = \cos\frac{\theta'}{2} + e^{i\varphi'}\sin\frac{\theta'}{2}$ and $\beta = \cos\frac{\theta'}{2} - e^{i\varphi'}\sin\frac{\theta'}{2}$ as defined above, the state after the interaction $|\psi_{IA}\rangle$ can be written as

$$
|\psi_{IA}\rangle = \alpha|H\rangle|\Phi_\epsilon\rangle + \beta|V\rangle|\Phi_{-\epsilon}\rangle.
\tag{A.18}
$$

For the postselection state $|\psi_F\rangle = \frac{1}{\sqrt{2}}(|H\rangle \pm |V\rangle)$ the probability of postselection $|\langle\psi_F|\psi_{IA}\rangle|^2$ becomes

$$
\begin{aligned}
|\langle\psi_F|\psi_{IA}\rangle|^2 &= \frac{1 \pm \operatorname{Re}\left[\alpha\beta^*\right]e^{-\frac{\epsilon^2}{2\Delta_0^2}}}{2} \\
&= \frac{1 \pm \cos\theta' e^{-\frac{\epsilon^2}{2\Delta_0^2}}}{2}.
\end{aligned}
\tag{A.19}
$$

Thus, for finite ϵ the probability of postselection is therefore always higher for preselection states from the same half of the Bloch sphere as the postselection state.

By executing both postselections and considering only the data corresponding to higher intensities, the exact DST scheme will always only evaluate weak values from the unamplified region of the eigenvalues, which correspond to the invertible region of the pointer response.

A.2.3. Inversion of Pointer Response

The inversion of eqs. (4.50) and (4.51) for $z = 0$ is facilitated if σ_w is expressed in polar form with

$$\sigma_w = \mathcal{A}_\sigma e^{i\varphi_\sigma}. \tag{A.20}$$

In this case the Ansatz for the modulus $\mathcal{A}_\sigma$ becomes

$$\frac{\mathcal{A}_\sigma^2}{\left[1 - \frac{1}{2}(1 - \mathcal{A}_\sigma^2)(1 - e^{-\frac{\epsilon^2}{2\Delta_0^2}})\right]^2} = (\delta\tilde{x})^2 + (\delta\tilde{p})^2, \tag{A.21}$$

which under the assumption $\mathcal{A}_\sigma \geq 0$ represents a quadratic equation with the normalized shifts $\delta\tilde{x}$ and $\delta\tilde{p}$ defined as

$$\delta\tilde{x} := \frac{\langle \hat{x} \rangle_F}{\epsilon}, \quad \delta\tilde{p} := \frac{2\Delta_0^2}{\hbar\epsilon e^{-\frac{\epsilon^2}{2\Delta_0^2}}} \langle \hat{p}_x \rangle_F. \tag{A.22}$$

Employing s_{xp} as a short notation for the measured shifts as

$$s_{xp} := (\delta\tilde{x})^2 + (\delta\tilde{p})^2 = \left(\frac{\langle \hat{x} \rangle_F}{\epsilon}\right)^2 + \left(\frac{2\Delta_0^2 \langle \hat{p}_x \rangle_F}{\hbar\epsilon e^{-\frac{\epsilon^2}{2\Delta_0^2}}}\right)^2, \tag{A.23}$$

the solution of eq. (A.21) can be expressed as

$$\mathcal{A}_\sigma = \frac{1 \pm \sqrt{1 - (1 - e^{-\frac{\epsilon}{\Delta_0^2}})s_{xp}}}{(1 - e^{-\frac{\epsilon}{2\Delta_0^2}})\sqrt{s_{xp}}}, \tag{A.24}$$

where "$-$" represents the desired solution.

For the calculation of the phase φ_σ various cases have to be distinguished as

$$\varphi_\sigma = \begin{cases} \arctan(\frac{\delta\tilde{p}}{\delta\tilde{x}}) & \text{if } \delta\tilde{x} > 0 \\ \arctan(\frac{\delta\tilde{p}}{\delta\tilde{x}}) + \pi & \text{if } \delta\tilde{x} < 0 \\ \frac{\pi}{2} & \text{if } \delta\tilde{x} = 0, \ \delta\tilde{p} > 0 \\ -\frac{\pi}{2} & \text{if } \delta\tilde{x} = 0, \ \delta\tilde{p} < 0 \end{cases}. \tag{A.25}$$

Bibliography

[1] Gerlach, W. and Stern, O., Practical measurement of joint weak values and their connection to the annihilation operator, *Zeitschrift für Physik*, **9**, 1, 349 (1922).

[2] Schlosshauer, M., Decoherence, the measurement problem, and interpretations of quantum mechanics, *Rev. Mod. Phys.*, **76**, 1267 (2005).

[3] Schlosshauer, M., Kofler, J., and Zeilinger, A., A snapshot of foundational attitudes toward quantum mechanics, *Studies in History and Philosophy of Science Part B: Studies in History and Philosophy of Modern Physics*, **44**, 3, 222 (2013).

[4] Aharonov, Y., Albert, D. Z., and Vaidman, L., How the result of a measurement of a component of the spin of a spin-1/2 particle can turn out to be 100, *Phys. Rev. Lett.*, **60**, 1351 (1988).

[5] Aharonov, Y., Bergmann, P. G., and Lebowitz, J. L., Time Symmetry in the Quantum Process of Measurement, *Phys. Rev.*, **134**, B1410 (1964).

[6] Peres, A., Quantum measurements with postselection, *Phys. Rev. Lett.*, **62**, 2326 (1989).

[7] Leggett, A. J., Comment on "How the result of a measurement of a component of the spin of a spin-1/2 particle can turn out to be 100", *Phys. Rev. Lett.*, **62**, 2325 (1989).

[8] Aharonov, Y. and Vaidman, L., Aharonov and Vaidman reply, *Phys. Rev. Lett.*, **62**, 2327 (1989).

[9] Duck, I. M., Stevenson, P. M., and Sudarshan, E. C. G., The sense in which a "weak measurement" of a spin-1/2 particle's spin component yields a value 100, *Phys. Rev. D*, **40**, 2112 (1989).

[10] Sokolovski, D., Are the Weak Measurements Really Measurements?, *Quanta*, **2**, 1, 50 (2013).

[11] Svensson, B. E. Y., What Is a Quantum-Mechanical "Weak Value" the Value of?, *Foundations of Physics*, **43**, 10, 1193 (2013).

Bibliography

[12] Vaidman, L., Past of a quantum particle, *Phys. Rev. A*, **87**, 052104 (2013).

[13] Danan, A., Farfurnik, D., Bar-Ad, S., and Vaidman, L., Asking Photons Where They Have Been, *Phys. Rev. Lett.*, **111**, 240402 (2013).

[14] Aharonov, Y., Popescu, S., Rohrlich, D., and Skrzypczyk, P., Quantum Cheshire Cats, *New Journal of Physics*, **15**, 11, 113015 (2013).

[15] Svensson, B. E. Y., On the interpretation of quantum mechanical weak values, *Physica Scripta*, **2014**, T163, 014025 (2014).

[16] Salih, H., Commentary: Asking photons where they have been without telling them what to say, *Frontiers in Physics*, **3**, 47 (2015).

[17] Vaidman, L., Danan, A., Farfurnik, D., and Bar-Ad, S., Response: "Commentary: Asking photons where they have been without telling them what to say", *Frontiers in Physics*, **3**, 48 (2015).

[18] Svensson, B. E. Y., Non-representative Quantum Mechanical Weak Values, *Foundations of Physics*, **45**, 12, 1645 (2015).

[19] Fu, L., Hashmi, F. A., Jun-Xiang, Z., and Shi-Yao, Z., An Ideal Experiment to Determine the "Past of a Particle" in the Nested Mach-Zehnder Interferometer, *Chinese Physics Letters*, **32**, 5, 050303 (2015).

[20] Sokolovski, D., Weak measurements measure probability amplitudes (and very little else), *Physics Letters A*, **380**, 18–19, 1593 (2016).

[21] Ritchie, N. W. M., Story, J. G., and Hulet, R. G., Realization of a measurement of a "weak value", *Phys. Rev. Lett.*, **66**, 1107 (1991).

[22] Hosten, O. and Kwiat, P., Observation of the Spin Hall Effect of Light via Weak Measurements, *Science*, **319**, 5864, 787 (2008).

[23] Lundeen, J. S., Sutherland, B., Patel, A., Stewart, C., and Bamber, C., Direct measurement of the quantum wavefunction, *Nature*, **474**, 7350, 188 (2011).

[24] Salvail, J. Z., Agnew, M., Johnson, A. S., Bolduc, E., Leach, J., and Boyd, R. W., Full characterization of polarization states of light via direct measurement, *Nat Photon*, **7**, 4, 316 (2013).

[25] Malik, M., Mirhosseini, M., Lavery, M. P. J., Leach, J., Padgett, M. J., and Boyd, R. W., Direct measurement of a 27-dimensional orbital-angular-momentum state vector, *Nat Commun*, **5**, (2014).

[26] Kofman, A. G., Ashhab, S., and Nori, F., Nonperturbative theory of weak pre- and post-selected measurements, *Physics Reports*, **520**, 2, 43 (2012).

[27] Aharonov, Y. and Vaidman, L., Time in Quantum Mechanics, chapter The Two-State Vector Formalism: An Updated Review, 399–447 (2008).

[28] Cohen-Tannoudji, C., Diu, B., and Laloë, F., Quantum Mechanics, volume 1 (2005).

[29] Nielsen, M. A. and Chuang, I. L., Quantum Computation and Quantum Information: 10th Anniversary Edition (2010).

[30] Sakurai, J. J., Modern Quantum Mechanics (1994).

[31] Cartwright, N., How the Laws of Physics Lie (2002).

[32] Hughes, R. I. G., The Structure and Interpretation of Quantum Mechanics (1992).

[33] Lambropoulos, P. and Petrosyan, D., Fundamentals of Quantum Optics and Quantum Information (2007).

[34] Braunstein, S. L. and van Loock, P., Quantum information with continuous variables, *Rev. Mod. Phys.*, **77**, 513 (2005).

[35] Barnett, S. M., Quantum Information (2009).

[36] Scully, M. O., Englert, B.-G., and Walther, H., Quantum optical tests of complementarity, *Nature*, **351**, 6322, 111 (1991).

[37] Maccone, L. and Rusconi, C. C., State estimation: A comparison between direct state measurement and tomography, *Phys. Rev. A*, **89**, 022122 (2014).

[38] Dressel, J., Malik, M., Miatto, F. M., Jordan, A. N., and Boyd, R. W., *Colloquium* : Understanding quantum weak values: Basics and applications, *Rev. Mod. Phys.*, **86**, 307 (2014).

[39] Horodecki, R., Horodecki, P., Horodecki, M., and Horodecki, K., Quantum entanglement, *Rev. Mod. Phys.*, **81**, 865 (2009).

[40] Gühne, O. and Tóth, G., Entanglement detection, *Physics Reports*, **474**, 1–6, 1 (2009).

[41] Braginsky, V. B. and Khalili, F. Y., Quantum Measurement (1999).

[42] Pusey, M. F., Barrett, J., and Rudolph, T., On the reality of the quantum state, *Nat Phys*, **8**, 6, 475 (2012).

Bibliography

[43] Neumann, J. v., Mathematische Grundlagen der Quantenmechanik (1996).

[44] Fischer, M. C., Gutiérrez-Medina, B., and Raizen, M. G., Observation of the Quantum Zeno and Anti-Zeno Effects in an Unstable System, *Phys. Rev. Lett.*, **87**, 040402 (2001).

[45] Misra, B. and Sudarshan, E. C. G., The Zeno's paradox in quantum theory, *Journal of Mathematical Physics*, **18**, 4, 756 (1977).

[46] Aharonov, Y., Albert, D., Casher, A., and Vaidman, L., Novel Properties of Preselected and Postselected Ensembles, *Annals of the New York Academy of Sciences*, **480**, 1, 417 (1986).

[47] Lundeen, J. and Resch, K., Practical measurement of joint weak values and their connection to the annihilation operator, *Physics Letters A*, **334**, 5 - 6, 337 (2005).

[48] Dressel, J. and Jordan, A. N., Weak Values are Universal in Von Neumann Measurements, *Phys. Rev. Lett.*, **109**, 230402 (2012).

[49] Wu, S. and Li, Y., Weak measurements beyond the Aharonov-Albert-Vaidman formalism, *Phys. Rev. A*, **83**, 052106 (2011).

[50] Peres, A., When Is a Quantum Measurement?, *Annals of the New York Academy of Sciences*, **480**, 1, 438 (1986).

[51] Herzog, T. J., Kwiat, P. G., Weinfurter, H., and Zeilinger, A., Complementarity and the Quantum Eraser, *Phys. Rev. Lett.*, **75**, 3034 (1995).

[52] Aharonov, Y., Anandan, J., and Vaidman, L., Meaning of the wave function, *Phys. Rev. A*, **47**, 4616 (1993).

[53] Shikano, Y., Measurements in Quantum Mechanics, chapter Theory of "Weak Value" and Quantum Mechanical Measurements, 75–100 (2012).

[54] Pryde, G. J., O'Brien, J. L., White, A. G., Ralph, T. C., and Wiseman, H. M., Measurement of Quantum Weak Values of Photon Polarization, *Phys. Rev. Lett.*, **94**, 220405 (2005).

[55] Parks, A. D. and Gray, J. E., Variance control in weak-value measurement pointers, *Phys. Rev. A*, **84**, 012116 (2011).

[56] Steinberg, A. M., Conditional probabilities in quantum theory and the tunneling-time controversy, *Phys. Rev. A*, **52**, 32 (1995).

[57] Hofmann, H. F., Complete characterization of post-selected quantum statistics using weak measurement tomography, *Phys. Rev. A*, **81**, 012103 (2010).

[58] Steinberg, A. M., Quantum measurement: A light touch, *Nature*, **463**, 7283, 890 (2010).

[59] Aharonov, Y., Cohen, E., and Elitzur, A. C., Foundations and applications of weak quantum measurements, *Phys. Rev. A*, **89**, 052105 (2014).

[60] Banaszek, K., Fidelity Balance in Quantum Operations, *Phys. Rev. Lett.*, **86**, 1366 (2001).

[61] Di Lorenzo, A., Full counting statistics of weak-value measurement, *Phys. Rev. A*, **85**, 032106 (2012).

[62] Aharonov, Y. and Vaidman, L., Properties of a quantum system during the time interval between two measurements, *Phys. Rev. A*, **41**, 11 (1990).

[63] Vaidman, L., Weak-measurement elements of reality, *Foundations of Physics*, **26**, 7, 895 (1996).

[64] Steinberg, A. M., How Much Time Does a Tunneling Particle Spend in the Barrier Region?, *Phys. Rev. Lett.*, **74**, 2405 (1995).

[65] Bub, J. and Brown, H., Curious Properties of Quantum Ensembles Which Have Been Both Preselected and Post-Selected, *Phys. Rev. Lett.*, **56**, 2337 (1986).

[66] Aharonov, Y. and Vaidman, L., Complete description of a quantum system at a given time, *Journal of Physics A: Mathematical and General*, **24**, 10, 2315 (1991).

[67] Sharp, W. D. and Shanks, N., The Rise and Fall of Time-Symmetrized Quantum Mechanics, *Philosophy of Science*, **60**, 3, 488 (1993).

[68] Kirkpatrick, K. A., Classical three-box "paradox", *Journal of Physics A: Mathematical and General*, **36**, 17, 4891 (2003).

[69] Jozsa, R., Complex weak values in quantum measurement, *Phys. Rev. A*, **76**, 044103 (2007).

[70] Zhu, X., Zhang, Y., Pang, S., Qiao, C., Liu, Q., and Wu, S., Quantum measurements with preselection and postselection, *Phys. Rev. A*, **84**, 052111 (2011).

[71] Lundeen, J. S. and Bamber, C., Procedure for Direct Measurement of General Quantum States Using Weak Measurement, *Phys. Rev. Lett.*, **108**, 070402 (2012).

Bibliography

[72] Kocsis, S., Braverman, B., Ravets, S., Stevens, M. J., Mirin, R. P., Shalm, L. K., and Steinberg, A. M., Observing the Average Trajectories of Single Photons in a Two-Slit Interferometer, *Science*, **332**, 6034, 1170 (2011).

[73] Wu, S., State tomography via weak measurements, *Scientific Reports*, **3**, 1193 (2013).

[74] Wu, S. and Mølmer, K., Weak measurements with a qubit meter, *Physics Letters A*, **374**, 1, 34 (2009).

[75] Hofmann, H. F., On the resolution of quantum paradoxes by weak measurements (2009).

[76] Saleh, B. E. A. and Teich, M. C., Fundamentals of Photonics (1991).

[77] Fox, M., Quantum Optics, An Introduction (2009).

[78] Hecht, E., Optik (2014).

[79] Zhu, X., Zhang, Y.-X., and Wu, S., Unbiased state reconstruction using modified weak measurement (2015).

[80] James, D. F. V., Kwiat, P. G., Munro, W. J., and White, A. G., Practical measurement of joint weak values and their connection to the annihilation operator, *Phys. Rev. A*, **64**, 052312 (2001).

[81] Knips, L., Schwemmer, C., Klein, N., Wieśniak, M., and Weinfurter, H., Multipartite entanglement detection with minimal effort (2014).

[82] Schwemmer, C., Tóth, G., Niggebaum, A., Moroder, T., Gross, D., Gühne, O., and Weinfurter, H., Experimental Comparison of Efficient Tomography Schemes for a Six-Qubit State, *Phys. Rev. Lett.*, **113**, 040503 (2014).

[83] Knips, L., Schwemmer, C., Klein, N., Reuter, J., Tóth, G., and Weinfurter, H., How long does it take to obtain a physical density matrix? (2015).

[84] Schwemmer, C., Knips, L., Richart, D., Weinfurter, H., Moroder, T., Kleinmann, M., and Gühne, O., Systematic Errors in Current Quantum State Tomography Tools, *Phys. Rev. Lett.*, **114**, 080403 (2015).

[85] Massar, S. and Popescu, S., Estimating preselected and postselected ensembles, *Phys. Rev. A*, **84**, 052106 (2011).

[86] Zhang, Y.-X., Wu, S., and Chen, Z.-B., Coupling-deformed pointer observables and weak values, *Phys. Rev. A*, **93**, 032128 (2016).

[87] Mirhosseini, M., Magaña Loaiza, O. S., Hashemi Rafsanjani, S. M., and Boyd, R. W., Compressive Direct Measurement of the Quantum Wave Function, *Phys. Rev. Lett.*, **113**, 090402 (2014).

[88] Berry, M. V., Dennis, M. R., McRoberts, B., and Shukla, P., Weak value distributions for spin-1/2, *Journal of Physics A: Mathematical and Theoretical*, **44**, 20, 205301 (2011).

[89] Iinuma, M., Suzuki, Y., Taguchi, G., Kadoya, Y., and Hofmann, H. F., Weak measurement of photon polarization by back-action-induced path interference, *New Journal of Physics*, **13**, 3, 033041 (2011).

[90] Knee, G. C., Briggs, G. A. D., Benjamin, S. C., and Gauger, E. M., Quantum sensors based on weak-value amplification cannot overcome decoherence, *Phys. Rev. A*, **87**, 012115 (2013).

[91] Brunner, N. and Simon, C., Measuring Small Longitudinal Phase Shifts: Weak Measurements or Standard Interferometry?, *Phys. Rev. Lett.*, **105**, 010405 (2010).

[92] Dixon, P. B., Starling, D. J., Jordan, A. N., and Howell, J. C., Ultrasensitive Beam Deflection Measurement via Interferometric Weak Value Amplification, *Phys. Rev. Lett.*, **102**, 173601 (2009).

[93] Xu, X.-Y., Kedem, Y., Sun, K., Vaidman, L., Li, C.-F., and Guo, G.-C., Phase Estimation with Weak Measurement Using a White Light Source, *Phys. Rev. Lett.*, **111**, 033604 (2013).

[94] Ferrie, C. and Combes, J., Weak Value Amplification is Suboptimal for Estimation and Detection, *Phys. Rev. Lett.*, **112**, 040406 (2014).

[95] Magaña Loaiza, O. S., Mirhosseini, M., Rodenburg, B., and Boyd, R. W., Amplification of Angular Rotations Using Weak Measurements, *Phys. Rev. Lett.*, **112**, 200401 (2014).

[96] Kneubühl, F. K. and Sigrist, M. W., Laser (2008).

[97] Meschede, D., Optik, Licht und Laser (2008).

[98] Young, M., Optik, Laser, Wellenleiter (1997).

[99] Zinth, W. and Zinth, U., Optik (2009).

[100] CODIXX AG, colorPol Polarizers, *www.codixx.de*.

[101] DataRay Inc., WinCamD series, *www.dataray.com*.

Bibliography

[102] Fox, M., Optical Properties of Solids (2012).

[103] Foctek Photonics, Inc., Birefringent Crystals: YVO4, *www.foctek.net*.

[104] Dmitriev, V. G., Gurzadyan, G. G., and Nikogosyan, D. N., Handbook of Nonlinear Optical Crystals (1997).

[105] Ravon, T. and Vaidman, L., The three-box paradox revisited, *Journal of Physics A: Mathematical and Theoretical*, **40**, 11, 2873 (2007).

[106] Cohen, O., Pre- and postselected quantum systems, counterfactual measurements, and consistent histories, *Phys. Rev. A*, **51**, 4373 (1995).

[107] Vaidman, L., Compendium of Quantum Physics, chapter Counterfactuals in Quantum Mechanics, 132–136 (2009).

[108] Ringbauer, M., Duffus, B., Branciard, C., Cavalcanti, E. G., White, A. G., and Fedrizzi, A., Measurements on the reality of the wavefunction, *Nat Phys*, **11**, 3, 249 (2015).

[109] Kirkpatrick, K. A., Reply to "The three-box paradox revisited" by T. Ravon and L. Vaidman, *Journal of Physics A: Mathematical and Theoretical*, **40**, 11, 2883 (2007).

[110] Wiseman, H. M., Grounding Bohmian mechanics in weak values and bayesianism, *New Journal of Physics*, **9**, 6, 165 (2007).

[111] Wiseman, H. M., Weak values, quantum trajectories, and the cavity-QED experiment on wave-particle correlation, *Phys. Rev. A*, **65**, 032111 (2002).

[112] Chang, H., Operationalism, in Zalta, E. N. (editor), The Stanford Encyclopedia of Philosophy (2009).

[113] Einstein, A., Podolsky, B., and Rosen, N., Can Quantum-Mechanical Description of Physical Reality Be Considered Complete?, *Phys. Rev.*, **47**, 777 (1935).

[114] Vaidman *et al.*, Eigenvalues, Weak values and Expectation values, (in preparation).

Acknowledgments